# SINGLE FREQUENCY WHOLE-BODY IMPEDANCE STUDIES

# IN

# CHILDREN WITH DIARRHOEAL DISEASE

# AND

# DEVELOPMENT OF A VARIABLE FREQUENCY SYSTEM

BY

DAVID CLIVE MOSHAL

MB.BCH

Thesis submitted in partial fulfillment of the requirements

for the degree of Master of Philosophy

in the Department of Biomedical Engineering

University of Cape Town

March 1993

I, David Clive Moshal, hereby declare that the work on which this thesis is based is my original work (except where acknowledgements indicate otherwise) and that neither the whole work nor any part of it has been, is being, or is to be submitted for another degree in this or any other University.

I empower the University to reproduce for the purpose of research either the whole or any portion of the contents in any manner whatsoever.

Signed by candidate

SIGNATURE

1 March 93

DATE

## ACKNOWLEDGEMENTS

I would like to thank the following people for making this work possible:

My supervisor Professor AE Bunn

Professors M Bowie and M Mann of the Institute of Child Health

Dr M Gold and the staff of ward A9 Red Cross War Memorial Childrens Hospital

Peter van den Berg and Victor Moissey of the department of Biomedical Engineering

The Duncan Baxter Foundation, University of Cape Town

Dr Colleen Fenton for help with data collection

## ABSTRACT

Diarrhoeal disease is a major cause of infant mortality in this and other developing countries.The assessment of the degree of dehydration in these children is often based on subjective findings alone. These have been shown to be inaccurate as an assessment of the degree of dehydration.

Whole-body impedance (WBI) is a method of measuring total body water which is used to assess body composition. This WBI technology, which operates at a single frequency, has been applied to the assessment of dehydration in children with diarrhoeal disease.

The normal range of WBI was determined on a group of normally hydrated children and was found to have a mean of 746 Ω , a standard deviation of 85 Ω and 95 % confidence interval for the mean from 720 Ω to 772 Ω. WBI did not depend on age, mass, height or sex. The WBI of a group of children dehydrated from infantile gastroenteritis was measured both before and after rehydration. The dehydrated group had a mean WBI on admission of 1089 Ω and a standard deviation of 149 Ω with a 95 % confidence interval for the mean from 950 Ω to 1109 Ω. This value was significantly greater than that of the normal group. The WBI of the dehydrated group after rehydration was not significantly different from the normal group.

In addition a variable frequency bioimpedance analyser was designed and tested. It was found to have an error of less than 1% over the frequency range 1 to 100 kHz. The device was evaluated on 11 normal and dehydrated children. Four dehydrated children were tested before and after rehydration and this data was compared to a standard electrical model for WBI. It was found that the model could represent the measured data over this frequency range. The extracellular resistive element of the model was mainly responsible for the changes seen during rehydration, suggesting that dehydration in gastroenteritis is mainly due to fluid loss from the ECF compartment.

# TABLE OF CONTENTS

APPENDICES

## LIST OF TABLES

## LIST OF FIGURES

## LIST OF ABBREVIATIONS

| | |
|---|---|
| ASCII | American Standard Code for Information Interchange |
| d.f. | Degrees of Freedom |
| ECF | Extracellular Fluid |
| EEG | Electroencephalogram |
| FFM | Fat Free Mass |
| Hz | Hertz |
| ICF | Intracellular Fluid |
| kHz | Kilohertz |
| LBM | Lean Body Mass |
| mA | Milliamperes |
| pA | Picoamperes |
| RMS | Root Mean Square |
| TBW | Total Body Water |
| μA | Microamperes |
| UNICEF | United Nations Children's Fund |
| WBI | Whole Body Impedance |
| WHO | World Health Organisation |

# CHAPTER 1
# INTRODUCTION AND OBJECTIVES

## 1.1 INTRODUCTION

Diarrhoeal disease is a major cause of infant mortality and morbidity in South Africa and in all developing countries. UNICEF and WHO estimate that one child dies of diarrhoea every 6 seconds [52]. Yach el al (1984)[67], on examining the death register compiled by the South African Central Statistical Services, found that 8984 children under 5 years of age died of diarrhoeal disease in 1984 in South Africa. This represented 27,7% of all registered deaths in that age group. Assuming a case/fatality ratio of 0,6% they estimated that 1,5 million cases of diarrhoeal disease occurred in children under 5 years of age in the RSA in 1984. The Red Cross War Memorial Childrens' Hospital had more than 10 000 admissions for gastroenteritis in 1991[1].

An estimated 60 to 70 % of deaths from diarrhoea are caused by dehydration [32], however a major difficulty arising in the management of diarrhoeal disease is the assessment of the degree of dehydration [47]. The fluid loss in diarrhoeal disease can only be determined accurately if the mass of the child just prior to the onset of the diarrhoea is known [31]. As this value is very seldom known the assessment of the degree of dehydration must be based on clinical signs of dehydration such as loss of skin turgor, sunken fontanelle, sunken eyes and dry mucous membranes [7]. However the clinical assessment of the degree of dehydration in children with diarrhoeal disease requires considerable experience and has been shown to be inaccurate [47]. A non-invasive, accurate and simple bed-side method of quantifying the degree of dehydration in children with diarrhoeal disease would be most useful. Such a system would also be of use in the assessment of the response to rehydration therapy

bed-side method of quantifying the degree of dehydration in children with diarrhoeal disease would be most useful. Such a system would also be of use in the assessment of the response to rehydration therapy particularly in outlying rehydration centers where clinical expertise may be lacking.

Bioelectrical Impedance (henceforth abbreviated to 'bioimpedance') is the impedance of biological tissue to the flow of electricity. A form of bioimpedance analysis, namely whole-body impedance (WBI), is conventionally obtained by passing an alternating electrical current (usually 50 kHz) through the whole body, from the right hand to the right foot and then measuring the voltage drop between these two sites at the wrist and ankle. WBI has been shown to correlate well with total body water (TBW), first by Thomasset in 1962 [65] using the bipolar (two electrode) method and further expanded upon by Hoffer et al in 1969 [33] using the now standard tetrapolar (four electrode) method.

TBW is separated into intracellular fluid (ICF) and extracellular fluid (ECF) compartments by cell membranes. The cell membranes act electrically as capacitors, allowing high frequency currents to pass through the cells while blocking low frequency currents. Thus by passing low frequency ( $< 5$ kHz ) currents through the body one should theoretically be able to measure the impedance of predominately the ECF and by passing high frequency ( $\geq 50$ kHz ) currents one should be measuring both compartments. This accounts for the good correlation between TBW and WBI at 50 kHz as reported in the literature. The possibility of using a variable frequency technique for accurate measurement of body water compartments has far reaching applications in both paediatric hydrational disorders and clinical medicine in general.

It is further postulated that bioimpedance analysis could be a useful method for quantifying dehydration in children with diarrhoeal disease. The method is non-invasive, safe and is simple to perform. Such a method would be most useful in outlying rehydration centers to monitor the response to rehydration therapy as well as to assess when to refer children to tertiary institutions for more advanced therapy.

## 1.2 OBJECTIVES OF THESIS

1. To review the literature on whole-body impedance (WBI) with regard to the underlying physical and physiological principles as well as to discuss clinical studies and applications of WBI technology with an emphasis on body water determinations.

2. To apply the WBI technique of measuring total body water (TBW) to the assessment of dehydration and rehydration in children with diarrhoeal disease using existing single frequency equipment operating at 50 kHz. The specific objectives of this part of the thesis are given in chapter 3.2.

3. To develop and test a variable frequency bioimpedance analyser able to measure WBI (and skin impedance) over a wide range of frequencies. This system will be tested on subjects and the data compared to a standard electrical equivalent model of WBI. This will be done in order to determine the accuracy of the model with regard to extracting useful intra- and extracellular body water parameters. The feasibility of this approach will be discussed in the light of the findings of this and related studies in the literature.

# CHAPTER 2
# WHOLE-BODY IMPEDANCE ANALYSIS: THEORY AND LITERATURE REVIEW

## 2.1 INTRODUCTION

This review presents the underlying physics and physiology relating to bioimpedance measurement. The measurement of WBI, and clinical applications are discussed. The electrical model of body fluid distribution is presented with regard to the assessment of body fluid compartments.

## 2.2 THEORETICAL AND PHYSIOLOGICAL CONSIDERATIONS

### 2.2.1 Ohms Law and the Resistance of a Conductor

All substances offer resistance to the flow of electrical current. Ohm's law states that the voltage drop across a conductor (V) is equal to the amount of current flowing through it (I) multiplied by its resistance (R), that is:

$$V = I \cdot R \qquad (2.1)$$

The resistance of an electrical conductor is dependent on its physical dimensions, its configuration and its specific electrical resistivity. The resistance (R) of a cylindrical electrical conductor of length (L) in centimeters, cross sectional area (A) in square centimeters and resistivity (rho) in ohm.centimeters is given by the following formula:

$$R = \rho \frac{L}{A} \qquad (2.2)$$

Thus the resistance of a conductor is proportional to the length of the conductor and inversely proportional to its cross sectional area. Resistivity (ρ) expresses the difficulty an electron has in moving through the material due to collisions it experiences with the atoms. Resistivity varies for different materials. A good conductor such as silver has a low resistivity ($\approx 10^{-6}$ Ω.cm) and a poor conductor, or insulator, such as glass has a high resistivity ($\approx 10^{14}$ Ω.cm). The resistivity of biological tissues and fluids depends on their ionic concentration. This varies from 63 Ω.cm for plasma, a good biological conductor, to 2500 Ω.cm for fat, a poor conductor [25].

### 2.2.2 Impedance, resistance and reactance

For an alternating current the voltage drop across the conductor divided by the current flowing through it yields impedance. Impedance is composed of resistance and a frequency dependent component called reactance which is due to the capacitive and/or inductive elements in the conductor. In alternating current theory impedance (Z) is expressed as a complex number with the real and imaginary components representing resistance (R) and reactance (X) respectively (equation 2.3).

$$Z = R + jX \qquad (2.3)$$

where:

$$j = \sqrt{-1} \qquad (2.4)$$

The magnitude of the impedance is equal to the square root of the sum of the squares of resistance and reactance.

$$|Z| = \sqrt{R^2 + X^2} \qquad (2.5)$$

The human body has no significant inductive elements and its reactance is predominantly capacitive, due to the bilipid layer of the cell membranes which behaves as the dielectric of a capacitor. This allows only high frequency currents to pass through the cells. Most measurements of WBI are performed at 50 kHz. At this frequency the reactance of the cell membranes is minimal, allowing electrical currents to pass through the cells. Some bioimpedance measuring equipment measure only impedance while others measure impedance, resistance and reactance. In practice whole body impedance is less than 0.5% greater than whole body resistance at 50 kHz [24]. This implies that the reactive elements of the body are of far less magnitude than the resistive elements at this frequency and can be effectively neglected.

### 2.2.3 Volume from impedance

The volume (V) of an electrical conductor can be calculated from the product of the resistivity (ρ) of the conductor and its length (L) squared divided by its impedance (Z) (see appendix A for derivation). That is:

$$V = \rho \frac{L^2}{Z} \qquad (2.6)$$

It follows from equation 2.6 that the change in volume (ΔV) of a conductor can be determined from the change in its impedance (ΔZ). If the length of a cylindrical conductor is constant and its volume is increased by an increase in its cross sectional area then the change in its volume can be calculated from the change in its impedance by the following equation [55]:

$$\Delta V = \rho L^2 \left(\frac{\Delta Z}{Z_1 . Z_2}\right) \qquad (2.7)$$

Where $\Delta Z = Z_2 - Z_1$ and $Z_1$ and $Z_2$ are the initial and final impedances respectively. (see appendix B for the derivation)

### 2.2.4 Resistivity of Body Fluids

Body fluids consist of electrolytes in solution and are thus able to conduct electricity. Resistivity ($\rho$) is considered inversely proportional to the number of free electrolytic ions ($N_i$). That is:

$$\rho = k\frac{V}{N_i} \qquad (2.8)$$

Where k is the constant of proportionality and V is the volume of the solution. The inverse of resistivity is called conductivity, which is therefore directly proportional to the electrolyte concentration. This equation has been shown to be accurate in both *in vivo* and *in vitro* experiments[21].

### 2.2.5 Distribution of body water

Total body water (TBW) is distributed into two main compartments namely the intracellular fluid (ICF) and extracellular fluid (ECF) compartments. The ECF is further divided into interstitial fluid and plasma.

At birth TBW constitutes about 80% of body mass but drops to the adult level of 60% by 1 year of age. The ECF is larger than the ICF in the foetus but this ratio falls to the adult level by 9 months of postnatal life[57]. The relative percentage of each compartment for an average adult is given in the table 2.1.

**TABLE 2.1 Distribution of total body water**

| Compartment | Percent of TBW |
|---|---|
| Extracellular fluid: | 33% |
| - Plasma | - 8% |
| - Interstitial fluid | - 25% |
| Intracellular fluid | 67% |

The volume of the body fluid compartments is currently measured indirectly using the indicator dilution principle. A known amount of an indicator substance is introduced into one of the compartments. Once the indicator has distributed evenly throughout the compartment its concentration is measured. As the amount of indicator introduced is known, the volume of the compartment can be calculated from its final concentration.

The method of choice for the measurement of TBW is $^{3}H_2O$, an unstable isotope of water [58]. The ECF volume is measured by saccharides such as inulin, sucrose, raffinose and mannitol, ions such as thiosulfate, thiocyanate and the radionucleotides of sulphate, chloride, bromide and sodium [8]. Plasma volume can be measured by using substances that are confined to the vascular system and do not enter red cells, such as Evans blue dye (T-1824), radioiodinated human serum albumin (RISA) and radioiodinated gamma globulin and fibrinogen. Plasma volume can also be measured by tagging red cells with radioisotopes of phosphorous, iron or chromium.

No substance is distributed only in the ICF so this compartment is measured by subtracting the ECF from the TBW [8, 62]. Likewise no substance is distributed only in the interstitial fluid so this compartment must be determined by subtracting the plasma volume from the ECF.

### 2.2.6 Impedance of living tissue: An electrical model

Tissues contain numerous cells bonded together. The cell cytoplasm contains electro-

lytes in solution and acts electrically as a conductor, the conductivity being proportional to the electrolyte concentration, as discussed above. The cell membrane contains a lipid bilayer which acts electrically as the dielectric of a capacitor. At low frequencies its reactance is high, preventing current from flowing through the cell while at high frequencies its reactance is low, allowing current to flow through the cell. Therefore direct current or low frequency alternating current will not travel through the intracellular fluid (ICF), due to the high impedance of the cell membranes, but will pass through the extracellular fluid (ECF) only. High frequency current will pass through both the extracellular and intracellular fluids, due to the low impedance of the cell membranes at high frequencies.

Living tissue has been modelled by a standard electrical circuit (see figure 2.1) consisting of a capacitor and two resistors [62]. The ECF is modelled as the resistor ($R_e$), representing the resistance to current through the plasma and the interstitial fluid. There are no reactive elements in this compartment. The ICF is modelled electrically as the resistor ($R_i$) in series with the capacitor (C). The resistor represents the resistance to current through the cytoplasm of the cells. The capacitor represents the reactance of the cell membranes. These two fluid compartments are connected in parallel.

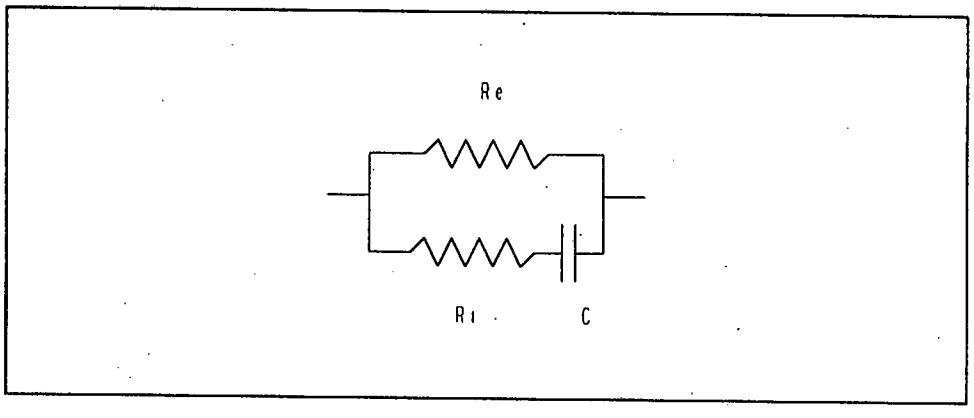


**FIGURE 2.1 Electrical Model of Biological Tissue**

Using this model the impedance of the human body can then be expressed in complex form as follows (see appendix C for derivation) :

$$Z = \frac{R_i \cdot R_e \cdot (R_i + R_e) + \frac{R_e}{(\omega C)^2}}{(R_i + R_e)^2 + \frac{1}{(\omega C)^2}} - j \cdot \frac{R_e^2}{\omega C \cdot (R_i + R_e)^2 + \frac{1}{\omega C}} \qquad (2.9)$$

$$(Where \ \omega = 2 \cdot \pi \cdot f)$$

Reactance (the imaginary part of the above equation) has been shown to contribute negligibly to WBI at 50 kHz [24], so the WBI (at 50 kHz) can be modelled by the real part of the equation as:

$$Z = \frac{R_i \cdot R_e \cdot (R_i + R_e) + \frac{R_e}{(\omega C)^2}}{(R_i + R_e)^2 + \frac{1}{(\omega C)^2}} \qquad (2.10)$$

## 2.3 MEASUREMENT OF WHOLE-BODY IMPEDANCE

Bioimpedance has been used since the 1940's to measure many different biological parameters. Nyboer (1959) [53] pioneered the use of bioimpedance in the study of dynamic changes in the volume of many organs including arterial pulse waveforms, lung volumes and cardiac output.

Whole body impedance is a bioimpedance measurement conventionally measured by passing a current through the whole-body from the right hand to the right foot and by measuring the impedance to that current. There are many techniques for measuring WBI. Thomasset (1962) [65] was the first to show that WBI correlates well with total body water (TBW). In these early experiments the bipolar method, in which the tissue under investigation is placed between two electrodes, was used. An alternating current, of constant peak amplitude and of fixed frequency, is passed between these electrodes and the voltage drop across them measured. From Ohms law (equation 2.1) the impedance of a conductor is equal to the voltage drop across the conductor divided by the current passing through it. As the current has a constant known amplitude, the voltage drop is then directly proportional to the impedance.

The impedance established in this way originates in part from impedances produced at the junction of the electrode and the tissue being examined. In WBI measurements it is important not to include skin impedance in the measurement. The skin has a very high impedance, particularly at low frequencies and can be modelled by the same electrical circuit [25] shown in figure 2.1. The early measurements of WBI by Thomasset in 1962 [65] employed the bipolar technique using needles inserted subcutaneously in order to overcome skin impedance (see figure 2.2). This measurement is invasive and uncomfortable for the patient. In addition it is known that the electric field produced by needle electrodes is far from homogeneous in the vicinity of the electrodes, which gives an additional error in the resulting impedance[20].

For these reasons the tetrapolar method, first described by Hoffer el al (1969) [33] is now the preferred method of measuring whole-body impedance. In this technique four

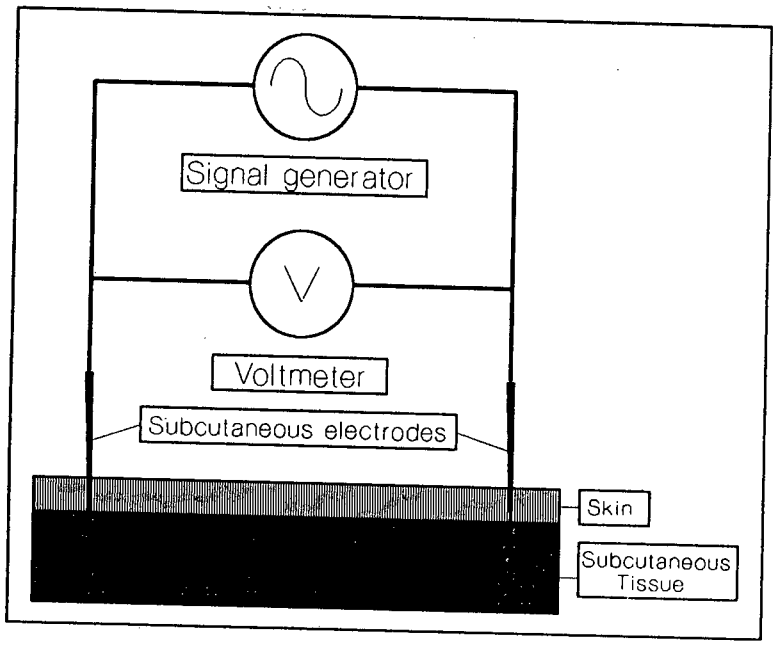


**FIGURE 2.2 Bipolar measurement of the impedance of biological tissue**

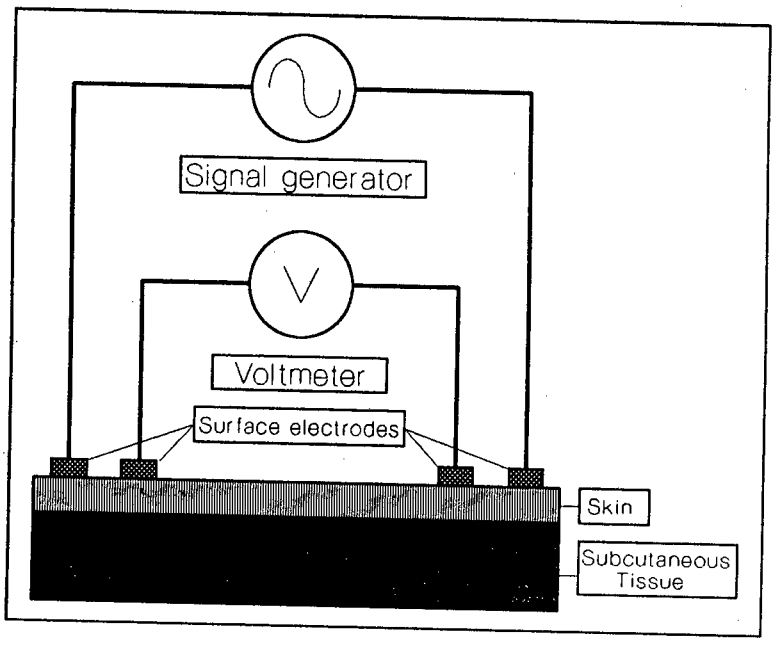


**FIGURE 2.3 Tetrapolar measurement of the impedance of biological tissue**

surface electrodes are placed on the skin using conductive gel (see figure 2.3). Two electrodes are used for injecting the constant current. By convention one of these electrodes is placed proximal to the second metacarpophalangeal joint of the right wrist and the other is placed proximal to the second metatarsophalangeal joint of the right foot. The second pair of electrodes are placed between this current path and are used to measure the voltage drop. One electrode is placed between the radial and ulnar styloid processes on the dorsal surface of the right wrist and the other is placed on the dorsal surface of the right ankle between the lateral and medial malleoli.

The voltage sensing equipment has a very high impedance ($\approx 10^{10}\Omega$), many orders of magnitude greater than the skin impedance, so only a negligible amount of current flows through the skin. Hence the voltage drop from the electrodes to the subcutaneous tissue, through the skin, is negligible compared with the voltage drop across the body (see appendix D for a more detailed explanation). Thus the tetrapolar method is able to overcome the problem of skin impedance. The distance between proximal and distal electrodes must be more than 4 cm [33,34] for a homogeneous current distribution to be obtained.

## 2.4 CLINICAL APPLICATIONS OF WHOLE-BODY IMPEDANCE MEASUREMENTS

### 2.4.1 Body composition

The major clinical application of whole-body impedance measurement to date has been in the assessment of body composition. Body fat is a poor conductor of electricity [43] and nearly all the current in WBI measurements is conducted by the fat-free mass (FFM) or lean body mass (LBM). Numerous studies have shown WBI to be an accurate and reproducible method of assessing body composition[4, 9, 10, 12, 18, 24, 33, 34, 38, 40, 44, 45, 56, 59, 60, 67]

Densitometry or 'underwater weighing' is the technique which employs Archimedes principle to determine body density and thereby derives FFM from assumptions based on the densities of fat and lean mass. Lukaski et al (1985) [44] and Segal et al (1985) [59] were the first to show that height squared / WBI and FFM (determined densitometrically) are highly correlated.

Segal et al (1988) [60] in a four-site cross-validation study involving 1567 adults found the correlation between height squared / WBI and FFM determined by densitometry to be very good, with r = 0.91. This has been further validated by numerous studies [4, 24, 38, 45]. The bipolar method of measuring WBI is also able to predict FFM [6] though is less accurate than the tetrapolar method and is less tolerated, as discussed above.

WBI has many advantages over other methods of determining body composition. Laboratory methods such as densitometry, computed tomography, total body electrical conductivity, isotope dilution, whole-body counting of potassium-40 and neutron activation analysis for total body calcium and $N_2$ are expensive and not suited for field studies. Other techniques developed for epidemiological surveys, such as anthropometry, skinfold thickness and infrared interactance have been shown to be less reliable indicators of body composition [45].

### 2.4.2 Total body water

Impedance measurements had been applied to the measurement of many biological parameters, such as arterial waveforms and pulsatile flow in many organs [54], before a relationship between total body water (TBW) and electrical impedance was first reported by Thomasset (1962) [65] using the bipolar technique. This was further improved upon by Hoffer et al (1969) [33] using the tetrapolar technique.

In the initial studies Hoffer et al [33, 34] showed that the regression of TBW, measured by tritiated water, on height squared / WBI, measured between electrodes on the hand and foot, in 20 subjects with normal hydrational status was 0.92. In 34 patients with abnormal hydrational status, due to either renal failure or congestive heart failure, the regression coefficient was 0.93. This has been validated by other studies comparing TBW, measured either by tritiated water [36] or deuterium [40], with whole-body impedance in people with normal and abnormal fluid status.

Height squared / WBI and TBW, determined by isotope dilution, have been found to be highly correlated in all age groups. In preterm infants Mayfield et al (1991) [49] found a regression coefficient of 0.90 for the above correlation. Davies et al (1988)[17] found a correlation of 0.97 in children and adolescents and this has been confirmed in the same age group by others [23, 28, 48]. In elderly subjects a regression coefficient of 0.98 has been found[17].

### 2.4.3 Extracellular water

At low frequencies (≈1 kHz) the reactance of cell membranes is high, so electrical current does not flow through the ICF. Thus WBI at 1 kHz has been used as a measure of ECF. A good correlation has been found between height squared / WBI and ECF, measured by a radioactive bromide isotope [36] and a radioactive sulphate isotope [61, 62].

### 2.4.4 Haemodialysis and transcellular fluid shifts

Hypotension is a frequent complication seen in haemodialysis [20]. The decrease in intravascular volume caused by ultrafiltration plays an important role in its pathogenesis. A transcellular fluid shift from the extracellular to the intracellular compartment may aggravate this depletion. Continuous recording of whole-body impedance at high and low frequencies during dialysis has been studied with a view to developing an on-line blood volume indicator [19, 20, 21, 27, 50, 64]. A good correlation between whole-body impedance and changes in blood volume during haemodialysis has been shown [20, 50]. Changes in the ratio of whole-body impedance at high frequencies to whole-body impedance at low frequencies has also been used to predict the change in blood volume during dialysis with good results [19].

## 2.5 SAFETY CONSIDERATIONS

Any procedure that passes electrical current through the body must be examined for possible hazards to the subject. The biological effect of electrical current depends on its frequency and strength. Alternating currents at mains power-line frequency (50 Hz) stimulate muscle and nerve cells with a threshold for sensation of a few milliamperes. Much higher currents elicit pain and involuntary muscle contractions. The threshold for perception of current increases with increasing frequency. For example, the perception of current using hand-held electrodes increases from 100 μA at 10 Hz to 2 mA at 1 kHz, to over 10 mA at 10 kHz [25, 62].

The usual mechanism for lethal shock is ventricular fibrillation although, at much higher and sustained current levels, respiratory paralysis and burns can result from 50 Hz currents [62], the power-line frequency in this country. At this frequency, a current of less than 100 μA passed directly into myocardial fibers can induce fibrillation [25]. When the frequency is raised to 200 Hz the threshold for fibrillation increases to over 1 mA and is much higher at frequencies above 1 kHz. Much larger currents are required to produce cardiac fibrillation when applied through external electrodes because only a small fraction of the total current passes through the heart. Cardiac fibrillation thresh-

olds in the dog, using external electrodes at 1 kHz are about 1 Ampere [25]. Thus the low current levels used in bioimpedance studies (≈ 300 μA) at the frequencies used (above 1 kHz) present no hazard to the patient, provided that the patient does not have a cardiac pacemaker or any other conductive leads in contact with the myocardium and that the instrumentation is well isolated from the 50 Hz mains supply.

# CHAPTER 3
# WHOLE-BODY IMPEDANCE IN THE ASSESSMENT OF DEHYDRATION IN CHILDREN WITH DIARRHOEAL DISEASE

## 3.1 INTRODUCTION: ACUTE INFECTIVE DIARRHOEA IN CHILDREN

Diarrhoea is an imprecise symptom manifested by the "too frequent passage of a too liquid stool" [2]. It can be defined numerically as faecal water loss exceeding 200 ml/m$^2$ body surface/day [15]. In developing countries it is the major cause of mortality and morbidity and is related more to socio-economic conditions than climate, to poverty more than place [14, 35].

### 3.1.1 Pathophysiology

Diarrhoea is the result of a disturbance of the normal physiology of the gastro-intestinal tract, usually involving the small bowel and sometimes the colon. Large volumes of fluid enter the proximal bowel through diet and endogenous secretions of the upper digestive tract. Water and electrolytes are secreted and reabsorbed into and out of the intestinal lumen with an overall net inward movement of water and electrolytes. Electrolytes are transported actively across the lumen and the osmotic gradient thus created is responsible for the passive transport of water. Diarrhoea occurs when the normal balance between absorption and secretion is disrupted. Diarrhoea is often divided into two broad groups, secretory and osmotic.

In secretory diarrhoea the balance between secretion and absorption is disrupted such that there is a net flux of water and electrolytes into the intestinal lumen. This may be due to damage to the enterocyte by the pathogen itself or a toxin released by the

pathogen. In osmotic diarrhoea the increased fluid flux is due to osmotically active particles in the intestinal lumen, such as lactose.

### 3.1.2 Body Fluid Compartments and Dehydration in Acute Diarrhoea in Children

The loss of fluid in children with acute diarrhoea is from the ECF with little or no change in the ICF [16, 37, 39]. This loss affects both the interstitial fluid and the intravascular fluid compartments of the ECF. Rapidly occuring dehydration may lead to shock from a precipitous fall in the circulating intravascular volume. Sodium is the major extracellular cation and is largely responsible for the osmotic pressure of this compartment. In cases of hypernatraemic dehydration (serum sodium ≥150 mmol/l) the osmolality of the ECF becomes greater than that of the ICF so there is a shift of fluid from the ICF to the ECF. Thus in cases of hypernatreamic dehydration the fluid loss is from both the ECF and the ICF [22]. This relative sparing of the ECF may mask the signs of dehydration in these children. A recent study of 3889 children with diarrhoea admitted to the drip room of the Red Cross Hospital over a twelve month period found that 3.8% were hypernatraemic [30]. In these children the degree of dehydration is often underestimated [31]. These children have a higher incidence of coma and convulsions than the normonatreamic dehydrated children. The mortality rate is higher in hypernatraemic dehydration [31].

### 3.1.3 Aetiology

An enteropathogen may be identified in about 50% to 70% of faecal specimens of cases of infantile gastroenteritis [11]. The aetilogical agent responsible may be bacterial, (such as *Esherichia coli*, *Campylobacter jejuni*, *Salmonella* or *Shigella*) viral (mostly rotavirus) or parasitic (such as *Giardia Lamblia*). In both developing and developed countries viruses are the major aetiological agent. In developing countries bacterial pathogens play a relatively larger aetiological role.

### 3.1.4 Clinical Features and Assessment of the degree of Dehydration

The clinical features of infantile gastroenteritis include diarrhoea and vomiting, signs of dehydration, signs of shock, signs of acidosis and signs of parenteral disease such as otitis media, respiratory or urinary tract infection. The signs of dehydration only appear after there has been significant water loss. These are: dry mucous membranes, decreased skin turgor, sunken eyes and fontanelle, decreased perfusion, acidotic breathing, oliguria, lethargy and absent tears [7,47]. The child is regarded as 5% dehydrated if these signs are present and 10% dehydrated if these signs are marked [15]. This assessment can be extremely subjective and has been shown to be unreliable.

Mackenzie et al [47], in a study of 102 children requiring admission for gastroenteritis, has shown that the degree of dehydration did not correlate with the presence of sunken eyes, dry mouth, sunken fontanelle or oliguria or the absence of tears .They found that dehydration was overestimated by a mean of 3.2% and that many of the children admitted because they were thought to be more than 5% dehydrated were found to be less than 4% dehydrated.

There is at present no simple, quantitative bed-side test able to display the level of dehydration. The degree of dehydration can only be determined accurately if the mass immediately prior to the onset of the gastroenteritis is known. This former value is very seldom available.

There are many problems with the use of tracer dilution techniques in the measurement of body fluid compartments in children with diarrhoeal disease. These measurements are expensive and time consuming [62]. They require several hours for equilibration of the tracer before blood or urine samples are collected and analyzed for the tracer substance. Many require repeated blood or urine collections over several hours. Some of these tracer techniques expose the subject to radioactivity and most require expensive equipment to measure concentrations of the tracer substance.

Furthermore in children with diarrhoeal disease the volume of the fluid compartment being measured is constantly changing due to fluid losses from the GIT and due to fluid replacement either orally or parenterally. The fluid compartment volume is therefore not constant throughout the measuring period, which may be many hours. In addition collection of blood and urine samples from small children is difficult and seldom well tolerated.

### 3.1.5 Management

In most cases the diarrhoeal disease is self-limiting and lasts only a few days. The prevention and correction of fluid and electrolyte losses remains the mainstay of treatment. Shock, if present, is treated with a plasma volume expander (Haemaccel). A volume of 20 milligrams per kilogram body weight is infused rapidly and the response assessed. A further bolus of half that volume is infused rapidly if the capillary perfusion remained poor.

The fluid deficit is calculated as 50 ml/kg for children assessed as 5% dehydrated and 100 ml/kg for children assessed as 10% dehydrated. Maintenance fluids requirements are calculated as 120 ml/kg for children younger than one year and 100 ml/kg for children from one to two years of age. The fluid deficit and maintenance requirements are combined and given over 24 hours [31].

Half-strength Darrow's solution in 5% dextrose water is used. Severe metabolic acidosis (pH < 7.25) is corrected with 8% sodium bicarbonate. The amount calculated to correct half the base deficit is given intravenously over 5 minutes.

At the Red Cross War Memorial Childrens Hospital the fluid is given by naso-gastric tube unless the child is vomiting or severely dehydrated. Antibiotics are only used if the child is very malnourished, very young (<1 month), has an identified pathogen known to responsive to specific therapy (such as *Shigella*, amoebae or *Giardia*) or has an intercurrent bacterial infection, in which case an appropriate agent is given. Anti-diarrhoeal agents are not used as these slow intestinal transit time which may encourage bacterial overgrowth.

## 3.2 OBJECTIVES OF STUDY

The object of this study was to apply the WBI technique of measuring TBW to the assessment of dehydration in children with diarrhoeal disease using existing single frequency equipment operating at 50 kHz (throughout this chapter WBI is the whole-body impedance at 50 kHz only). It is postulated that whole-body impedance could offer an objective method of assessing the degree of dehydration in children with diarrhoeal disease.

The specific objectives were:

1. To derive normal values of WBI for infants and to evaluate the effect of the interfering variables of age, height, sex and mass on whole-body impedance at 50 kHz in this population.

2. To determine if there is a significant difference between the WBI of dehydrated children and normally hydrated children and to see how the WBI after rehydration compares with that of the normal group.

3. To determine whether correcting for changes in electrolyte concentrations can improve the accuracy of WBI as a measure of degree of dehydration.

4. To examine the correlation of height squared / WBI on mass in normal and dehydrated children.

5. To examine the correlation of measured change in body mass of dehydrated children before and after rehydration on the change in body mass calculated from the change in WBI.

## 3.3 METHODS OF STUDY

### 3.3.1 Clinical Material

The investigation was undertaken on 43 children with normal fluid status and 16 infants with acute dehydrating diarrhoeal disease. The normals were children seen at the medical outpatient department of the Red Cross War Memorial Children's Hospital, Cape Town. They were children who had minor medical complaints or who were being followed up for previous illness. None had gastrointestinal or respiratory signs or symptoms. The dehydrated children were all patients requiring admission to the Drip room, ward A9, of the same hospital.

### 3.3.2 Selection Criteria for the Dehydrated Children

The following general selection criteria were applied:

1. A history of recent onset of diarrhoea with or without vomiting.
2. Clinical evidence of dehydration requiring admission to hospital for rehydration with intravenous fluids.
3. The absence of associated systemic infections such as pneumonia.
4. Absence of clinical or biochemical evidence of kwashiorkor or protein losing enteropathy.
5. Body mass more than 60% of expected for age, so that marasmic children were excluded.

### 3.3.3 Study design

WBI, mass, electrolyte status and acid-base status were measured on each child initially and then every 8 hours on each child during rehydration. Age, sex and height were also recorded for each child with the initial measurement. Clinical assessment of dehydration was recorded at each reading. The treatment regime used by the staff of ward A9 has been described previously (see 3.1.5) and this was in no way altered.

Informed parental consent was obtained in order to perform the WBI measurements on each child. Percentage dehydration was calculated from the initial and final weights (Wi and Wf) using the formula: 100 (Wf - Wi) / Wf.

### 3.3.4 Measurement of whole-body impedance

Determination of WBI was made using a four terminal bioimpedance analyser (Bodystat 500) which generates a current of 300 μA RMS. It is powered by two 9V batteries and is unable to produce an unsafe current or voltage output. The tetrapolar method was used to overcome skin impedance (see appendix D) . EEG contact electrodes were used with Elefix EEG Paste (Nihon Kohden, Japan) which has adhesive properties. The distal electrode pair (current inducing electrodes) were positioned with one electrode in the middle of the dorsal surface of the right hand just proximal to the metacarpophalangeal joint and the other electrode in the middle of the dorsal surface of the right foot just proximal to the metatarsophalangeal joint. The proximal pair of electrodes (the voltage sensing electrodes) were positioned with one electrode on the dorsal surface of the right wrist between the distal prominences of the radius and the ulna and the other electrode on the dorsal surface of the right foot between the medial and lateral malleoli. Care was taken to ensure that the children were held motionless in the prone position with their arms and legs held away from the trunk. Insulating gloves were used to ensure that the current did not flow through the assistant resulting in a false WBI reading. All readings were taken by the same operator. These guidelines are summarized in appendix E.

Testing of the Bodystat 500 showed that it could deliver a constant current of 300 μA at 50 kHz into a load impedance $\leq$ 5 kΩ at $\leq$ 1 % error. The testing procedure to determine the maximum impedance that the Bodystat 500 could accurately determine WBI is given in appendix I.

### 3.3.5 Data Analysis

#### (a) Normally Hydrated Subjects

The mean, standard deviation and range for WBI, age, mass and height of the normally hydrated group were obtained. Linear regression analysis was used to determine the correlation of WBI on height, age and mass. A p-value of 0.05 or less was regarded as significant and a p-value of 0.01 or less was regarded as very significant. The WBI of the male and female subjects were compared using the *t*-test and the same p-values were used to assess significance. The WBI of the children older and younger than 3 months were compared as the percentage TBW of body mass and the ratio of ECF to ICF are known to change from foetal levels to adult levels during the first year of life, as discussed earlier (see section 2.2.5).

At birth TBW constitutes about 80% of body mass but drops to the adult level of 60% by 1 year of age. The ECF is larger than the ICF in the foetus but this ratio falls to the adult level by 9 months of postnatal life [57]. The relative percentage of each compartment for an average adult is given in the table 2.1.

#### (b) Dehydrated Subjects

The mean, standard deviation and range for WBI, age, mass and height of the dehydrated subjects were obtained before and after rehydration. The 95 % confidence intervals for the population mean were obtained for the WBI before and after rehydration and compared with those of the normally hydrated children using the *t*-test.

#### (c) Height squared / WBI and Mass

Height squared / WBI is known to correlated well with TBW and this has been used in the assessment of FFM and body composition. Linear regression analysis was used to examine the correlation between height squared / WBI and mass in the normal children and in the dehydrated children before and after rehydration.

**(d) Correction for electrolyte abnormalities**

Electrical current is conducted through body fluids due to the electrolyte content of biological tissue. As discussed (section 2.2.4) the resistivity of the body fluids is inversely proportional to the electrolyte concentration. In children the normal serum sodium concentration is from 136 - 143 mmol/l and the normal serum potassium concentration is from 3.8 - 5.0 mmol/l [5]. The WBI was corrected for serum sodium by multiplying by the sodium concentration and dividing by the mid-point between the upper and lower limits of the above normal values (139.5 mmol/l). Similarly WBI was corrected for serum potassium concentration by multiplying by the potassium concentration and dividing by the mid-point between the upper and lower limits of the above normal values (4.4 mmol/l). The correlation between height squared divided by the WBI corrected for sodium concentration on mass was examined. The same was performed for height squared divided by the WBI corrected for potassium concentration.

**(e) Ethical approval**

Approval was obtained from the Ethics Committee of the faculty of Medicine, University of Cape Town.

## 3.4 RESULTS

### 3.4.1 Whole-body impedance in the normally hydrated children

Forty-three normally hydrated children were measured. Twenty were female and twenty-three male. The range, mean and standard deviation for whole-body impedance, age, mass and height are given in table 3.1 below. The results for the individual normal children are given in appendix F.

**TABLE 3.1 Whole-body impedance, age, mass and height of 43 normally hydrated children**

| Variable | WBI ( in Ω ) | Age ( in months ) | Mass ( in kg ) | Height ( in cm ) |
|---|---|---|---|---|
| Mean | 746 | 8.8 | 8.24 | 69.1 |
| Standard deviation | 85 | 5.6 | 2.37 | 9.11 |
| Minimum | 575 | 1.1 | 3.86 | 54.0 |
| Maximum | 903 | 23.1 | 14.50 | 87.6 |

**(a) Correlation between mass and height squared / WBI in the normally hydrated children**

Figure 3.1 shows the scatter plot of mass on height squared / WBI for the normal group. Linear regression analysis shows a significant correlation ( correlation coefficient = 0.93, Intercept = 0.25, Slope = 0.77).

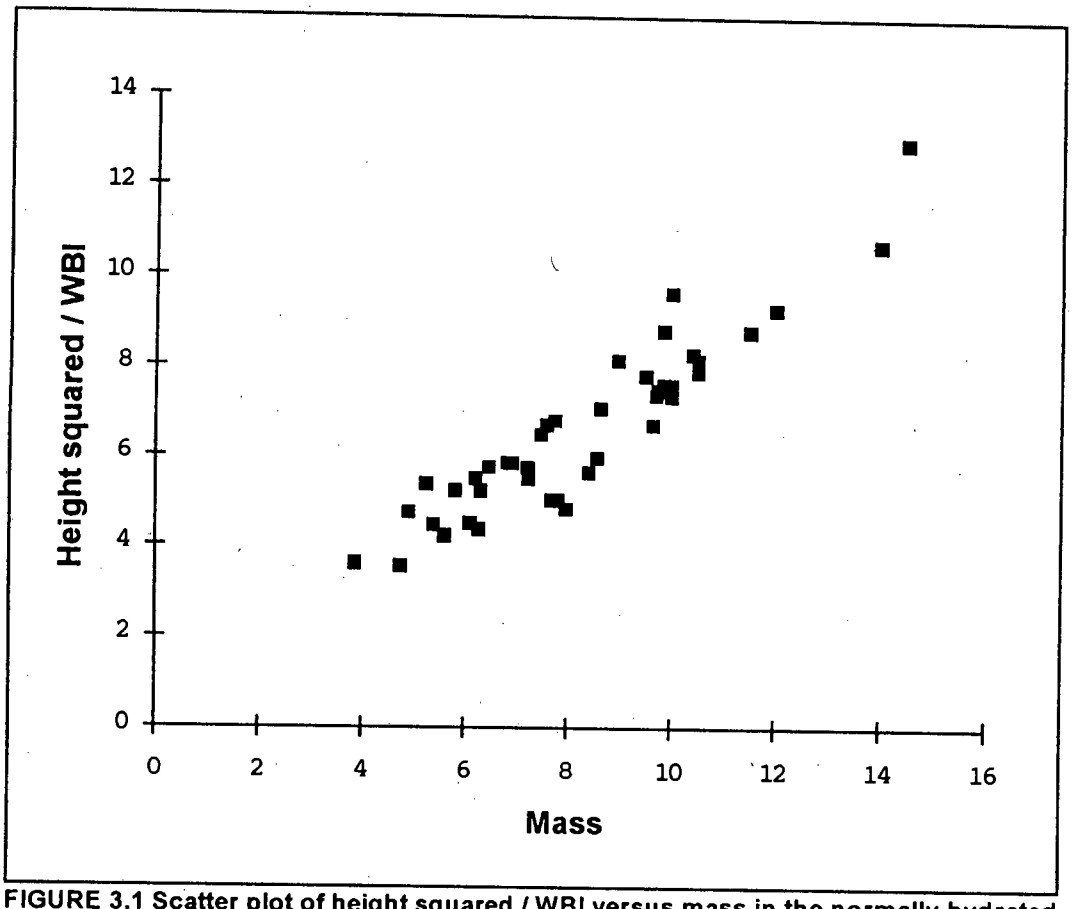


**FIGURE 3.1 Scatter plot of height squared / WBI versus mass in the normally hydrated children**

## (b) Whole-body impedance and sex

The statistics for the WBI of the normally hydrated children by sex are given in table 3.2 and compared in figure 3.2. The difference between the WBI of normally hydrated male and female children was not significant at the $p \leq 0.05$ level ( p value = 0.20, t value = 1.33 at 41 d.f.) .

TABLE 3.2 Whole-body impedance of normally hydrated children by sex

| Variable | All normals | Males | Females |
|---|---|---|---|
| Sample size | 43 | 23 | 20 |
| Mean WBI (Ω) | 746 | 730 | 764 |
| Standard deviation (Ω) | 85 | 84 | 85 |

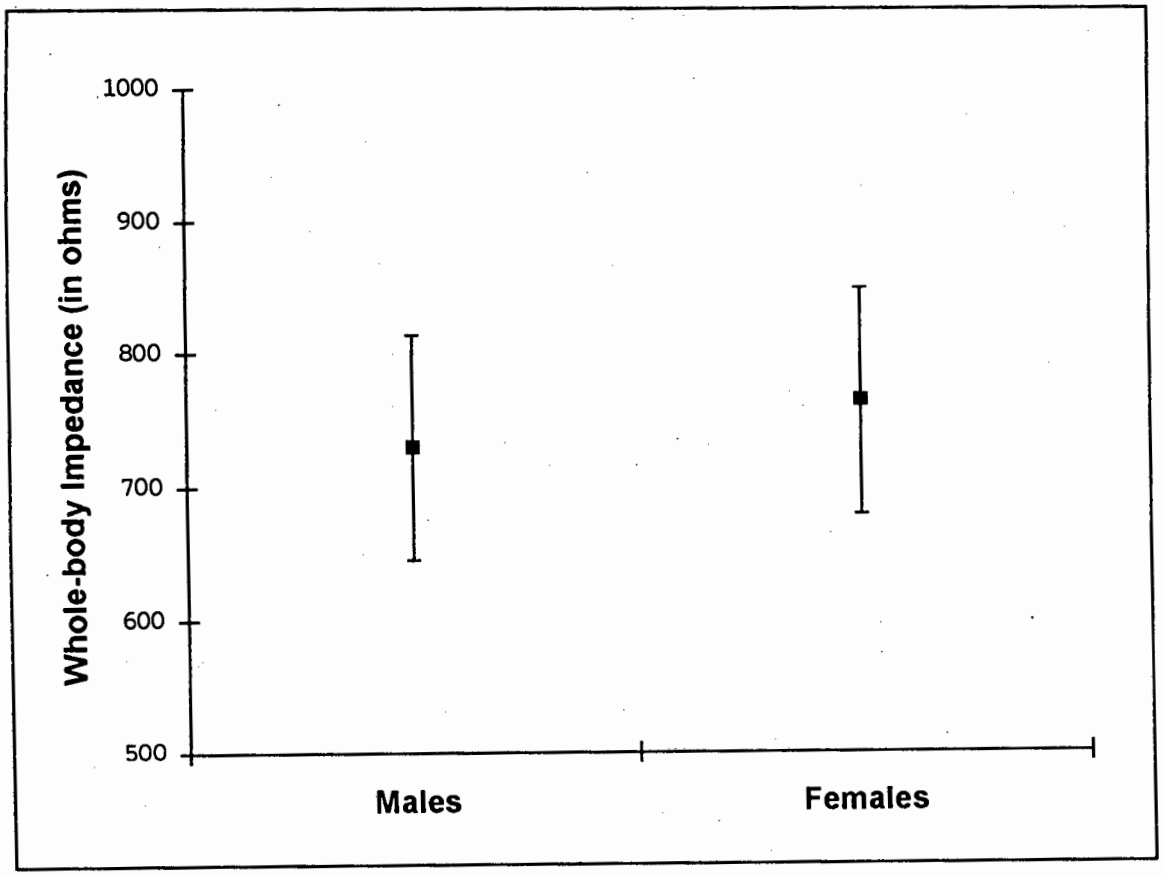


FIGURE 3.2 Mean and standard deviation of Whole-Body Impedance by Sex

## (c) Whole-body impedance and age

A scatter plot of WBI on age is given in figure 3.3. Linear regression analysis shows no significant correlation between age and WBI ( correlation coefficient = 0,03 R-squared = 0.09 %, SEE = 86.3). The difference between the WBI of children younger and older than 3 months was not significant at the $p \leq 0.05$ % level ( p value = 0.87, t value = 0.16, d.f. = 41). The statistics of these two groups are given in table 3.3 and compared in figure 3.4.

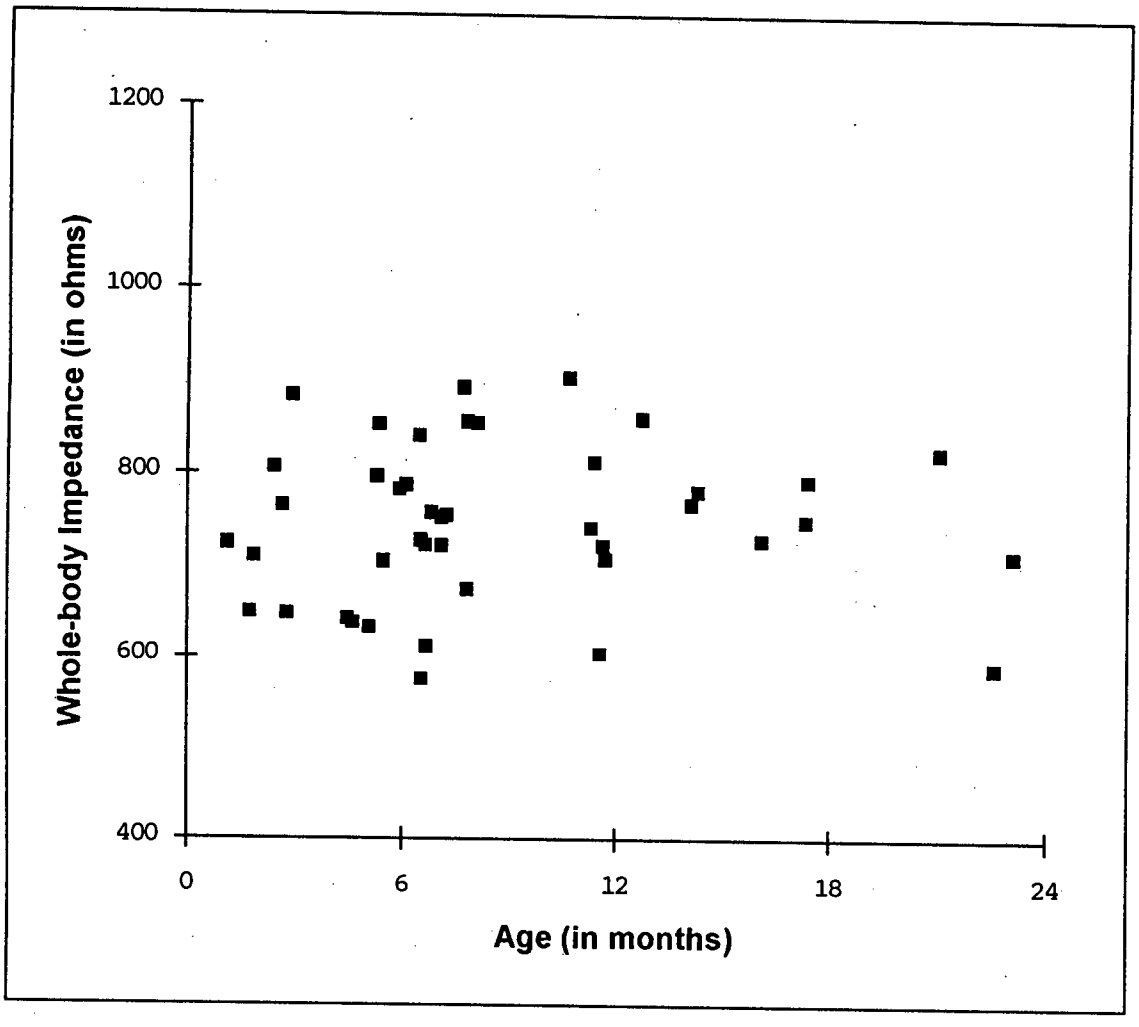


**FIGURE 3.3 Plot of Whole-body Impedance (in Ω) versus age (in months) for the normal group**

TABLE 3.3 Whole-body impedance of the normal children above and below 3 months

| Variable | All normals | Age ≤ 3 months | Age > 3 months |
|---|---|---|---|
| Sample size | 43 | 7 | 36 |
| Mean WBI (Ω) | 746 | 741 | 747 |
| Standard Deviation (Ω) | 85 | 85 | 86 |

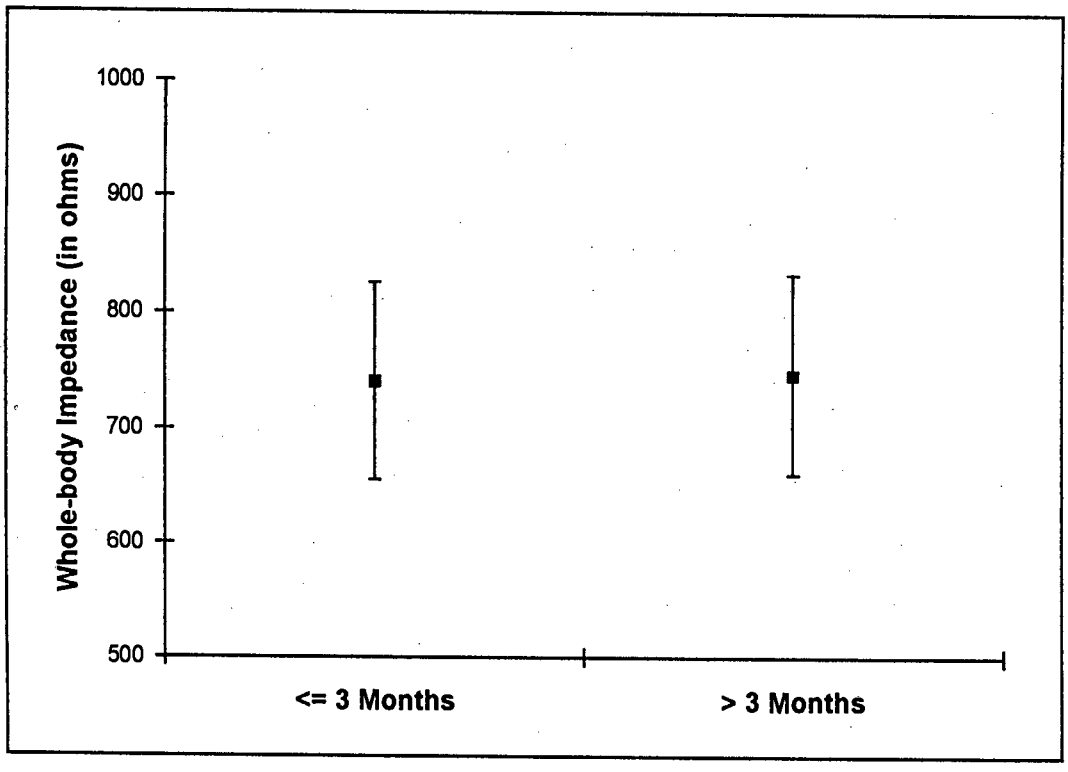


FIGURE 3.4 Mean and standard deviation of Whole-Body Impedance for children older and younger than 3 months

**(d) Whole-body impedance and height**

A scatter plot of WBI on height is given in figure 3.5. Linear regression analysis shows no significant correlation between height and WBI (correlation coefficient = 0,016 R-squared = 0.026 %).

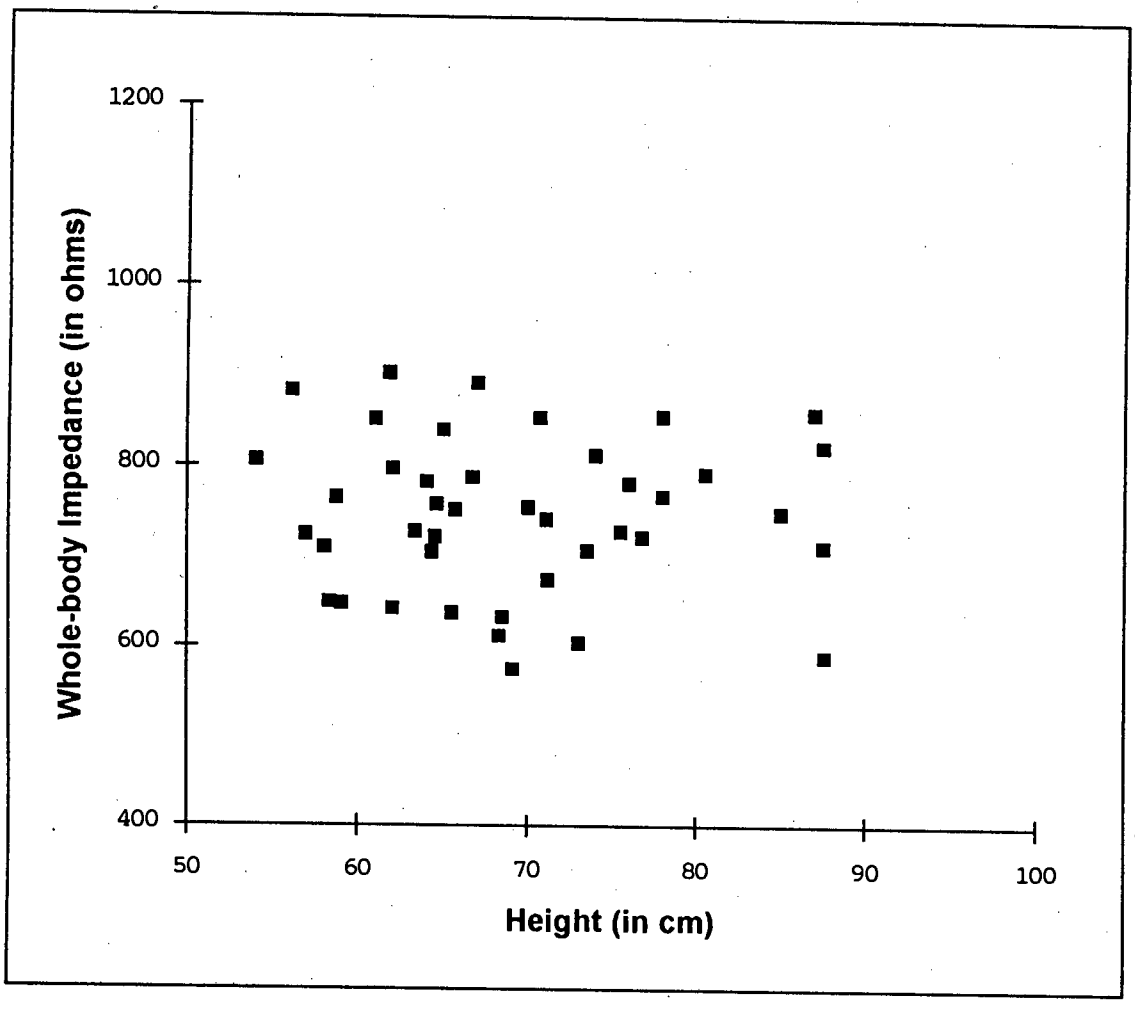


**FIGURE 3.5 Plot of Whole-body Impedance (in Ω) versus height (in cm) for the normal group**

## (e) Whole-body impedance and mass

A scatter plot of WBI on mass is given in figure 3.6. Linear regression analysis shows no significant correlation between mass and WBI (correlation coefficient = -0,26 R-squared = 6.76 %).

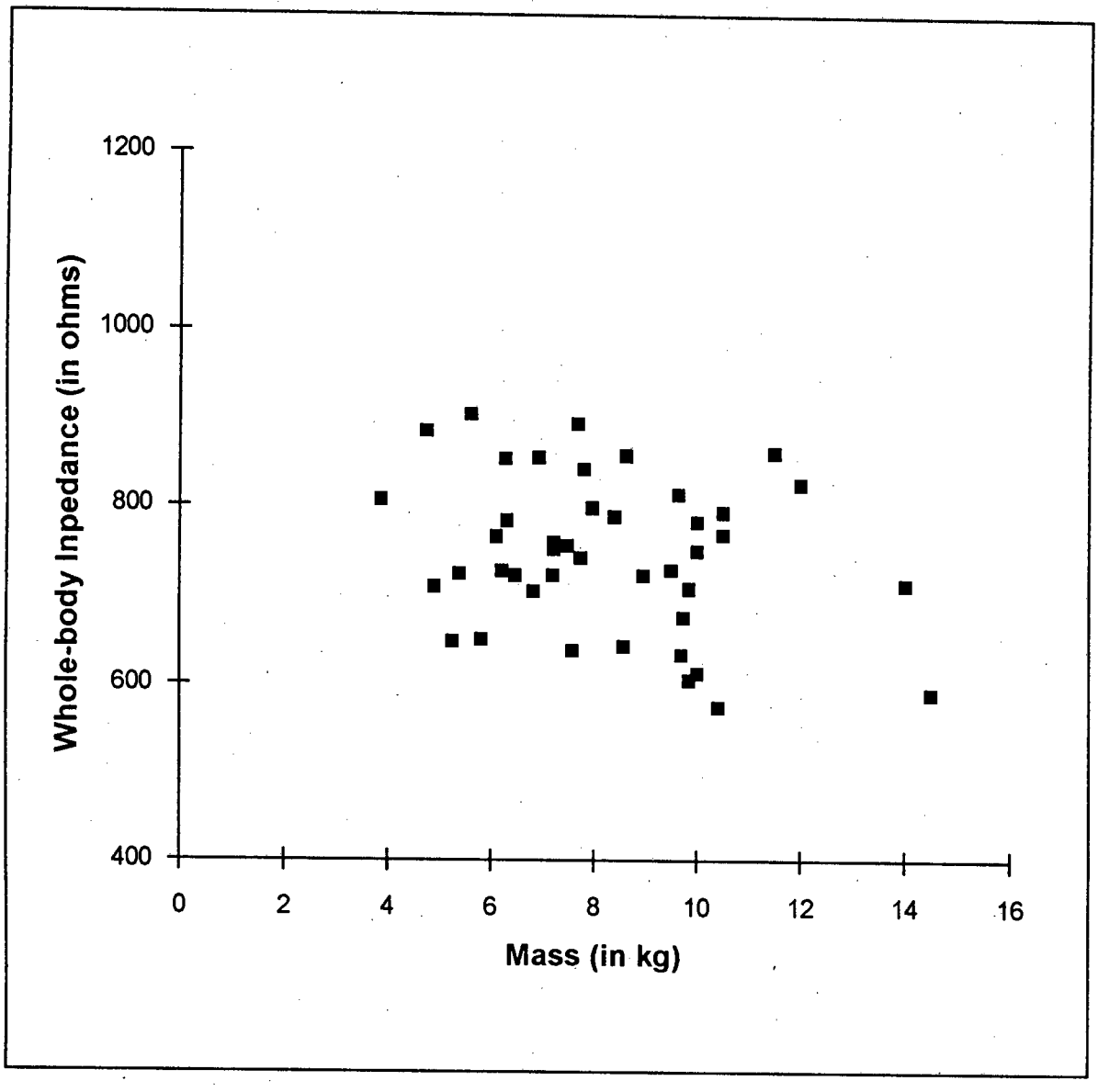


**FIGURE 3.6 Plot of Whole-body Impedance (in Ω) versus mass (in kg) for the normal group**

### 3.4.2 Whole-body impedance in dehydrated children and comparison with the normals

Sixteen dehydrated children were measured comprising of seven males and nine females. The mean, range and standard deviation for age, rehydrated mass, height and percentage dehydration are given in table 3.4. The results for the individual dehydrated children are given in appendix G.

**TABLE 3.4 Physical characteristics, age and percentage dehydration for the dehydrated subjects**

| Variable | Age (months) | Height (cm) | Mass (kg) | Percentage Dehydration |
|---|---|---|---|---|
| Mean | 9.0 | 67.2 | 7.0 | 8.9 |
| Standard Deviation | 6.1 | 10.3 | 2.4 | 3.4 |
| Minimum | 2.1 | 49.9 | 3.2 | 4.3 |
| Maximum | 19.1 | 83.5 | 10.8 | 16.3 |

#### (a) Correlation between the age, mass and height of the normal and dehydrated children

The difference between the age of the normal and the dehydrated children was not significant at the $p \leq 0.05$ level ( p value = 0.87, t value = 0.16, d.f. = 57 ).

The difference between the mass of the normal and the dehydrated children was not significant at the $p \leq 0.05$ level ( p value = 0.08, t value = 1.77, d.f. = 57 ).

The difference between the height of the normal and the dehydrated children was not significant at the $p \leq 0.05$ level ( p value = 0.50, t value = 0.67, d.f. = 57 ).

The statistics for the initial WBI of the dehydrated children and their final WBI once rehydrated are shown in table 3.5 together with the statistics for the WBI of the normally hydrated children, added for comparison.

**TABLE 3.5 Whole-body impedance of the dehydrated children before and after rehydration and normal children**

| Variable | Dehydrated WBI (in Ω) | Rehydrated WBI (in Ω) | Normal WBI (in Ω) |
|---|---|---|---|
| Mean | 1029 | 728 | 746 |
| Standard Deviation | 149 | 62 | 85 |
| Minimum | 847 | 595 | 575 |
| Maximum | 1296 | 807 | 903 |

Paired one-sample hypothesis testing using the *t*-test showed that the difference between the WBI of the dehydrated children and the rehydrated children was significant at the $p < 0.001$ level ( t value = 46.9, d.f. = 15).

Two-sample hypothesis testing using the *t*-test showed that the difference between the WBI of the dehydrated children and the normally hydrated children was also significant at the $p < 0.001$ level ( t value = 9.16, d.f. = 57).

The difference between the WBI of the rehydrated children and the normally hydrated children was not significant at the $p \leq 0.05$ level using the same test ( p value = 0.43, t value = 0.79, d.f. = 57).The 95% confidence intervals for the population mean of these groups are given in table 3.6 and shown in figure 3.7.

TABLE 3.6 Confidence intervals for the whole-body impedance of the dehydrated, rehydrated and normally hydrated children

| Group | 95% Confidence Intervals for the population mean | |
|---|---|---|
| | lower limit (Ω) | upper limit (Ω) |
| Dehydrated | 950 | 1109 |
| Rehydrated | 695 | 761 |
| Normal | 720 | 772 |

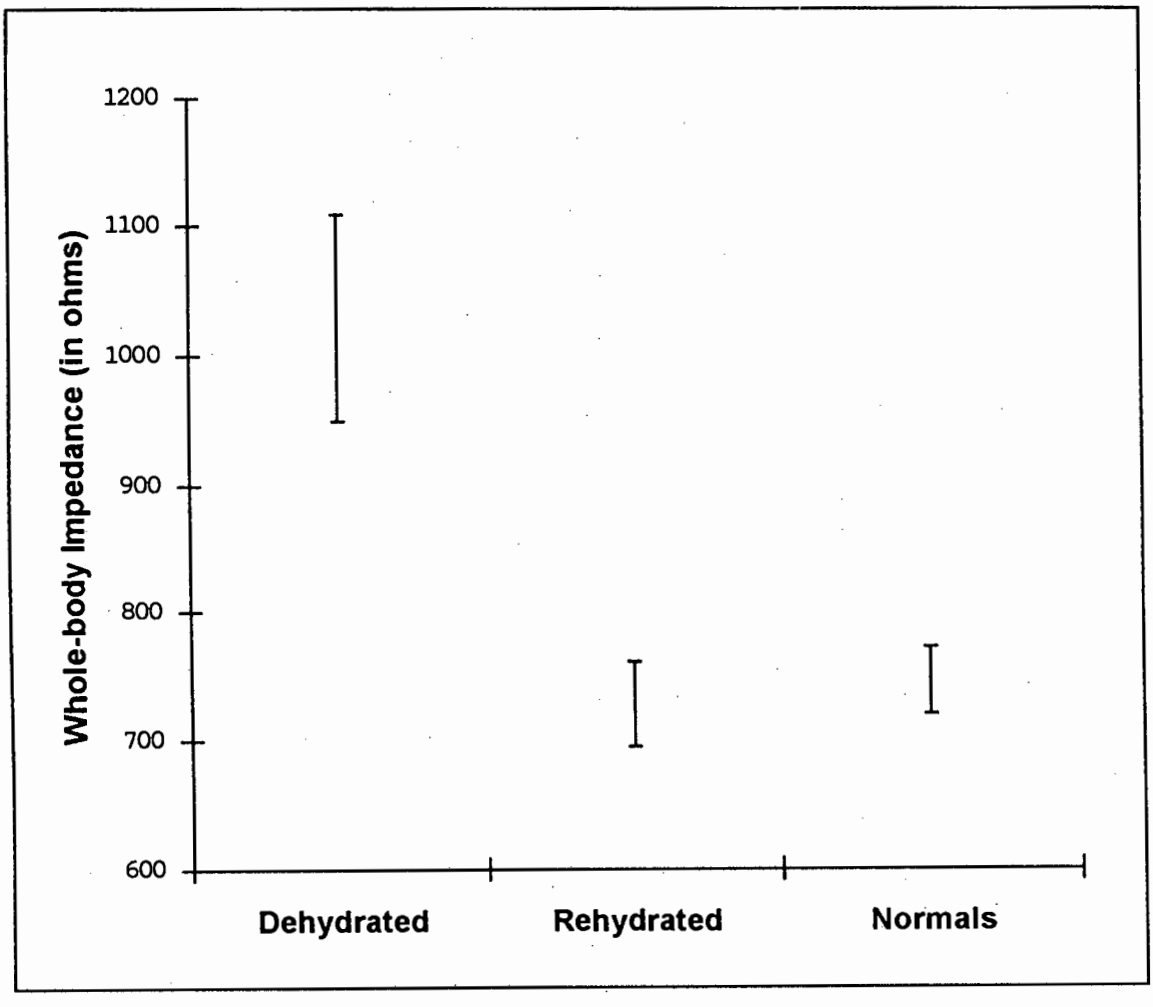


FIGURE 3.7 Graph of the 95% confidence limits for the population mean for the dehydrated, rehydrated and normal children

## (b) Prediction of percentage dehydration from Whole-Body Impedance

A scatter plot of the initial whole-body impedance of the dehydrated children on admission versus their percentage dehydration on admission is given in figure 3.8. Linear regression analysis shows a correlation coefficient of 0.61 ($r^2$ = 37.18 % SEE = 2.75).

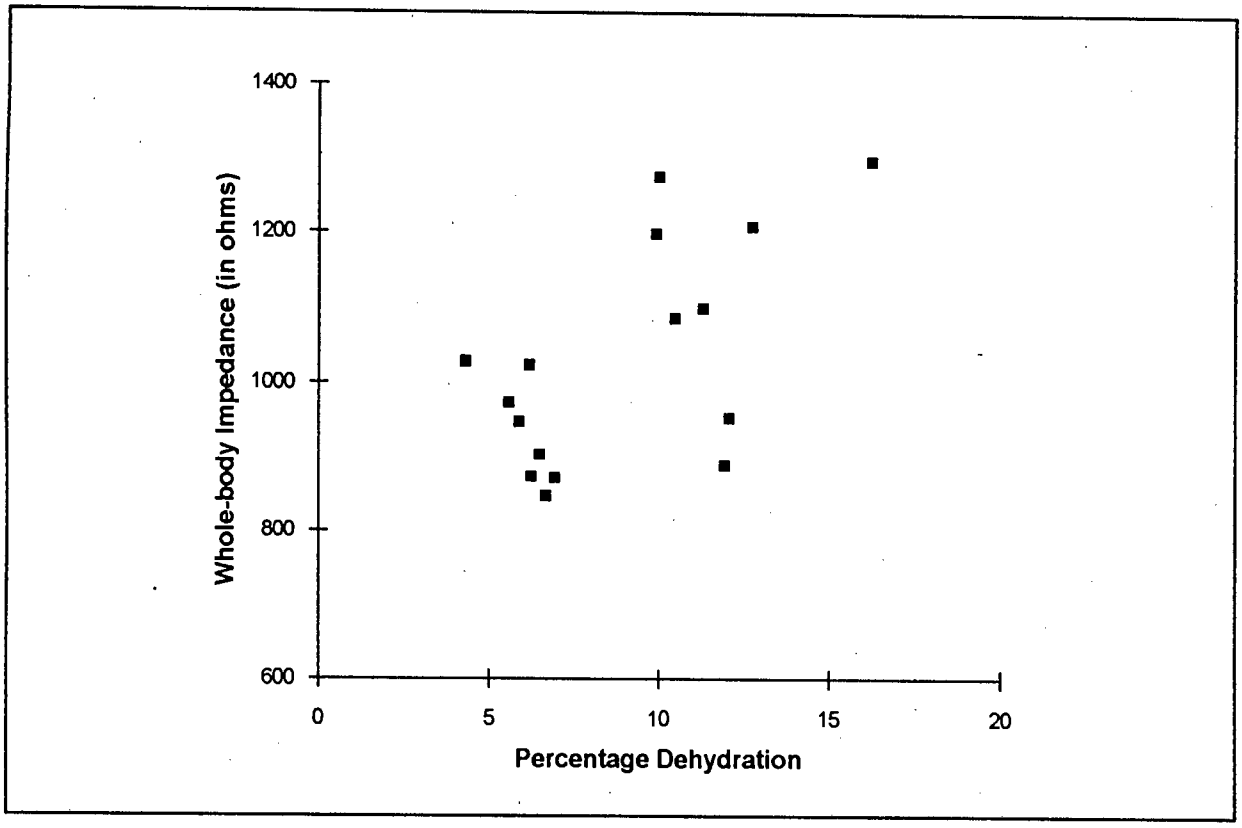


**Figure 3.8 A scatter plot of the initial (dehydrated) whole-body impedance (in Ω) versus the initial percentage dehydration**

**(c) Correlation between mass and height squared / WBI in the dehydrated children**

The scatter plot of mass on height squared / WBI for the dehydrated group before and after rehydration is given in figure 3.9. Linear regression analysis shows a significant correlation between height squared / WBI and mass for the dehydrated group (correlation coefficient = 0.91, Intercept = 0.69, Slope = 0.62) and for the same group after rehydration (correlation coefficient = 0.94, Intercept = 1.26, Slope = 0.73).

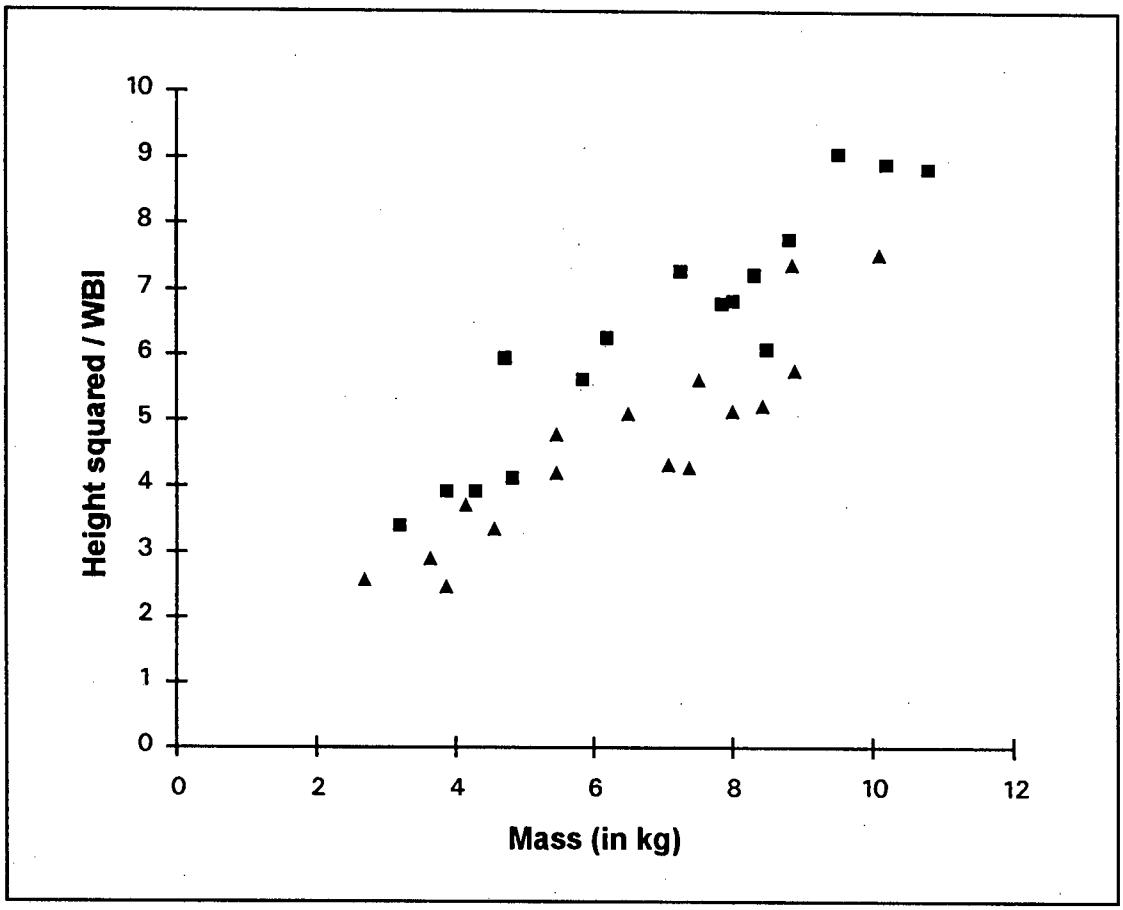


**FIGURE 3.9 Scatter plot of height squared / WBI (in $cm^2/\Omega$) versus mass (in kg) in the dehydrated children (■) and in the same children after rehydration (▲)**

**(d) Whole-body impedance in dehydrated children and the effect of electrolytes**

The sodium concentrations of the dehydrated children on admission were found to range from 121 to 153 mmol/l ( mean = 135.6, s.d. = 8.5 ). Nine children had initial sodium concentrations below the normal range ( 136 - 143 mmol/l [5] ) and two were hypernatraemic (both with an initial sodium concentration of 153 mmol/l).

The potassium concentrations of the dehydrated children on admission were found to range from 1.6 to 5.2 mmol/l ( mean = 3.1, s.d. = 0.88 ). Eleven children were hypokalaemic and none were hyperkalaemic ( the normal range is 3,8 to 5.0 [5] ).

Sodium concentration and WBI were poorly correlated ( correlation coefficient = - 0.43, $r^2$ = 18.1 % ) as were potassium concentration and WBI ( correlation coefficient = - 0.31, $r^2$ = 9.7 % ).

The scatter plot of height squared / WBI corrected for serum sodium concentration ( section 3.5.5 of data analysis methods ) on mass is given in figure 3.10 and the scatter plot of height squared / WBI corrected for serum potassium concentration on mass is given in figure 3.11.

Linear regression analysis shows that the correlation of height squared / WBI corrected for serum sodium concentration on mass is good ( correlation coefficient = 0.93 ) but this is exactly the same as the uncorrected correlation.

Linear regression analysis shows that the correlation of height squared / WBI corrected for serum potassium concentration is worse ( correlation coefficient = 0.71 ) than the uncorrected correlation.

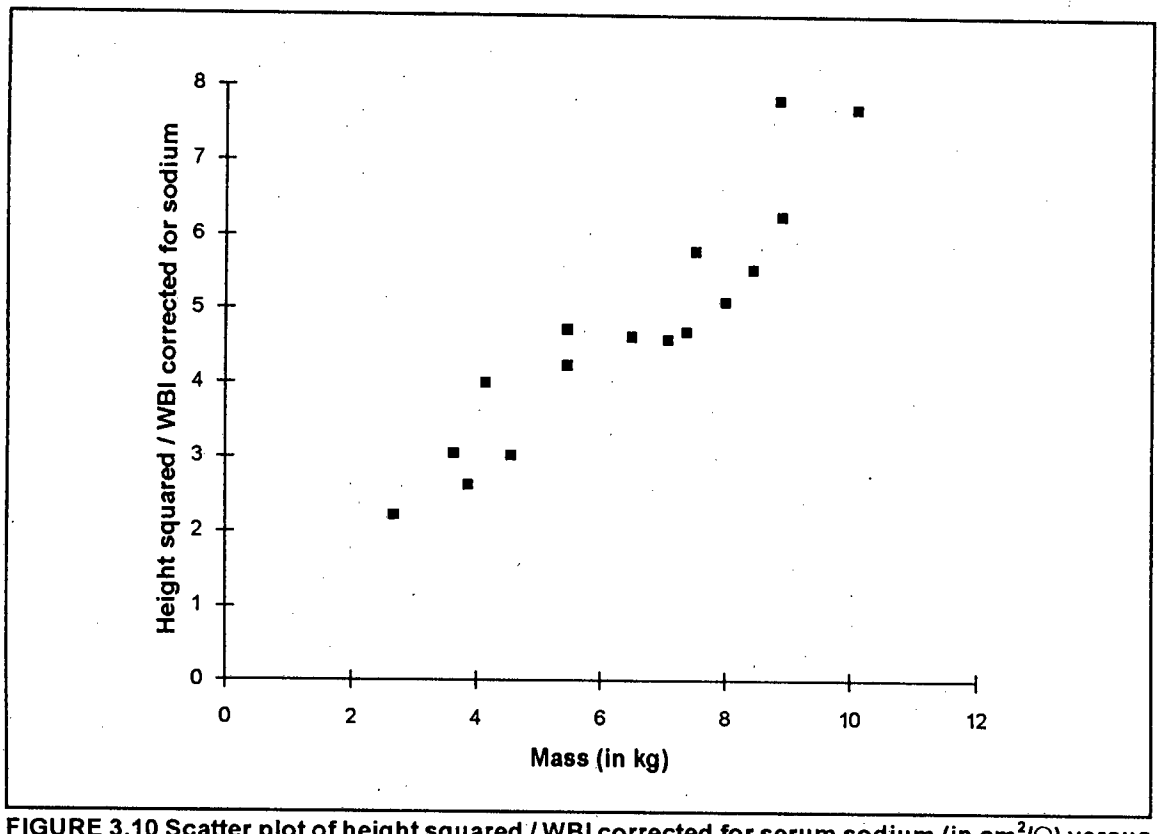


**FIGURE 3.10 Scatter plot of height squared / WBI corrected for serum sodium (in $cm^2/\Omega$) versus mass (in kg) in the dehydrated children**

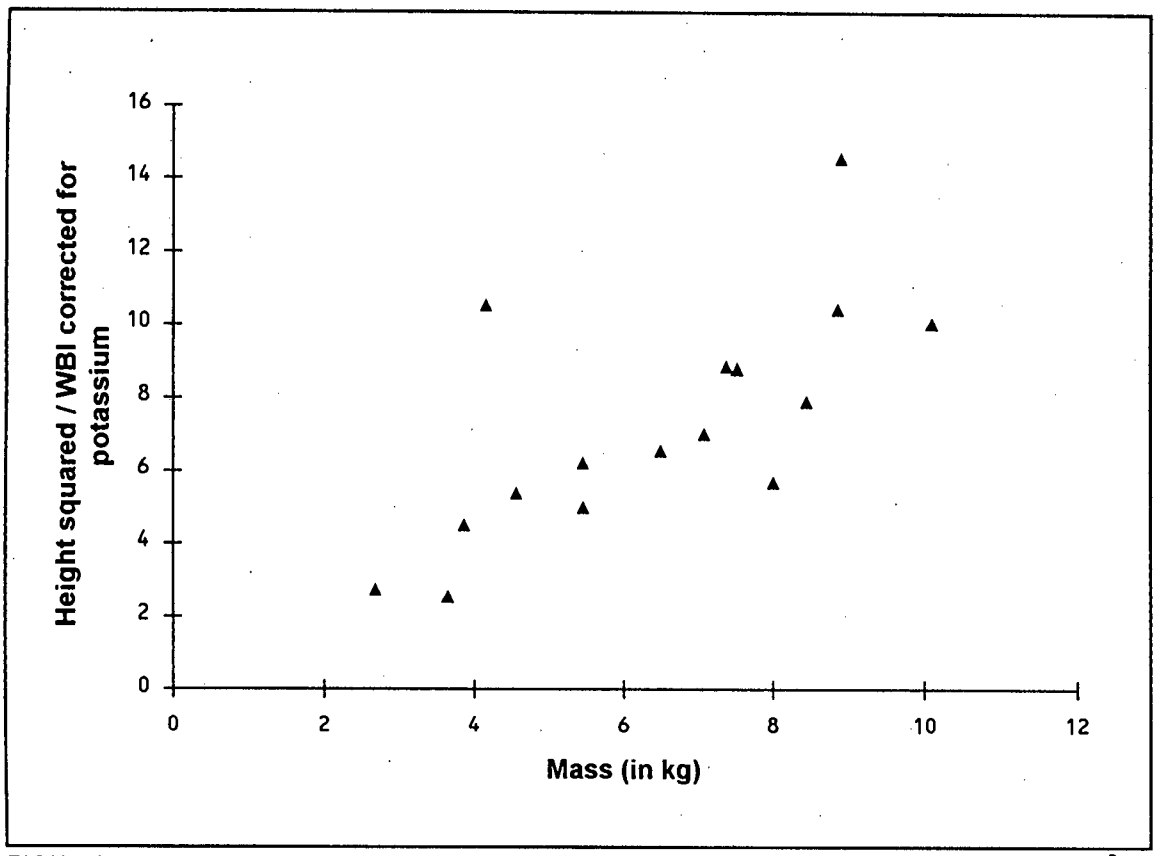


**FIGURE 3.11 Scatter plot of height squared / WBI corrected for serum potassium (in $cm^2/\Omega$) versus mass (in kg) in the dehydrated children**

**(e) Prediction of change in mass from change in impedance**

A scatter plot of the change in mass calculated from change in impedance (see appendix B and section 2.2.3 earlier) on the measured change in mass between the initial (dehydrated) measurements and the final (rehydrated) measurements is given in figure 3.12. Linear regression analysis shows a correlation coefficient of 0.74 ( $r^2$ = 54.94 % SEE = 0.50 ).

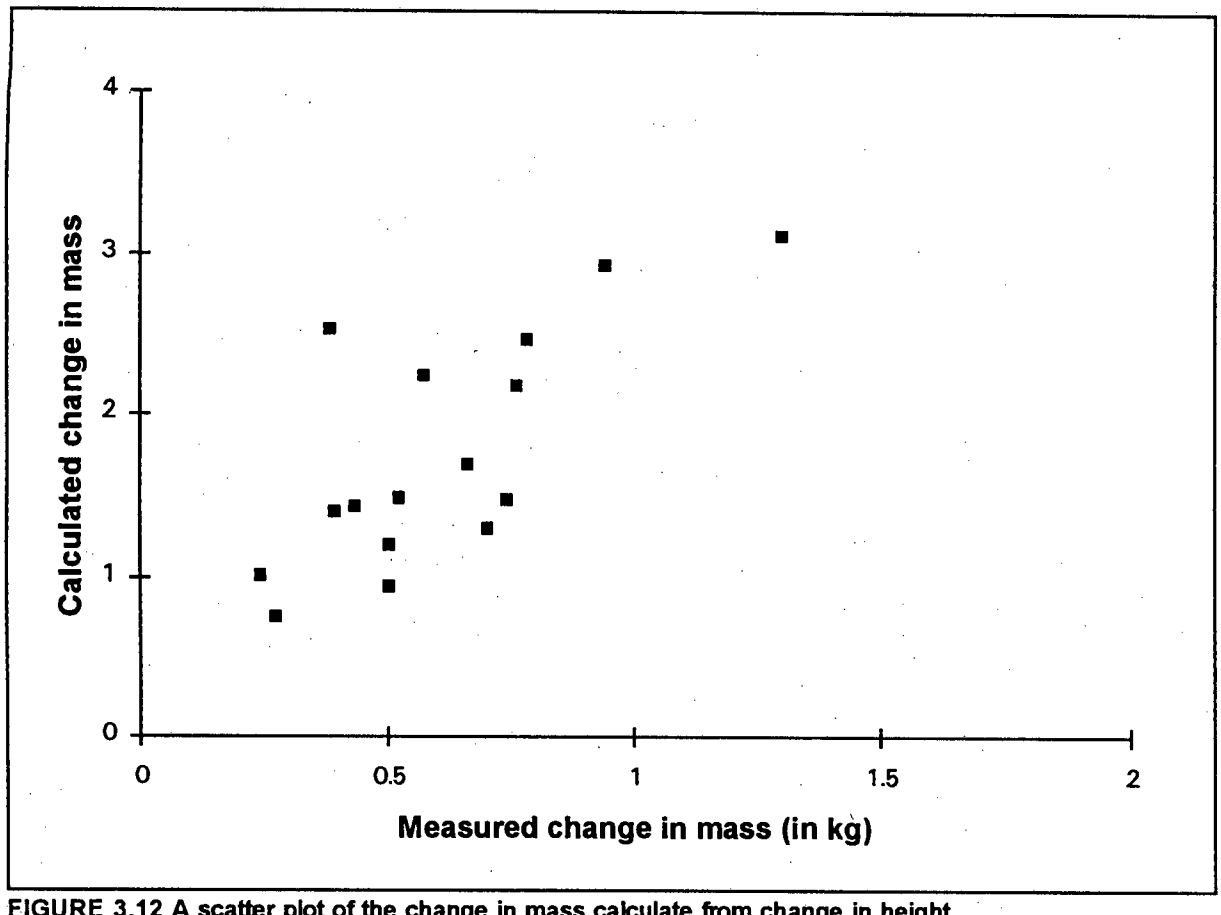


**FIGURE 3.12 A scatter plot of the change in mass calculate from change in height squared / WBI (in $cm^2/\Omega$) versus the measured change in mass (in kg)**

## 3.5 DISCUSSION

### 3.5.1 Whole-body impedance in normally hydrated and dehydrated children

Forty-three normally hydrated and sixteen dehydrated children were measured. The dehydrated children ranged from 2 to 19 months of age with a mean of 9.0 months. The normal group was aged from 1 to 23 months with a mean of 8.8 months. A study of 2095 patients admitted to a hospital in this country with acute gastroenteritis shows that 94% were 24 months or less of age with the highest distribution in the 6 to 12 month age group [28]. Thus this study has included the major age group of interest in this condition in this country.

The mean WBI of the normals was 746 Ω with a standard deviation of 85 Ω and the 95 % confidence interval for the mean was from 720 Ω to 772 Ω. There was no difference between the WBI of the normal males and females ($p > 0.05$). There was no correlation between the WBI of the normal group and their age, mass or height ($p > 0.05$ for all three). In addition the WBI of the children older than 3 months of age was no different from that of the younger children ($p > 0.05$).

There was no difference between the age, mass and height of the normal group and the dehydrated children ($p > 0.05$ for all three). The dehydrated children were 4.3 % to 16.3 % dehydrated. The mean WBI of the these children on admission was 1029 Ω with a standard deviation of 149 Ω and the 95 % confidence interval for the mean was from 950 Ω to 1109 Ω. This was very significantly greater than the WBI of the normal group ($p < 0.001$).

Once rehydrated these children had a mean WBI of 728 Ω with a standard deviation of 62 Ω. The 95 % confidence intervals for the mean WBI once rehydrated was from 695 Ω to 761 Ω which was no different from that of the normal group ($p>0.05$). Thus WBI was significantly greater in the dehydrated children than the normal group, who were of similar age, mass and height and was not different from the normal group after rehydration.

The correlation between percentage dehydration and WBI ( r = 0.61 ) suggests that the problem of the degree of dehydration in children with diarrhoeal disease can be determined from the WBI alone although it is suggested that this correlation be examined in a larger series of dehydrated children. However it appears that WBI is able to clearly distinguish between dehydrated children needing intervention and normally hydrated children even though the degree of dehydration may not be accurately quantifiable using this technique.

### 3.5.2 Correlation between mass and height squared / WBI in normal and dehydrated patients

Numerous studies have validated the use of the height squared / WBI as a measure of total body water and of fat-free mass in both adults and children. It is this good correlation that has lead to the use of this technique in the clinical assessment of body composition. In this study the height squared / WBI index was highly correlated with mass in the normals ( r = 0.93 ), the dehydrated children ( r = 0.94 ) and the same children after rehydration ( r = 0.93 ). It is of note that mass is highly correlated with WBI even during severe dehydration and even after rehydration.

### 3.5.3 Effect of electrolytes

The conduction of electrical current in biological tissues is due to the presence of ions in solution [25]. In this study WBI was found to be poorly correlated with the serum concentrations of sodium and potassium. Potassium did not improve the correlation of height squared / WBI on mass but the same correlation ( r = 0.93 ) was unchanged when corrected for sodium. Sodium is the major ECF cation and potassium is the major ICF cation [41] . Only 2% of the total body potassium is present in the ECF [41] and the ECF concentration of potassium does not correlate with its ICF concentration [41]. WBI measurements at 50 kHz measure both the ECF and the ICF as current at this frequency is able to flow through cell membranes. Thus the poor correlation of WBI measurements of TBW corrected for ECF potassium is to be expected.

### 3.5.4 Change in Whole Body Impedance during dehydration

The impedance of a conductor is proportional to its length and resistivity and inversely proportional to its cross sectional area (see section 2.2.1 and appendix A). In this study the whole-body impedance of sixteen dehydrated children, measured between the right hand and right foot, was higher than the whole-body impedance of the same children, measured between the same points after rehydration (figure 3.7). The conductor length and geometrical configuration were the same before and after rehydration so the change in WBI could either have been due to either a change in cross sectional area or to a change in resistivity or both.

The regression of height$^2$ / WBI on mass for the dehydrated and rehydrated groups is given in figure 3.9. The slope of this regression line is inversely proportional to resistivity (appendix A, equation A5). The slope of the dehydrated group is slightly less than that of the rehydrated group (0.62 versus 0.73) suggesting that the resistivity of the dehydrated group is greater than the rehydrated group. The increase in WBI during dehydration may thus be due to an increase in resistivity. GIT fluids are known to be hypotonic in relation to the ECF and ICF. The loss of more water than electrolyte in the stool may result in greater concentration of electrolytes in the ICF and ECF. Resistivity is inversely proportional to electrolyte concentration ( section 2.3.1 ) so it follows that an increase in electrolyte concentration in dehydration should result in a decrease in resistivity (increase in the slope of the above regression line), however this was not seen.

If the length of the conductor remains constant the change in volume must be due to a change in the cross sectional area. Impedance is inversely proportional to cross-sectional area so it is possible that the increase in WBI during dehydration is due to an increase in resistivity together with a decease in cross-sectional area.

### 3.5.5 Prediction of change in mass from change in impedance

Whole-body impedance measurements have been used in haemodialysis patients to measure changes in body fluid volumes from the WBI [19, 20, 21, 55] and the theory is described in appendix B. In this study the change in mass calculated with this method ( from the change in WBI ) was well correlated with the measured change in mass ( $r = 0.74$ ). This suggests that WBI measurements may be useful as an alternative method for the assessment of progress during rehydration.

A very interesting observation has been made in this regard. In all of the cases examined the rehydrated impedance was lower than the initial impedance on admission and each impedance reading during rehydration was lower than the preceding one. In this series some of the children showed a transient decrease in mass during rehydration even though clinically they appeared to be improving and their WBI was decreasing. This transient decrease in mass during rehydration is a phenomenon often seen during rehydration. These children appear to be improving clinically yet this is not reflected in the early mass measurements. The WBI measurements however are seen to fall steadily with each successive measurement during rehydration which is consistent with the clinical impression.

One possible explanation is as follows: During rehydration the child is receiving parenteral infusions, or oral solutions that are easily absorbed, so that the body fluid compartments are being rehydrated. Losses in the stool are continuing however and in the early course of treatment the loss from the stool may exceed oral and parenteral gain even though the gain into the body fluid compartments may still be greater than the loss from the body fluid compartments into the stool, particularly in the case of parenteral fluids. Thus the child will have an improved fluid status ( due to the rehydration solution entering the body fluid compartments ) even though the child's mass may decrease, owing to an even greater loss from the stool.

The trunk has a very large diameter relative to the diameter of the arms and legs. Impedance is inversely proportional to cross-sectional area ( see appendix A ) and

thus the trunk contributes only about 10% to the WBI reading [24]. Fluids in the trunk such as the gastro-intestinal fluids and bladder fluids therefore contribute very little to the WBI measurements [55]. For this reason WBI measurements may reflect more accurately the true hydrational status than mass, which includes gastro-intestinal and bladder fluids. WBI may also be a reasonable substitute to weighing in those dehydrated children who are too moribund to disturb or who may be requiring oxygen therapy or intensive monitoring.

# CHAPTER 4
# DEVELOPMENT OF A VARIABLE FREQUENCY TETRAPOLAR BIOIMPEDANCE ANALYSER

## 4.1 INTRODUCTION AND OBJECTIVES

The distribution of fluid between the ECF and ICF is known to be abnormal in renal, cardiac and gastrointestinal conditions. In addition malnourished children may also have abnormalities of fluid distribution. This is particularly the case in children with kwashiorkor who develop oedema. The measurement of the distribution of fluid in these conditions would be of clinical importance but the present method involves using isotope dilution (see section 2.6.1) which is expensive, complicated, invasive and cannot be used to monitor rapid changes of fluid distribution [61].

The strong correlation between WBI and fat-free mass (determined using densitometry) or total body water (measured by isotope dilution) has been discussed in earlier chapters. In most studies the measurement of WBI has been performed at the single frequency of 50 kHz. It is known that at this frequency current travels through both the extracellular and intracellular fluid compartments (see section 2.3. for a more detailed description of the electrical model of biological tissue). In our study of WBI in dehydrated children the WBI at 50 kHz was found to be significantly increased during dehydration and to return to normal after rehydration.

Early studies by Jenin et al (1975) [36] suggested that ECF volume (measured using isotopes of bromide and sulphate) might be strongly correlated with WBI measured at low frequencies (1 kHz), in keeping with the electrical model for biological tissue. This finding has been confirmed by other studies [61,62]. In these studies the frequency used

for the measurement of ECF is either 1 kHz or 5 kHz and that used to measure TBW is either 50 kHz or 100 kHz. It has been suggested that the ratio between $WBI_{1\ kHz}$ and $WBI_{100\ kHz}$ is a relatively fixed value in normally hydrated subjects but may vary markedly in subjects with abnormal fluid distribution [36].

The objectives of this part of the study were to design, build and test an instrument capable of measuring WBI at all frequencies throughout the range 1 kHz to 100 kHz, safely and accurately in order to evaluate the electrical model described in section 2.2.6. Such a model would allow electronic measurement of ECF and ICF compartments which may lead to many useful clinical applications.

## 4.2 DESIGN CONSIDERATIONS

### 4.2.1 Frequency range

WBI measured at 50 kHz and at 100 kHz has been used to measure TBW and WBI measured at 1 kHz and at 5 khz has been used to measure ECF [36]. In order to evaluate the electrical model a variable frequency bioimpedance analyser capable of measuring WBI at all frequencies from 1 kHz to 100 kHz is required.

### 4.2.2 Output Current

The safety considerations for electrical equipment passing current through the human body were given earlier (see section 2.5). It was decided that the patient be isolated from all equipment using mains voltages and that the equipment in direct contact with the patient be battery operated only. An output current of 300 μA RMS, well below the safety limits at these frequencies was regarded as safe. The equipment must be able to produce this current across the large skin impedance found in dehydrated children.

### 4.2.3 Skin electrodes

The tetrapolar method of measuring WBI requires that four surface electrodes be applied. It is necessary that these electrodes be placed not less than 4 cm apart

As children tend not to be as compliant as adults it important for these electrodes to be small, lightweight, easy to apply so that they will be well tolerated even by small and frightened children.

## 4.3 HARDWARE COMPONENTS

The following hardware components are used :

1. An IBM compatible 80286 AT computer with a 40 megabyte hard disk drive and 1 megabyte of RAM.

2. A PC-30D analogue to digital convertor card from Eagle Electric. This card has sixteen analogue to digital convertor channels, which can be configured as unipolar or bipolar inputs. Each channel has 12-bit resolution and 200 kHz throughput rate with less than ± 0.75 least significant bit non-linearity. The card has four digital to analogue convertor channels each with a 130 kHz throughput rate. Two channels have 12-bit resolution and two have 8-bit resolution each with less than 0.01% full scale range non-linearity.

3. A function generator : Escort EGC-2230 used in the 1 kHz to 100 kHz range at less than 0.1% distortion.

4. A custom built 'Bioimpedance Analyser' containing the isolation transformers, a constant current source and a precision full wave rectifier and averaging filter.

## 4.4 CIRCUIT DESCRIPTION

A simplified circuit diagram of the variable frequency bioimpedance analyser is given in figure 4.1 and the full circuit diagram of the interface between the computer and the patient is given in appendix H.

The Escort function generator can be configured as a VCO and an external voltage of 0 to -2V can be used to provide a frequency range of 1 kHz to 100 kHz. This voltage was provided by microprocessor via an analog-to-digital convertor (ADC).

This alternating current is then passed through an isolation transformer to protect the

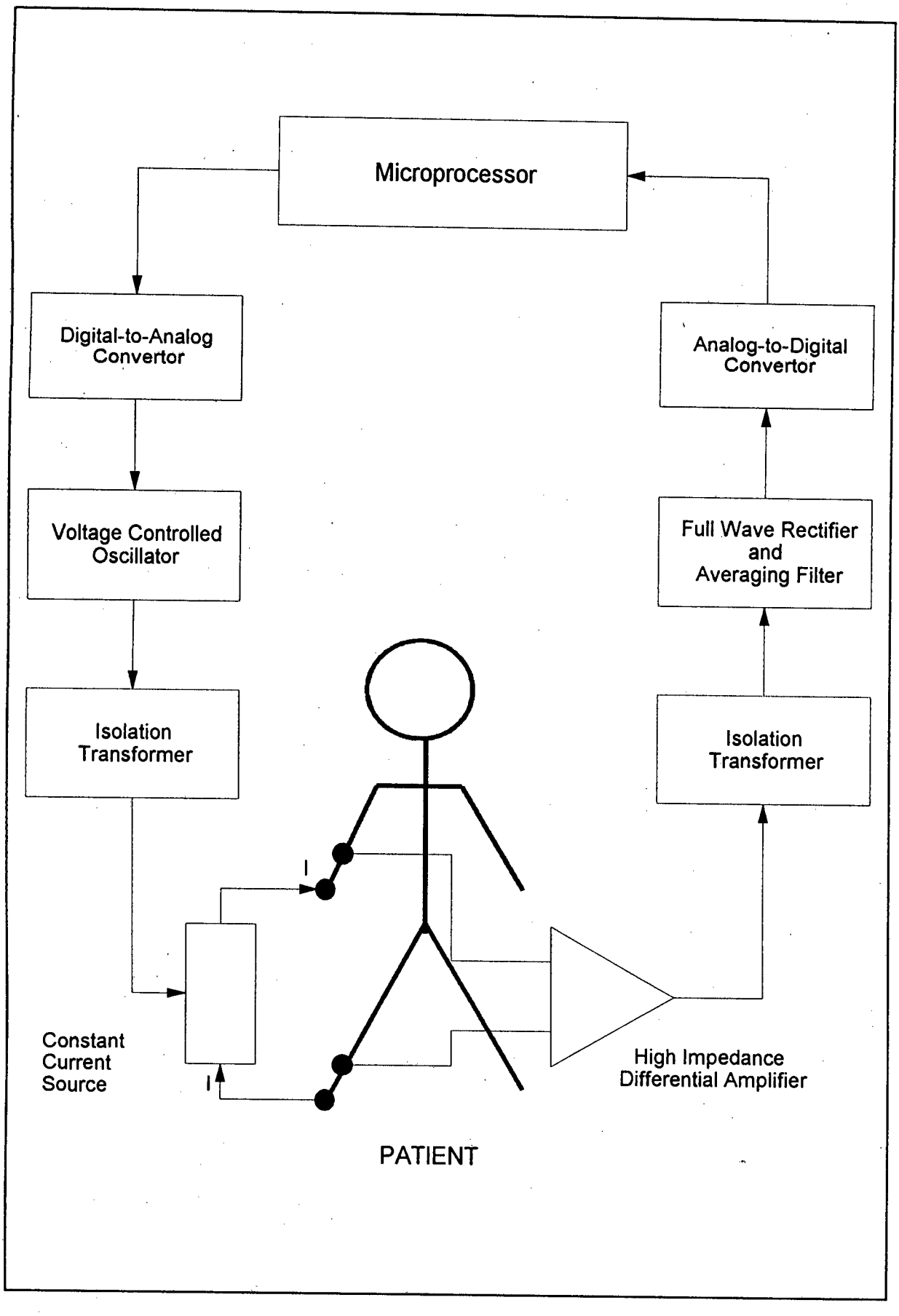


**FIGURE 4.1 Simplified circuit diagram of the Variable Frequency Bioimpedance Analyser**

patient from any mains currents passing through the computer or VCO..

A constant current source is then used to produce an alternating current of constant RMS amplitude (300 μA RMS) which is then passed through the patient, through leads placed distally on the right hand and foot. These are the current injecting electrodes.

The proximal leads are connected to the patient proximal to the current injecting electrodes (see figure 4.1). A high impedance differential amplifier is used to measure the differential voltage between these leads. This current is then passed through an isolation transformer for patient protection. A full wave rectifier and averaging filter is used to obtain a direct current output voltage equal in amplitude to the peak current of the constant current source multiplied by the WBI. An analog-to-digital (ADC) converter converts this rectified voltage to a digital code which is then read by the microprocessor. The electrical components on the patient side of the isolation transformers are all powered by a 9V battery.

## 4.5 SOFTWARE DESCRIPTION

The program was developed using Borland Turbo Pascal version 5.5 as the PC 30 ADC card came supplied with Pascal drivers and the language is easy to learn and implement.

The software program was developed to perform the following tasks:

1. To control the Escort Function generator via a digital-to-analog converter in order to generate frequencies from 1 kHz to 100 kHz using
2. To measure and display the whole-body impedance at each frequency using an analog-to-digital converter.
3. To store and retrieve data on each patient tested.
4. To allow the user to enter values for the intracellular and extracellular resistances and the cell wall capacitance and to compute the expected response using the model developed earlier (see appendix C).

### 4.5.1 Main Program

The flow chart of the main program is given in figure 4.2. After initialising and testing the hardware and initialising the variables a user friendly environment is displayed offering four main procedures: sample, retrieve, calibrate and model. If the hardware diagnostic test fails then the program is halted.

### 4.5.2 Sample Procedure

The sample procedure (see figure 4.3) controls the VCO through the DAC channel 0 and reads the rectified voltage through the ADC channel 0. The VCO is set to 1 kHz and allowed 20 msec to settle. The rectified voltage is then measured and displayed on the screen. The process is then repeated in 1 kHz increments until the WBI at 100 kHz is measured. These 100 readings take 2 seconds to perform. The frequency is then incremented by 1 kHz and This data is then displayed on a graphics screen in the form of a plot of WBI against frequency. Two sample ranges are provided. The

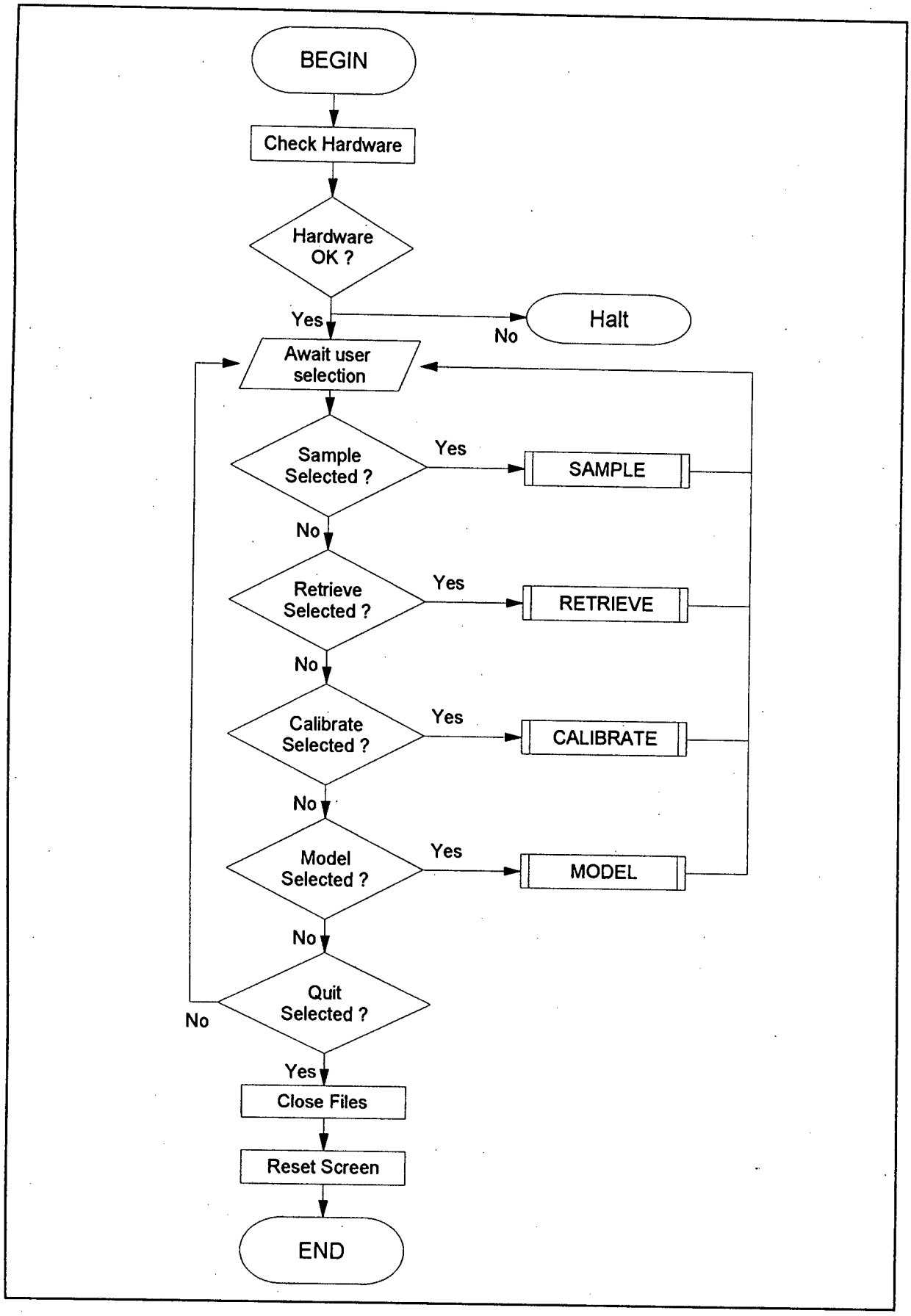


**FIGURE 4.2 Flow diagram of the main software procedure**

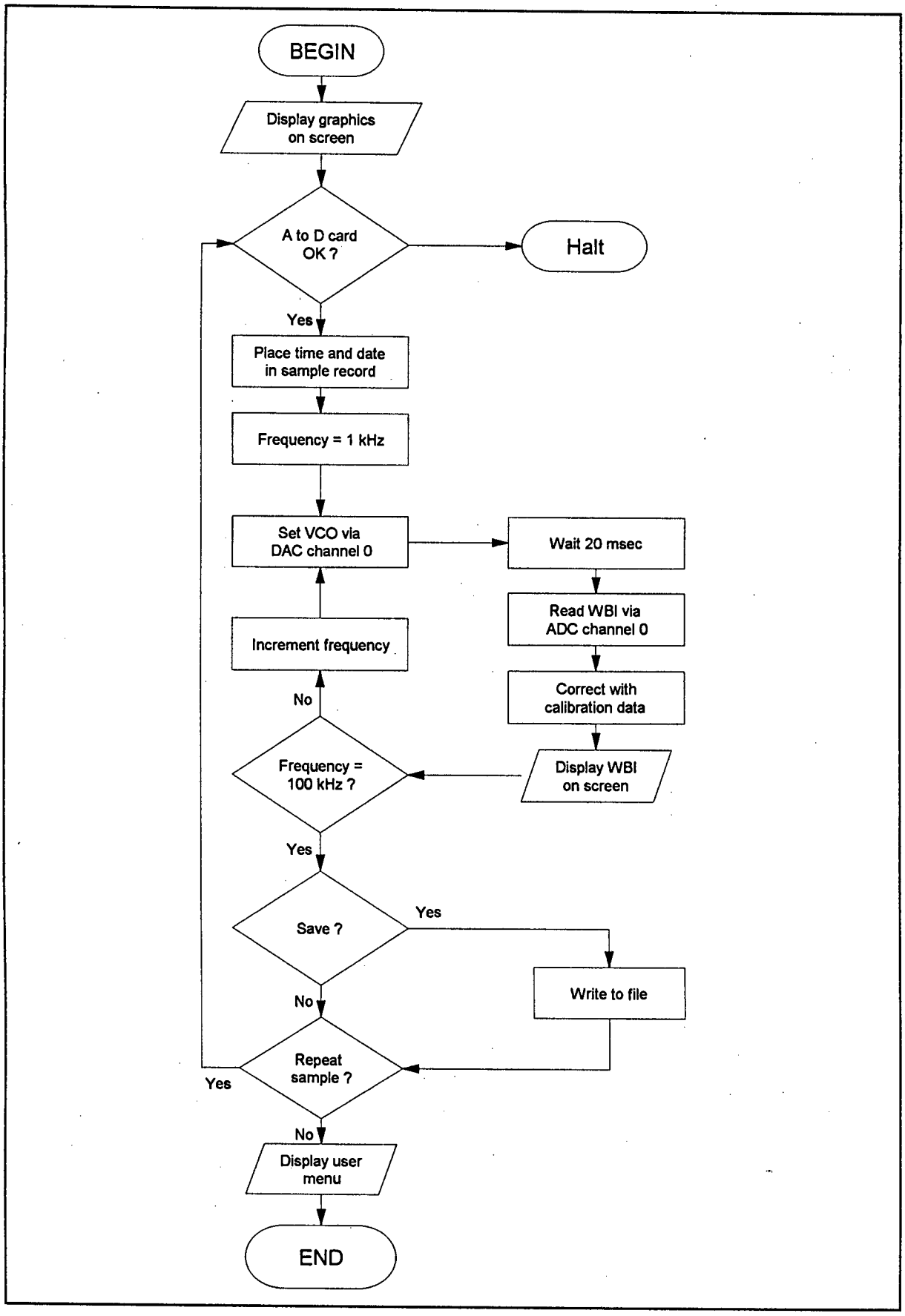


**FIGURE 4.3 Flow diagram of the Sample procedure**

high range measures impedance from 0 to 20 kΩ which is necessary for measuring skin impedance. The low range measures impedance from 0 to 2 kΩ which is necessary for the measurement of WBI. The user then has the option of saving the data for further analysis. Data is saved in ASCII format so that it may easily imported into word processor and spreadsheet computer programs. If a further sample is not required the user is returned to the main menu.

### 4.5.3 Retrieve Procedure

The retrieve procedure (figure 4.4) allows the user to view the results of previous samples. This procedure first finds all files with the extension 'bia' in the default directory and displays these file names on the screen. The user is then prompted for the name of a file to retrieve. Error checking warns if the desired file is not found or if any other disk operating system error occurs. If found the file is displayed on the screen. The user may then either retrieve another file or return to the main menu screen.

### 4.5.4 Calibration Procedure

The calibration procedure (see figure 4.5) is used to calibrate the Escort function generator and to create a look-up table to correct the measured WBI for impedance losses due to the inductance of the isolation transformers and to the capacitance in the leads connecting the equipment to the patient. The VCO is set to 1 kHz and is then calibrated manually (the Escort function generator has a built-in frequency counter. A precision 1500 Ω resistor is then placed between the current injecting electrodes. The current sensing electrodes are attached to either end of the resistor and the impedance is measured from 1 kHz to 100 kHz using the ADC channel 0 as in the sample procedure. The inverse of each impedance measurement multiplied by 1500 thus becomes the calibration factor for each frequency.

### 4.5.5 Model Procedure

The model procedure allows the user to enter values for the intracellular and extracellular resistances (Ri and Re respectively) and the cell membrane capacitance (C). A plot of the expected impedance for each frequency is then produced using the following equation for the electrical model of biological tissue:

$$WBI = \frac{R_i \cdot R_e \cdot (R_i + R_e) + \dfrac{R_e}{(\omega C)^2}}{(R_i + R_e)^2 + \dfrac{1}{(\omega C)^2}} \qquad (4.1)$$

$$( \textit{where } \omega = 2 \cdot \pi \cdot f )$$

See appendix C for the full derivation. A flow chart of this procedure is given in figure 4.6.

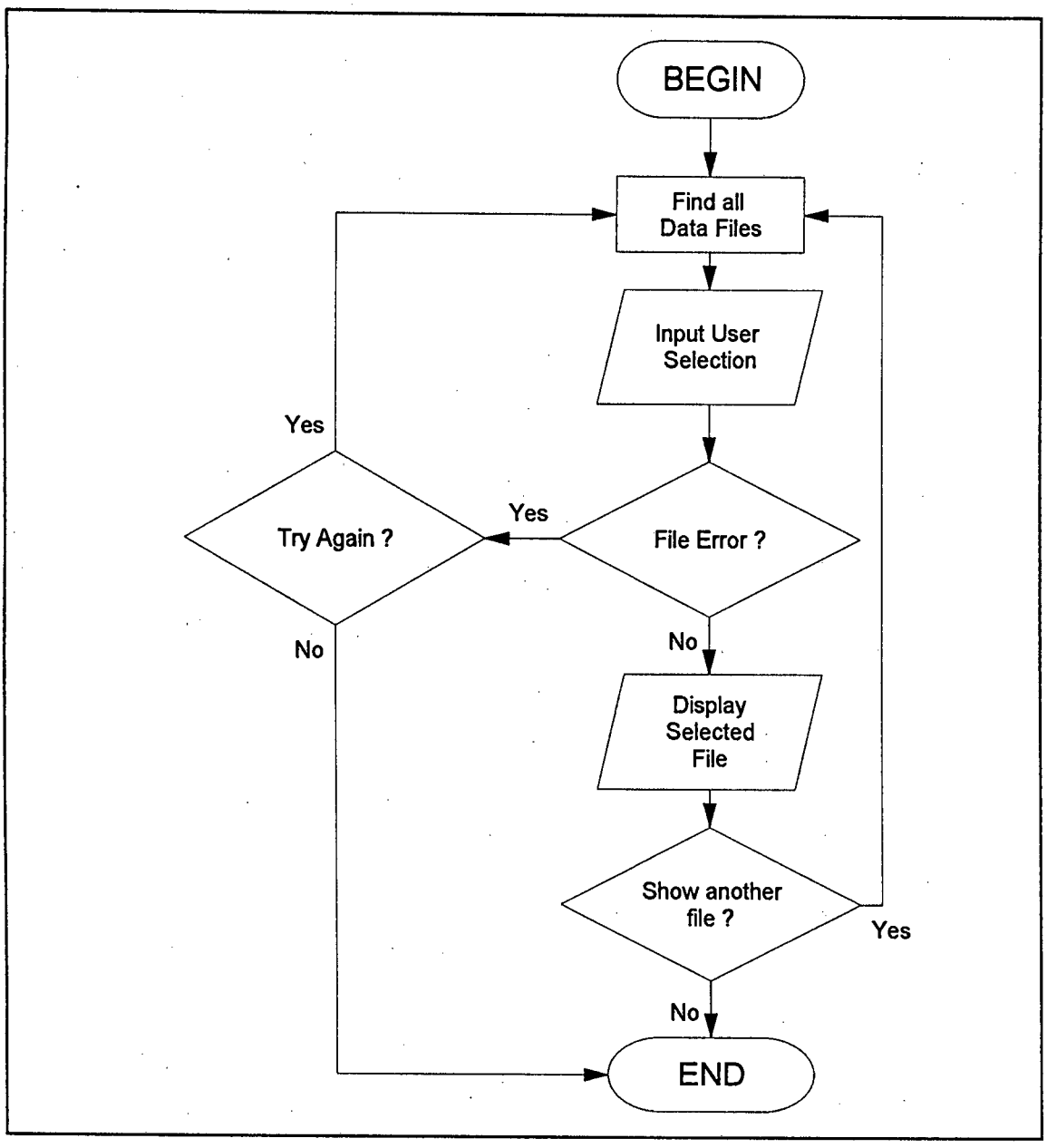


**FIGURE 4.4 Flow diagram of the Retrieve procedure**

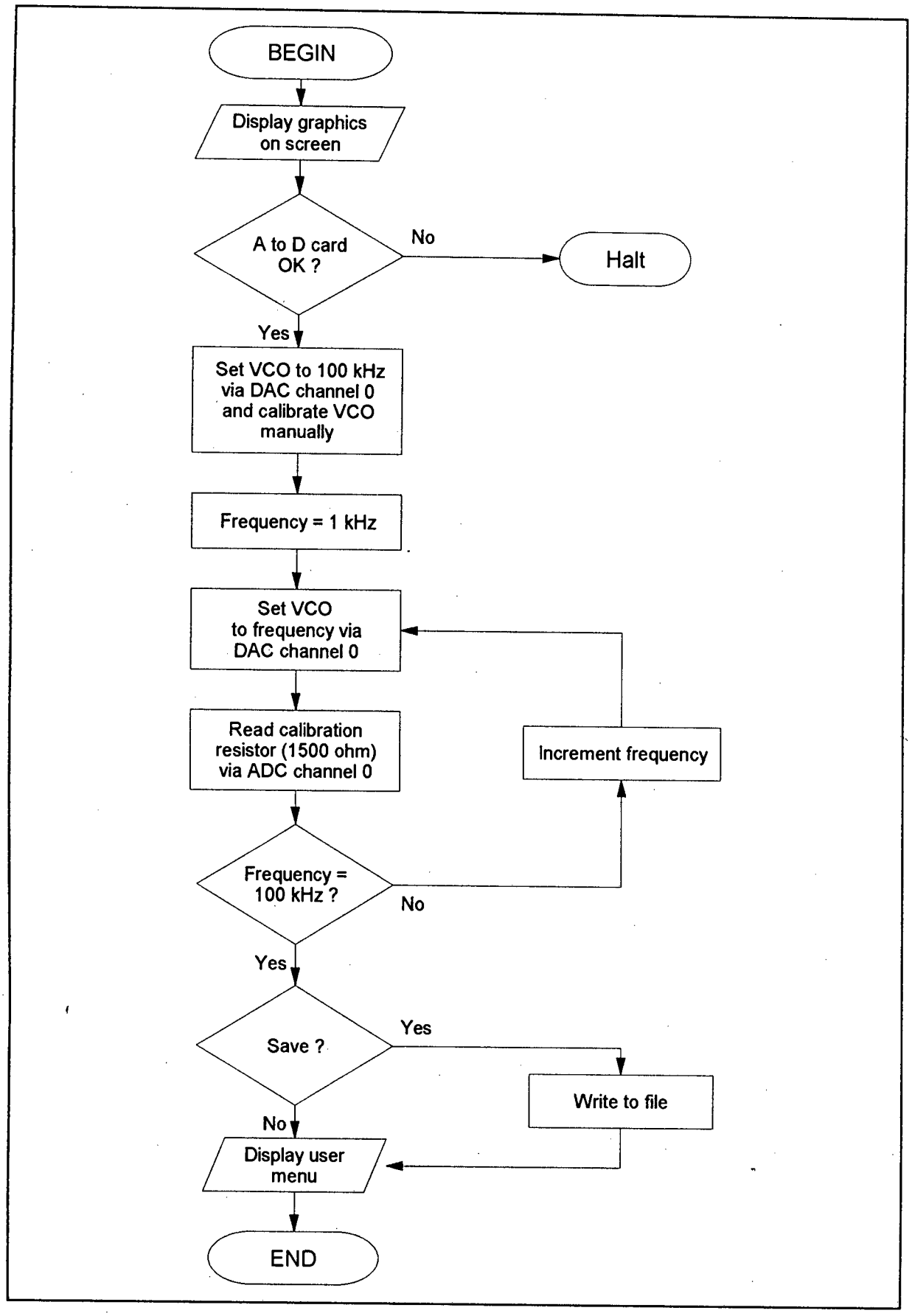


**FIGURE 4.5 Flow diagram of the Calibration procedure**

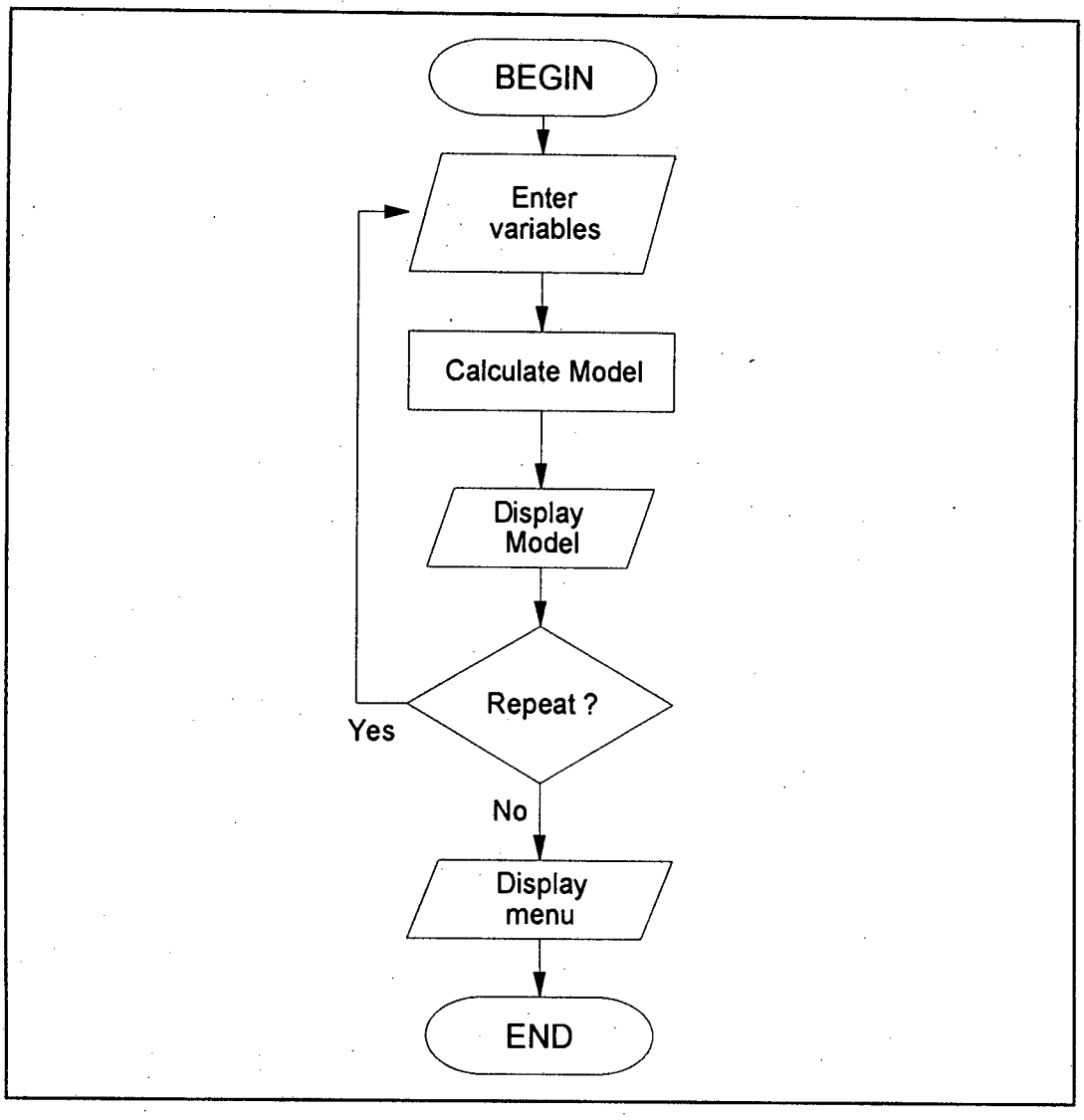


**FIGURE 4.6 Flow diagram of the Model procedure**

## 4.6 IMPLEMENTATION OF THE VARIABLE FREQUENCY BIOIMPEDANCE ANALYSER

### 4.6.1 INTRODUCTION

Implementing the variable frequency whole-body impedance analyser required the following :

1. Determining the impedance range over which the Variable Frequency WBI Analyser could operate with less than 1 % error.

2. Measuring the impedance seen by the current source in a small sample of dehydrated and normally hydrated children.

3. Measuring the WBI from 1 to 100 kHz of a small sample of dehydrated children before and after rehydration.

4. Using the computer model for WBI based on the electrical model of biological tissue (equation 4.1) to simulate the change in WBI seen in dehydrated children during rehydration.

### 4.6.2 METHODS

#### (a) Accuracy of Variable Frequency Whole Body Impedance Analyser

The equipment was tested firstly by measuring the impedance of prescision resistors and capacitors of known value. The method used is described in appendix I. These tests showed the range of impedances that could be measured accurately at each frequency.

**(b) Total impedance load seen by the constant current source in a sample of normally hydrated and dehydrated children**

A random sample of eleven children was selected from ward A9 of the Red Cross War Memorial Childrens' Hospital. Six had acute gastroenteritis and were dehydrated and five were normally hydrated children seen in the outpatient department of the same hospital. WBI was measured using the guidelines described earlier and given in appendix G with the current injecting electrodes placed distally. The voltage sensing electrodes were then connected to the current injecting electrodes so that the total voltage drop between the current injecting electrodes was measured. The current passes from one electrode through the skin, through the body fluids and through the skin again to the second electrode (see appendix D). Thus the voltage drop across the current injecting electrodes is equal to WBI plus twice the skin impedance and is the actual impedance seen by the constant current source. Macmed ECG electrodes (Macmed Cape Town, # P810) were used. These were cut into strips of 1 cm by 3 cm and these dimensions were kept constant for all measurements as skin impedance is a function of the electrode size.

**(c) Whole Body Impedance of Dehydrated Children at variable frequencies during rehydration**

The WBI of four dehydrated children selected at random from ward A9 of the same hospital was measured. The measurement protocol and electrodes placement described in appendix G was used. WBI was measured from 1 to 100 kHz before and after rehydration. Figures 4.7 and 4.8 shown the equipment used and a measurement being taken.

**FIGURE 4.7 Picture of the WBI Analyzer with the Escort function generator on top of it and the personal computer showing a typical measurement on the screen**

**FIGURE 4.8 Picture showing the measurement of WBI in subject MP before rehydration**

## (d) Comparison of Measured values of Whole-Body Impedance at variable frequencies with the Electrical Model

The electrical model of the body (equation 4.1) was used to simulate the change in WBI seen with rehydration and to examine the effect of varying each of the components of the equation (intracellular resistance, extracellular resistance and cell membrane capacitance).

## 4.6.3 RESULTS

### (a) Variable Frequency Whole Body Impedance Analyser Accuracy

The shaded area of figure 4.9 shows the region in which the instrument is able to measure impedance with ≤ 1% error. The equipment is able to measure impedance with less than 1 % error from 200 Ω to 11 kΩ at 1kHz and from 200 Ω to 5 k Ω at 100 kHz.

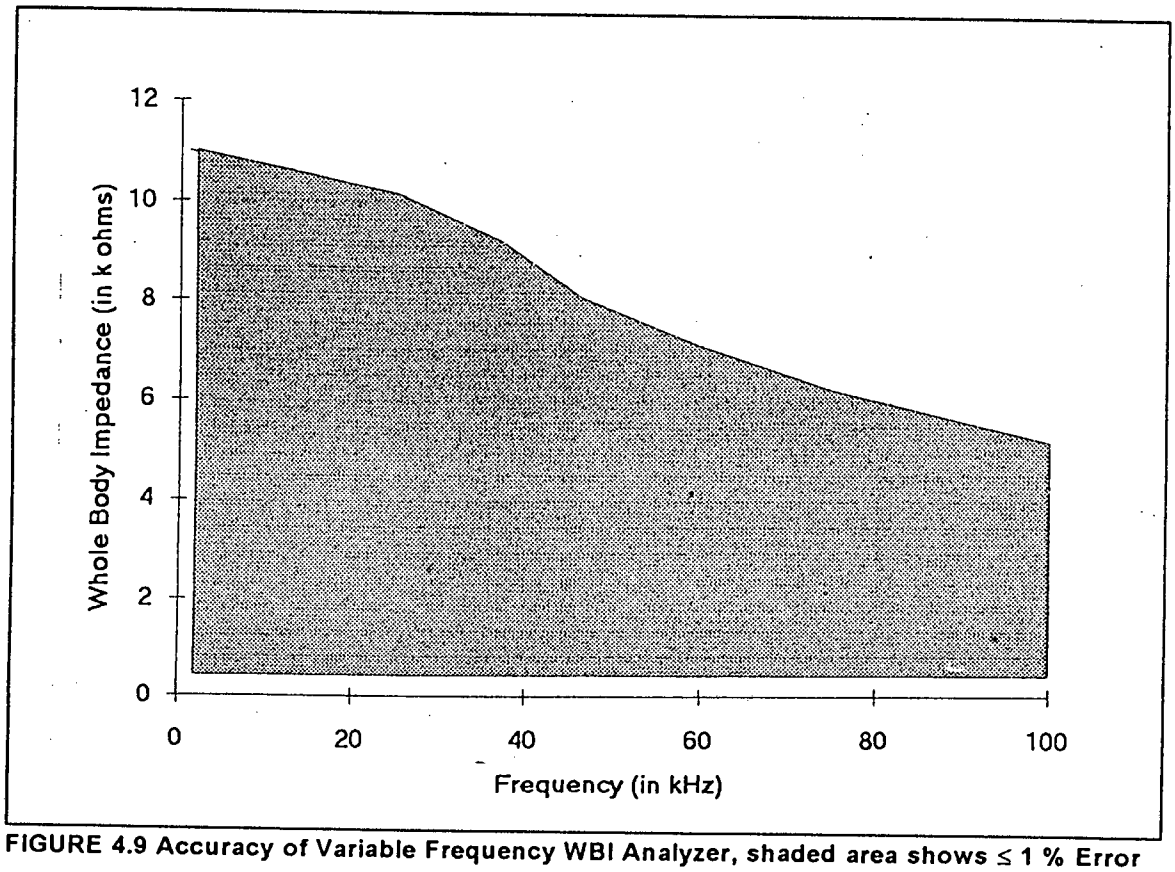


**FIGURE 4.9 Accuracy of Variable Frequency WBI Analyzer, shaded area shows ≤ 1 % Error**

**(b) Total impedance load seen by the constant current source in a sample of normally hydrated and dehydrated children**

Figure 4.10 shows the range of impedances seen by the current source, measured between the current injecting electrodes. The upper limit of the 1 % error range is shown again for comparison. Eleven children were sampled. Six were dehydrated and five were normally hydrated. Five were male and six female. The minimum mass was 2.84 kg and the maximum 12 kg. The minimum height was 50 cm and the maximum 87.5 cm.

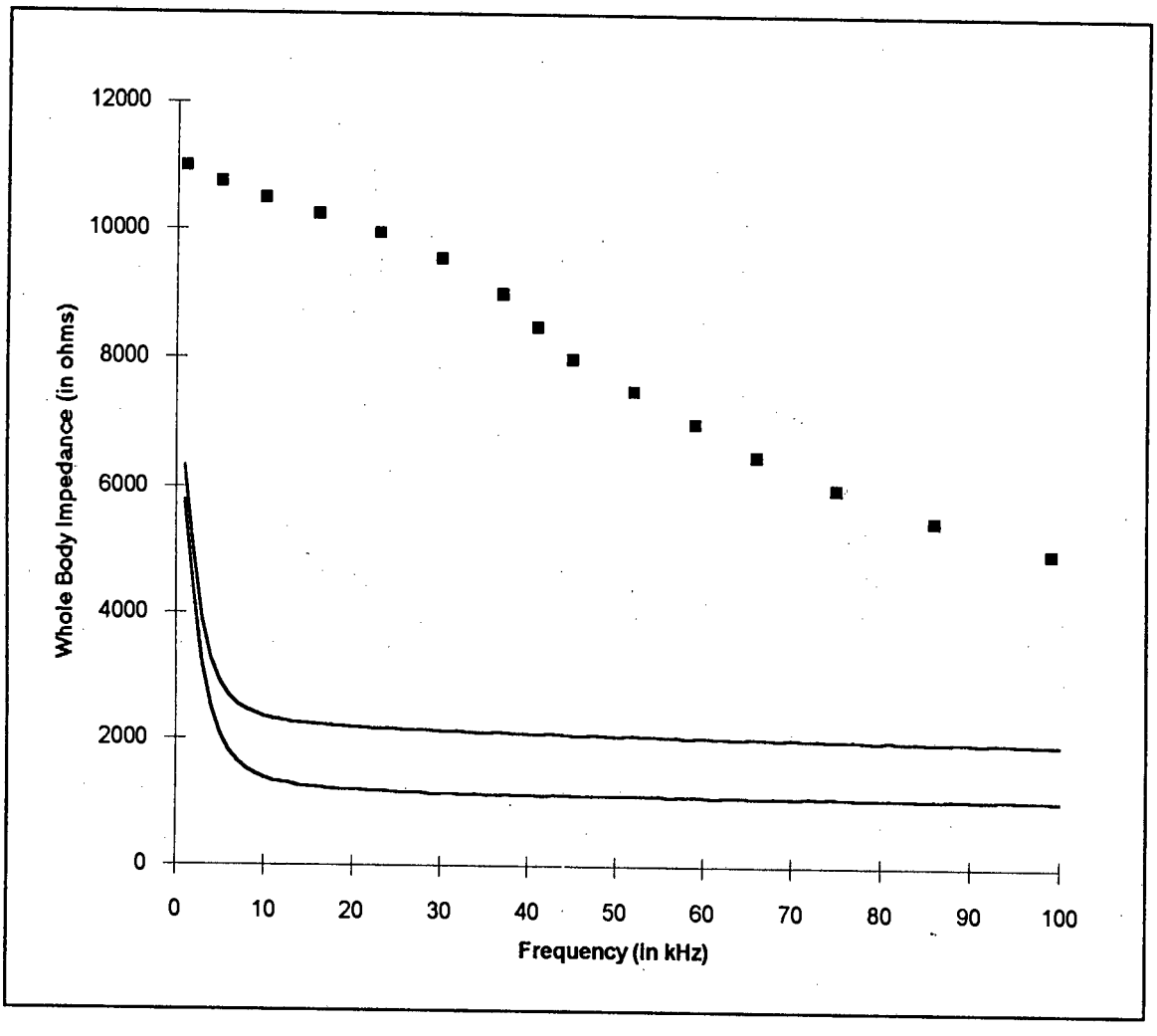


**FIGURE 4.10 Upper and lower limits of impedances between the current sensing electrodes. Markers ( ■ ) show the upper limit of the equipment for accurate readings**

## (c) Whole Body Impedance of Dehydrated Children at variable frequencies during rehydration

Figures 4.11 to 4.14 show the WBI at each frequency between 1 kHz and 100 kHz of dehydrated children before and after rehydration for four different children. Age, sex, mass, height and percentage dehydration are given in table 4.1 below.

**TABLE 4.1 Age, sex, mass, height and % dehydration of the group measured for variable frequency WBI**

| Name | Age (in months) | Sex | Height (in cm) | Rehydrated Mass (in kg) | % Dehydration |
|---|---|---|---|---|---|
| PM | 11.1 | M | 73.3 | 8.82 | 4.3 |
| CS | 4.9 | F | 54.5 | 3.88 | 6.2 |
| KN | 9.8 | F | 68.7 | 8.32 | 11.3 |
| CJ | 6.4 | M | 65.3 | 6.2 | 11.9 |

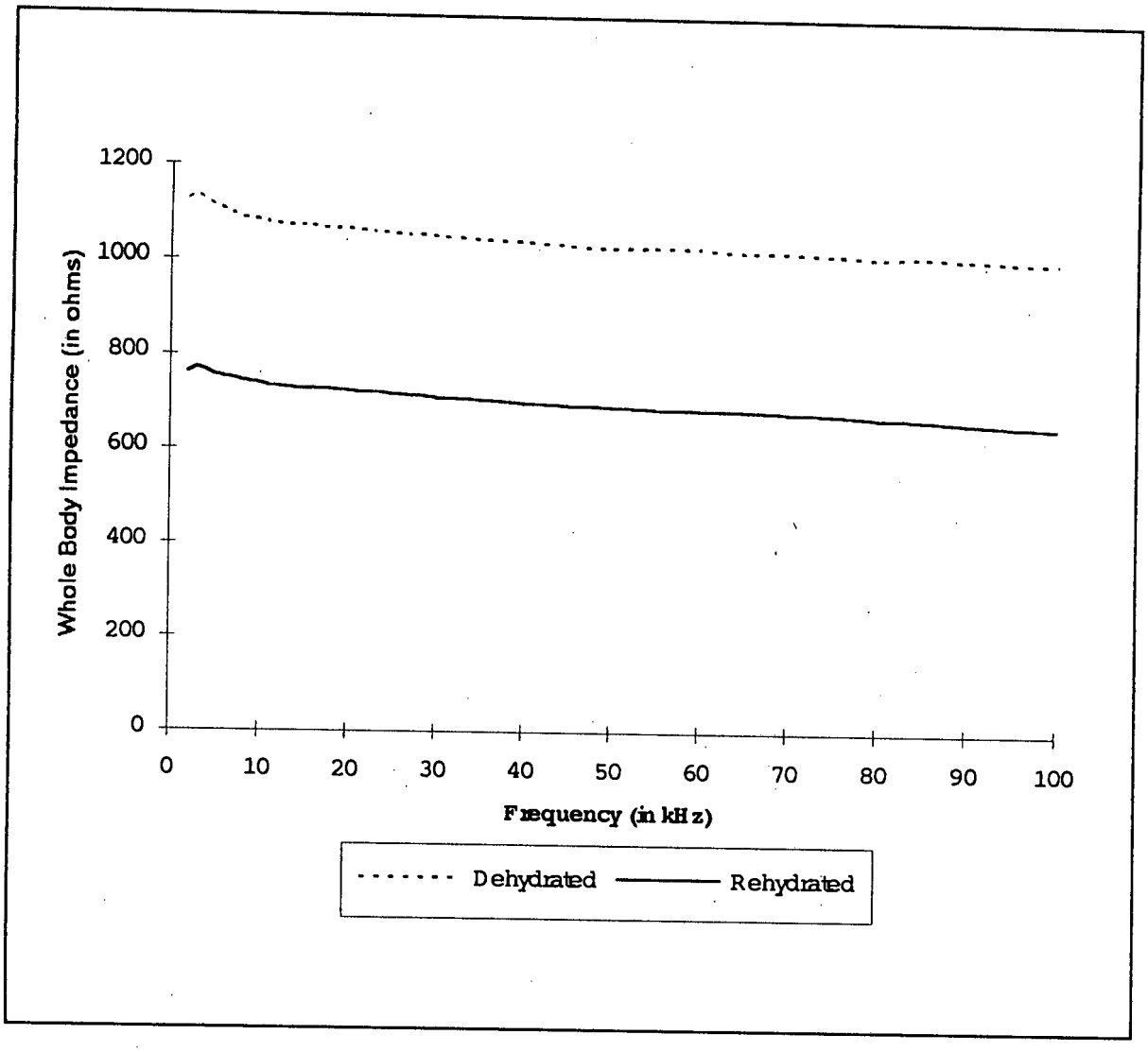


**FIGURE 4.11 WBI from 2 kHz to 100 kHz before and after rehydration in subject PM**

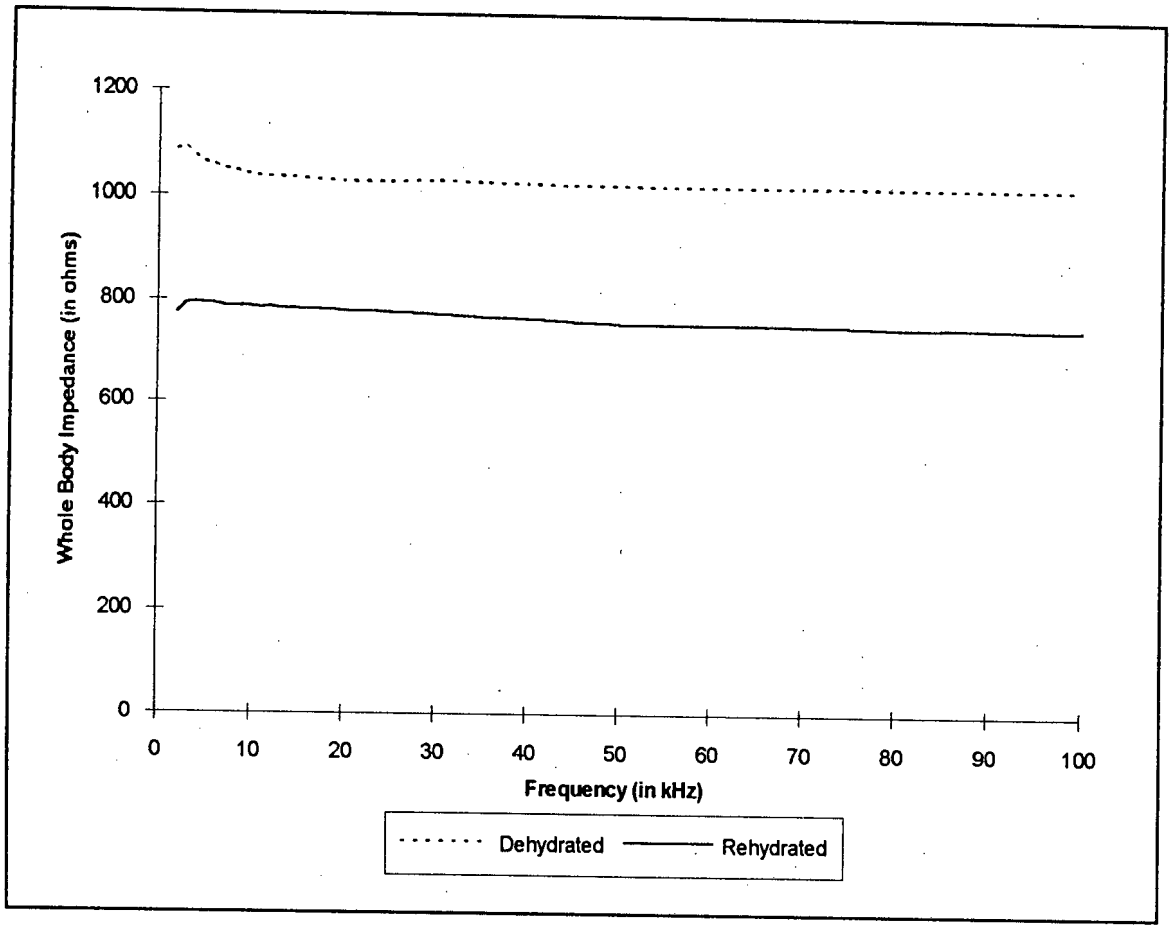


**FIGURE 4.12 WBI from 2 kHz to 100 kHz before and after rehydration in subject CS**

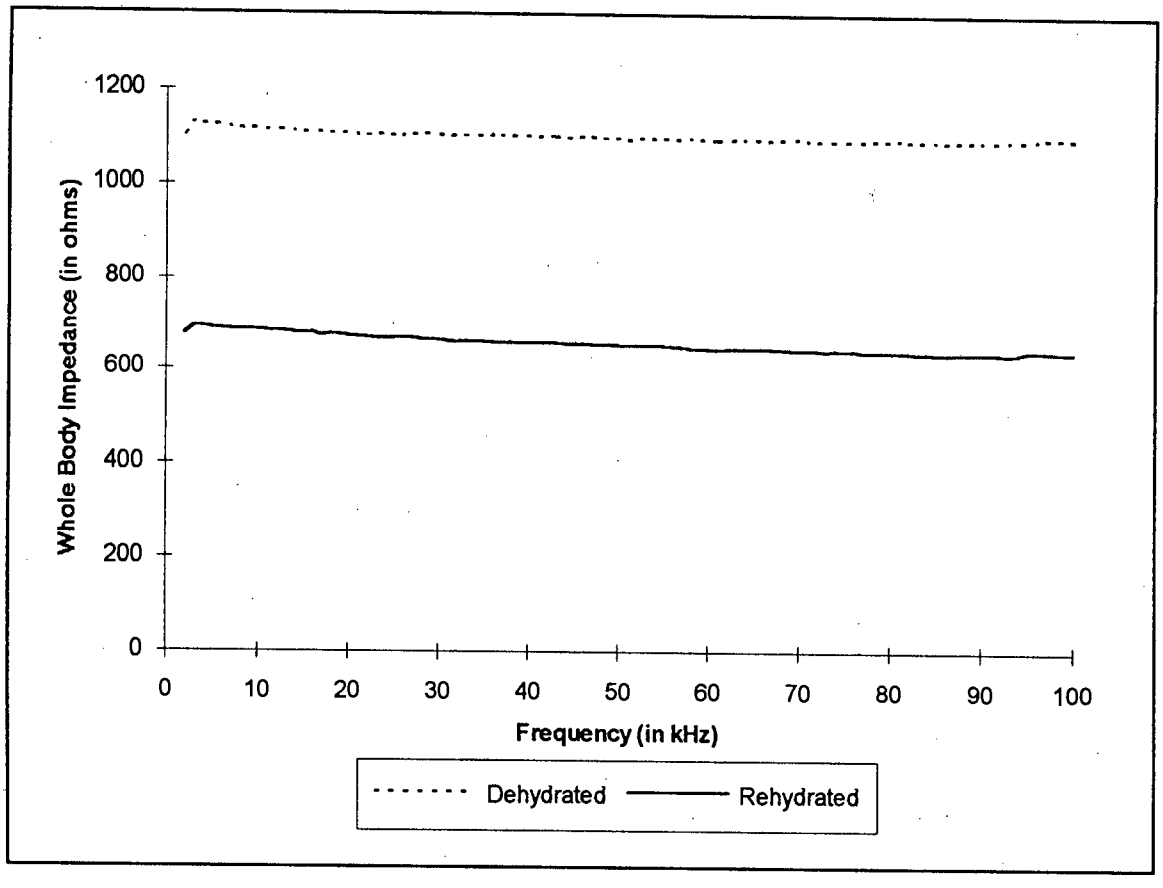


**FIGURE 4.13 WBI from 2 kHz to 100 kHz before and after rehydration in subject KN**

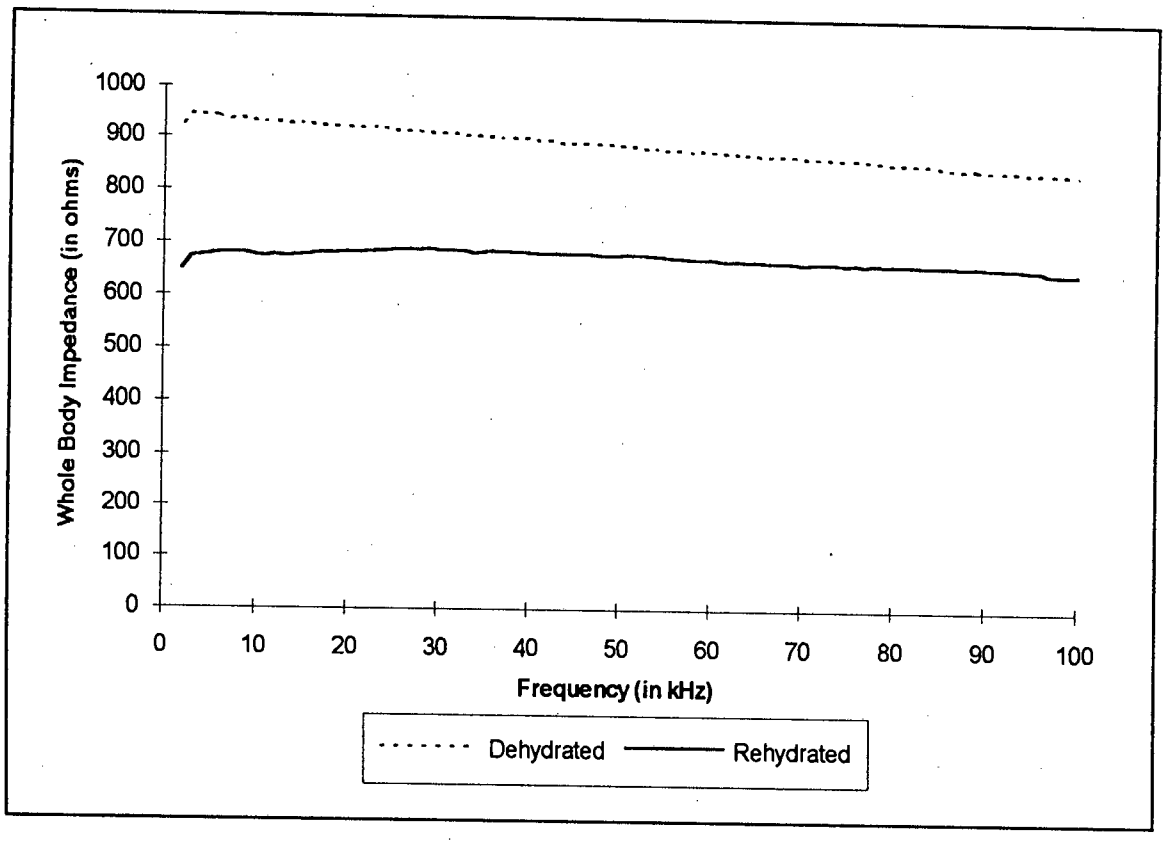


**FIGURE 4.14 WBI from 2 kHz to 100 kHz before and after rehydration in subject CJ**

## (d) Comparison of Measured change in Whole Body Impedance at variable frequencies versus that predicted from the model

Figures 4.15 to 4.17 show the changes in WBI resulting from changing one of the values of the intracellular resistance (Ri), the extracellular resistance (Re) or the cell membrane capacitance (C) using the model given in equation 4.1 and keeping the other variables constant.

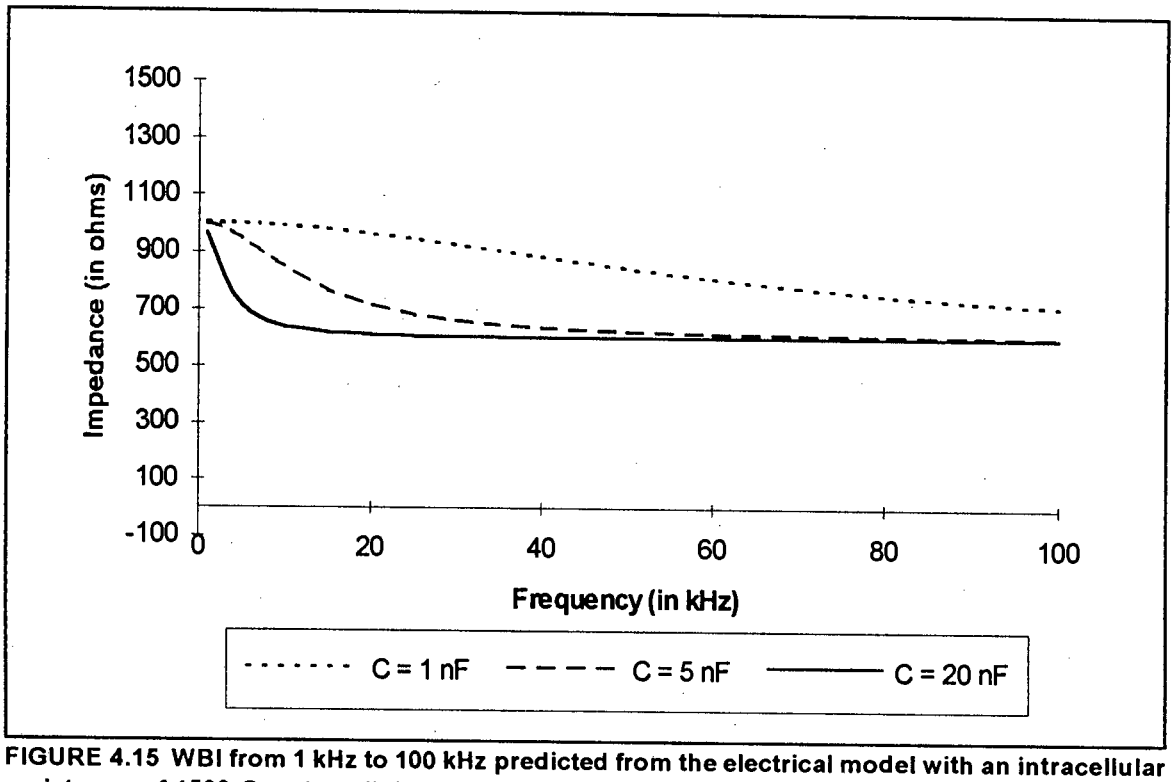


**FIGURE 4.15 WBI from 1 kHz to 100 kHz predicted from the electrical model with an intracellular resistance of 1500 Ω, extracellular resistance of 1000 Ω and varying capacitance**

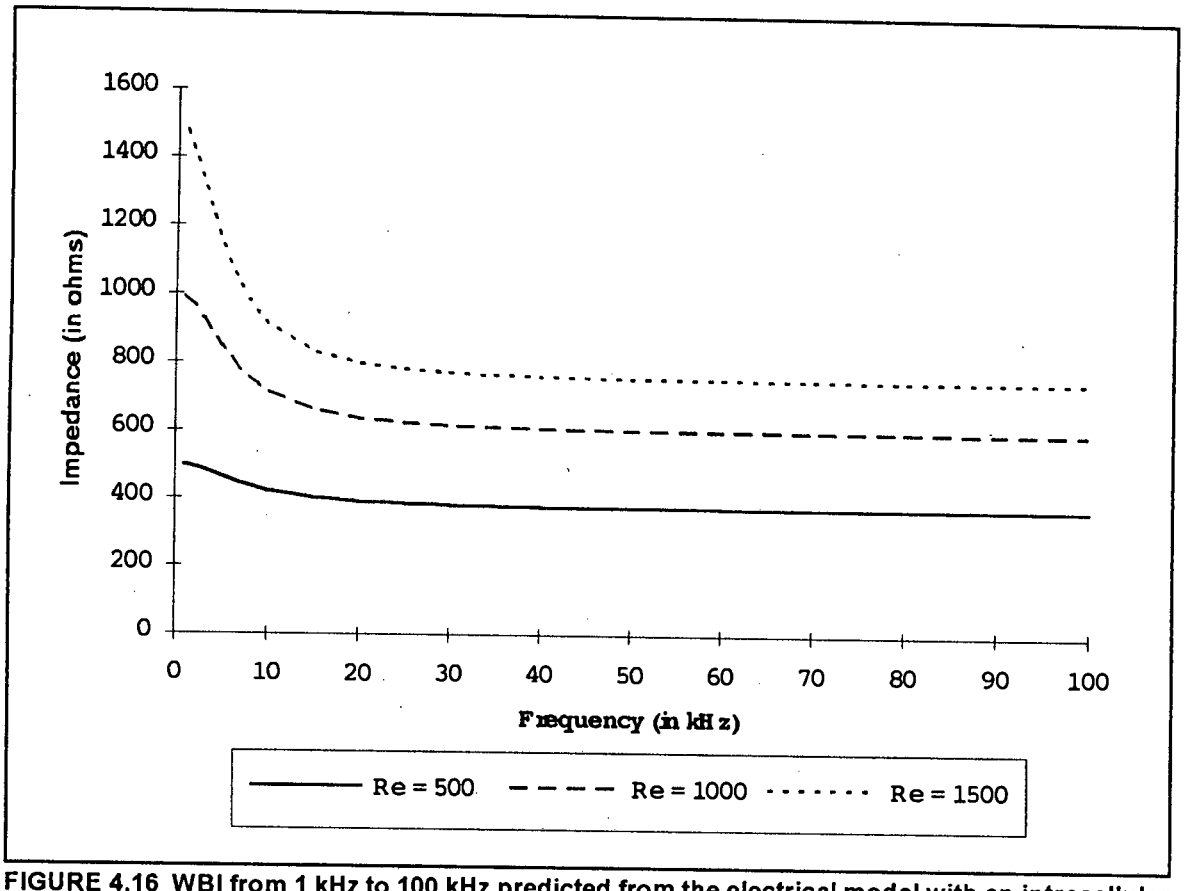


**FIGURE 4.16 WBI from 1 kHz to 100 kHz predicted from the electrical model with an intracellular resistance of 1500 Ω, capacitance of 10 nF and varying extracellular resistance**

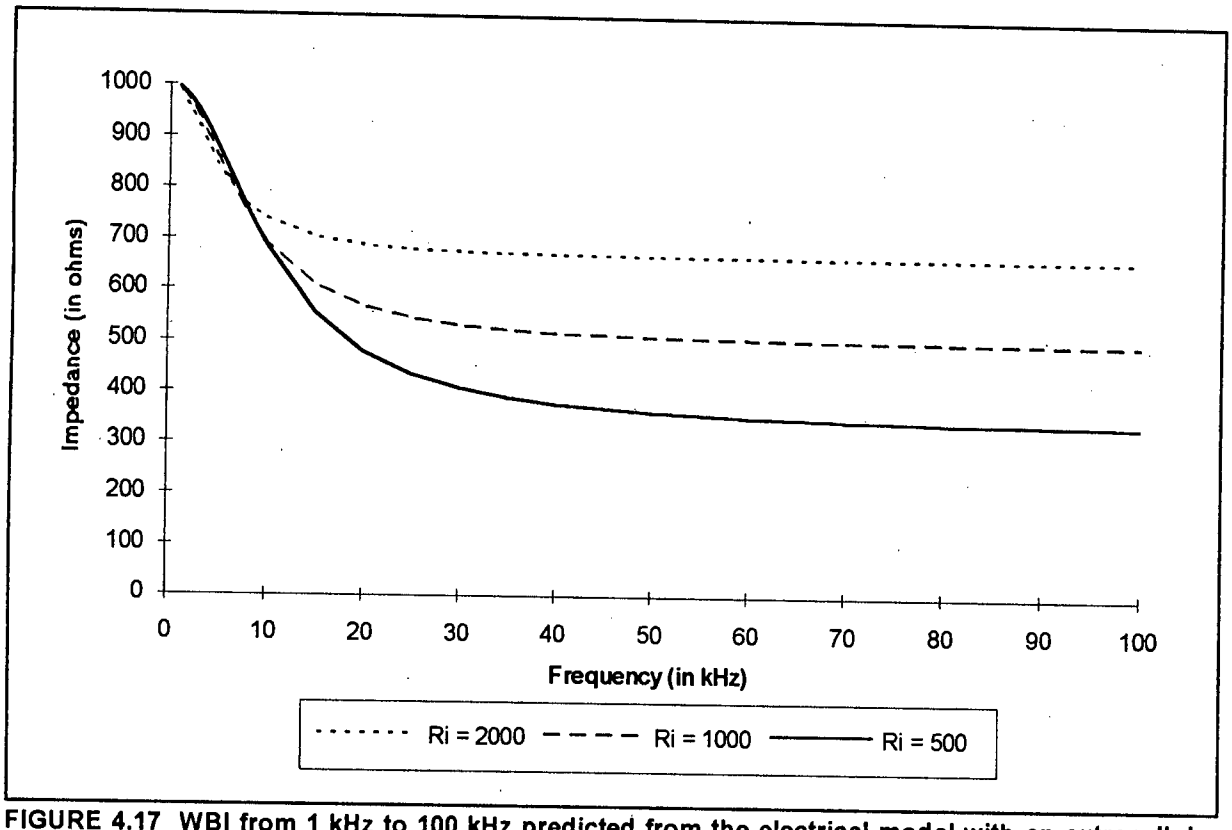


**FIGURE 4.17 WBI from 1 kHz to 100 kHz predicted from the electrical model with an extracellular resistance of 1000 Ω, capacitance of 10 nF and varying intracellular resistance**

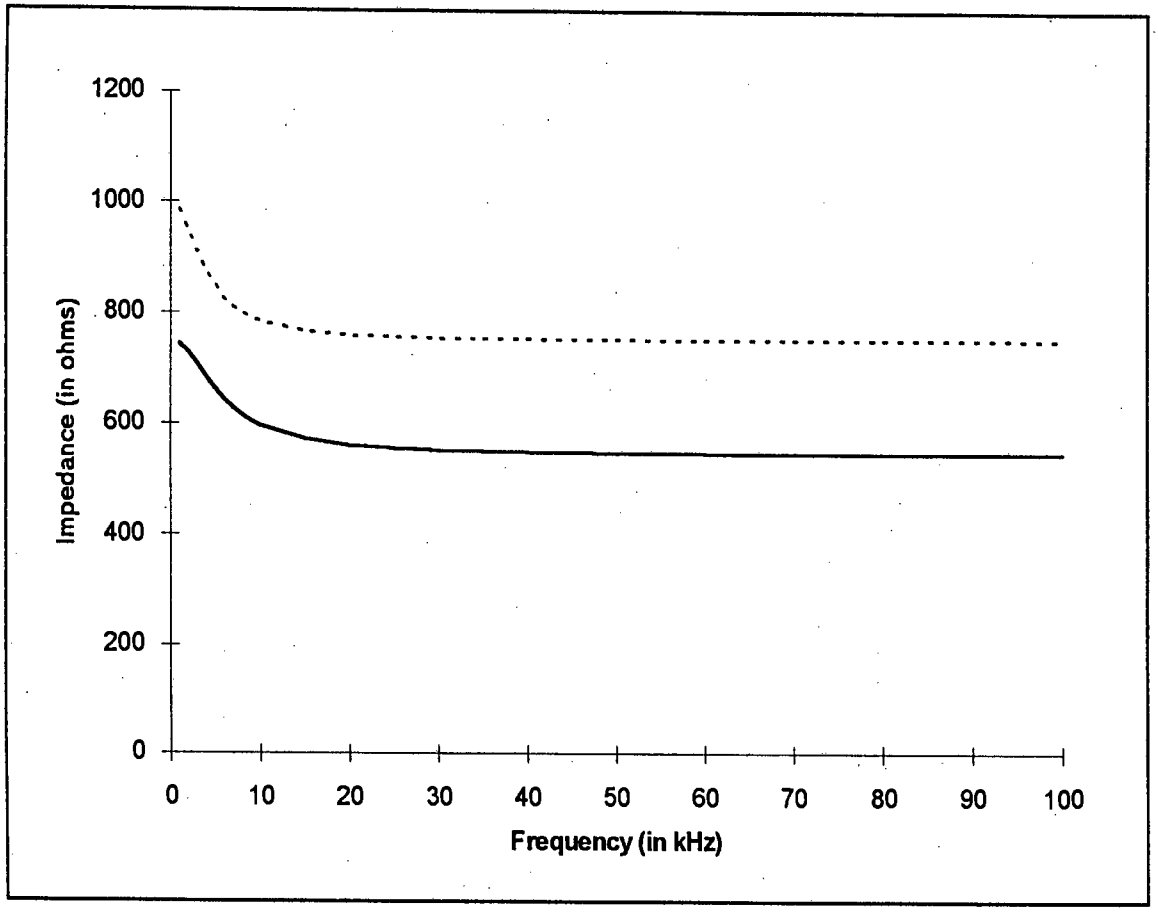


**FIGURE 4.18 Before (....) and after (__) rehydration simulated by changing the values for the intracellular and extracellular resistances in the electrical model.**

### 4.6.4 DISCUSSION

#### (a) Variable Frequency Whole Body Impedance Analyser Accuracy

Whole-body impedance is measured by passing a small alternating current through the body and measuring the potential difference developed across the body by this current. Two techniques have been described: the bipolar and the tetrapolar techniques. The bipolar method is invasive, requiring the placement of subcutaneous electrodes and in addition results in a non-homogenous electrical field in the vicinity of the electrodes which gives rise to additional errors in the measurement of bioimpedance [20]. For these reasons the tetrapolar method was used. A detailed description of the tetrapolar method is given in appendix D.

The constant current source must operate into an impedance load which is equal to the WBI and twice the skin impedance. Thus it was important to derive the range of load impedances over which the constant current source could operate accurately. A constant current of 300 μA was used which is well within the limits for electrical safety (see section 2.5). Figure 4.9 shows the impedance range at which the constant current source could operate to within 1% accuracy when tested as shown in appendix D. Load impedances down to 200 Ω at all frequencies could be measured accurately. The voltage drop across a load at 200 Ω is 1% of the resolution of the digital to analog convertor hence impedance loads lower than this cannot be measured accurately.

The upper range of load impedances for accurate measurement varied with frequency (Figure 4.9). At the low frequency limit (1 kHz) this was found to be 11 kΩ. A current of 300 μA RMS passing through an impedance load of 11 kΩ produces a voltage drop of 3.3 V RMS, or ± 4.67 V peak to peak. This instrument is battery operated so this voltage is enough to result in clipping by the operational amplifiers with resulting deterioration of accuracy. At the high frequency limit (100 kHz) the upper range for accurate measurement of load impedance was 5 kΩ.

**(b) Total impedance load in a sample of normally hydrated and dehydrated children**

The total impedance load seen by the current source was measured on 11 children, 6 were dehydrated and 5 normally hydrated. Figure 4.10 shows the upper and lower limits of impedances measured, together with the limits at which the instrument is accurate to 1%. As described above this is the sum of WBI and twice the skin impedance. As can be seen the range of impedances measured was from 5.8 kΩ to 6.2 kΩ at 1 kHz decreasing to 1 kΩ to 2.5 kΩ at 100 kHz.

Skin impedance is wide-ranging varying from a few hundred to a few thousand ohms per square centimeter of electrode area depending on the measurement frequency, skin wetness and the integrity of the stratum corneum [62]. In this study electrodes measuring 1 cm by 3 cm (3 $cm^2$) were used. It has been claimed that electrodes with less than 5 $cm^2$ should not be used for measuring frequencies less than 10 kHz [62]. More importantly, however, electrodes should not be less than 4 cm apart [34]. In children with small hands it may not be possible to satisfy both of these pre-requisites and for this reason small electrodes were used and as can be seen from figure 4.10 they were found to be accurate. As the sample tested was small it is accepted that there may be children whose skin impedance is greater than 11 kΩ at 1 kHz. Hence the recommendation is that wherever possible electrodes of at least 6 $cm^2$ (2 cm by 3 cm) be used for the current injecting electrodes (the distal pair) but that in children with smaller hands the 3 $cm^2$ electrodes may be necessary to maintain an adequate distance between the proximal and distal electrodes. The proximal electrodes (voltage sensing electrodes) are the inputs to the high impedance differential amplifier and have minimal current passing through them (a few pA) hence their size is far less critical.

**(c) Measurement of Whole Body Impedance at variable frequencies during rehydration**

Figures 4.11 to 4.14 show the change in WBI from 1 kHz to 100 kHz for four dehydrated children before and after rehydration. Three important observations are made. Firstly, the WBI of all the children, whether dehydrated or not, is greater at lower frequencies than at higher frequencies. Secondly, as with the WBI measurements done at 50 kHz, the WBI decreases during rehydration and this is seen over the entire frequency range. Thirdly, measurement of WBI at all frequencies from 1 kHz to 100 kHz is probably unnecessary and measurement of WBI at three frequencies namely: 1 kHz, 50 kHz and 100 kHz would probably be adequate. The decrease in impedance seen during rehydration is due to an increase in fluid in the body fluid compartments with a resultant decrease in the body compartment resistance.

**(d) The electrical model for the impedance of biological tissue**

The effect of varying individual components of the electrical model for the impedance of biological tissue is shown in figures 4.15 to 4.17. Varying the value of the cell membrane capacitance while the resistance of the external and internal fluid compartments remain constant (figure 4.15) seems to alter the impedance at higher frequencies more than at lower frequencies. Reactance is inversely proportional to capacitance so the larger the capacitor the smaller its reactance at a given frequency.

Decreasing the resistance of the extracellular fluid compartment (figure 4.16) decreases the impedance over the entire frequency range, while decreasing the value of the intracellular fluid compartment resistance decreases the impedance only at higher frequencies. This would be expected as the current only passes through this compartment at higher frequencies due to the reactance of the cell membrane.

The striking feature of the impedance curves measured before and after rehydration (figures 4.11 to 4.14) is the decrease in impedance over the entire frequency range. This is similar to that seen in the model when only the value of the resistance of the

extracellular compartment is decreased (figure 4.16). By substituting values for the other components the impedance change from dehydrated to rehydrated can be simulated (figure 4.18). The impression is that the change in impedance during rehydration occurs predominantly in the extracellular compartment. This is in agreement with previous studies [31].

From the model one would expect that the whole body impedance would increase significantly at lower frequencies. It is of note that this occurs when skin impedance is measured (figure 4.10). It is possible that this marked increase in WBI would be seen if measured at even lower frequencies. Measuring of WBI at lower frequencies may be dangerous because of the larger voltages required and the frequency of the constant source may be within the physiological range.

# CHAPTER 5
# CONCLUSION AND RECOMMENDATIONS

## 5.1 Single Frequency Studies at 50 kHz

Whole body impedance, measured at 50 kHz, in children aged 1 month to 2 years, was shown to be significantly greater in a group of dehydrated children than in a group of normally hydrated children of similar age, height and mass. After rehydration the WBI of the rehydrated group was no different from that of the normally hydrated group. The good correlation between height squared / WBI and mass is well established and this was found to be so for the three groups. There was no significant correlation between WBI and mass, height or age. The difference between the WBI of males and females in children of this age group was not significant.

It is hoped that this may form the basis for the electronic assessment of degree of dehydration in children with diarrhoeal disease and in children with other abnormalities of fluid balance. In addition the insensitivity of this method to GIT fluids makes this method ideal for assessing response to therapy in these children .

## 5.2 Variable frequency studies

A variable frequency whole body impedance analyzer able to measure WBI from 1kHz to 100 kHz was designed and tested. It was able to accurately measure impedance loads from 200 Ω to 11 kΩ at the lowest frequency (1 kHz) and from 200 Ω to 5 kΩ at the highest frequency (100 kΩ). The impedance load of the body seen by the constant current generator is equal to the sum of WBI and twice the skin impedance. This was measured on a small sample of dehydrated and normally hydrated children using 3 $cm^2$ electrodes and was found to be well with these accuracy limits. In order

to avoid inaccurate readings it is recommended that electrodes of 6 $cm^2$ be used particularly if lower frequencies are to be measured.

The electrical model for the impedance of biological tissues was compared to the measurements recorded on a small sample of dehydrated children. It was found that the change in impedance during rehydration most closely resembled the change seen when the resistance of the extracellular compartment was decreased. The implication is that the fluid gain during rehydration is predominantly into this compartment.

### 5.3 Future Studies

Whole-body impedance offers an objective method of assessing the degree of dehydration in children with diarrhoeal disease and in children with other abnormalities of fluid balance. Due to its low cost, ease of use and non-invasive nature it is ideally suited to use in the primary health care centers of the third world where many of these illnesses are seen. In this setting it may be of use as an adjunct to clinical skills in the assessment of degree of dehydration, response to oral rehydration therapy and as an indication for referral to more advanced treatment centers. It is recommended that further studies be carried out with this equipment in the primary health care setting.

The ratio of WBI measured at 1 kHz to WBI measured at 100 kHz has been proposed as a method of assessing the distribution of fluid between the ECF (WBI at 1 kHz) and TBW (WBI at 100 kHz) [36]. Such a ratio may be independent of age, mass, height, sex and other interfering variables and hence it is proposed that this ratio be measured in gastroenteritis and in other conditions of abnormal fluid balance.

Children with nutritional disorders such as protein losing enteropathy, kwashiorkor and marasmus are known to have abnormal distribution of body fluid. In particular, children with kwashiorkor (protein energy malnutrition) are often oedematous due to increased extracellular fluid. This fluid is known to shift into the intracellular compartment during treatment. Measurement of WBI at both high and low frequencies may be a useful method of assessing the severity of kwashiorkor and response to therapy.

## REFERENCES


1. ANONYMOUS
1992
Red Cross War Memorial Childrens' Hospital Annual Report for 1990/1991.
Cape Town.

2. BANWELL JG.
1986
Pathophysiology of diarrhea
In: Gorbach SL ed. *Infectious diarrhoea*
Boston: Blackwell.

3. BAUMGARTNER RN, CHUMLEA WC AND ROCHE AF.
1989
Estimation of body composition from bioelectric impedance of body segments.
*Am J Clin Nutr*, **50**: 221-6.

4. BEATTY DW, MANN MD, DE V. HEESE H, BERGER GMB.
1974
Acute Dehydrating Gastro-enteritis in Undernourished Infants.
*S Afr Med J*, **48**: 1563-1568.

5. BERGER GMB AND SACKS SS
1987
Chemical Pathology
In : Cook R ed. Peadriatric Handbook 1st Ed.
Pretoria : HAUM.

6. BOULIER A, FRICKER J, THOMASSET AL AND APFELBAUM.
1990
Fat-free mass estimation by the two-electrode impedance method.
*Am J Clin Nutr*, **52**: 581-5.

7. BOWIE MD.
1960
The management of gastro-enteritis with dehydration in out-patients.
*S Afr Med J* ; **34**: 344-348.

8. BULLOCK J.
1984
Renal Physiology
In: Bullock J,Boyle J, Wang MB,Ajello RR eds. *Physiology*
Pennsylvania: Harwal

9. CHALET MA, MCCUTCHEON MJ, REDDY S, PEARMAN PL, HUNTER GR, WEINER RL.
1988
Electrical impedance in assessing human body composition: the BIA method. *Am J Clin Nutr* ; **47**: 798-792.

10. CHUMLEA WC, BAUMGARTNER RN, ROCHE AF
1988
Specific resistivity used to estimate fat-free mass from segmental body measures of bioelectrical impedance.
*Am J Clin Nutr* ;**48**: 7-15

11. COHEN MB.
1991
Etiology and mechanisms of acute infectious diarrhoea in infants in the United States. *J Paeds* ; **118(4) part 2**; S34-S39.

12. COHN SH.
1985
How valid are bioelectric impedance measurements in body composition studies?
*Am J Clin Nutr* ; **42**: 889-890.

13. CONWAY JM, NORRIS KH AND BODWELL CE.
1984
A new approach for the estimation of body composition: infrared interactance.
*Am J Clin Nutr* ; **40**: 1123-1130.

14. COOVADIA HM.
1984
Gastro-Intestinal Disorders.
In: Coovadia HM and Loening WEK, eds. *Paediatrics and child health.*
Cape Town : Oxford University Press.

15. COTTERILL AM AND WALKER-SMITH JA .
1986
Gastro-Intestinal Tract.
*Br Med Bull* ; **42(2)**: 176-180.

16. DARROW D.
1946
The retention of electrolyte during recovery from severe dehydration due to diarrhoea. *J Pediatr* ; **28(5)**: 515-540.

17. DAVIES PSW, PREECE MA, HICKS CJ, HALLIDAY D.
1988
The prediction of total body water using bioelectrical impedance in children and adolescents.
*Ann Hum Biol* ; **15(3)**: 237-240.

18. DEURENBERG P, VAN DER KOOIJ, EVERS P AND HULSHOF T.
1990
Assessment of body composition by bioelectrical impedance in a population aged > 60 years.
*Am J Clin Nutr* ; **51**: 3-6.

19. DE VRIES PMJM, MEIJER JH, OE LP, VAN BRONSWIJK H, SCHNEIDER H AND DONKER AJM.
1987
Conductivity measurements for analysis of transcellular fluid shifts during haemodialysis.
*Trans Am Soc Artif Intern Organs* ; **33**: 554-556.

20. DE VRIES PMJM, KOUW PM, MEIJER JH, OE LP, SCHNEIDER H AND DONKER AJM.
1988
Changes in blood parameters during haemodialysis as determined by conductivity measurements.
*Trans Am Soc Artif Organs* ; **34**: 623-626.

21. DE VRIES PMJM, MEIJER JH, VLAANDEREN K, VISSER V, OE PL, DONKER AJM AND SCHNEIDER H.
1989
Measurement of transcellular fluid shift during haemodialysis: part 2 *In vitro* and clinical evaluation.
*Med & Biol Eng & Comput* ; **27**: 152-158.

22. FEIG PU AND MCCURDY DK.
1977
The hypertonic state.
*N Engl J Med* ; **297(26)**: 1444-1453.

23. FJELD CR, FREUNDT-THURNE J, SCHOELLER DA.
1990
Total Body Water Measured by 18O Dilution and Bioelectrical Impedance in Well and Malnourished Children.
*Ped Res* ; **27(1)**: 98-102.

24. FULLER NJ AND ELIA M.
1989
Potential use of bioelectrical impedance of the 'whole body' and of body segments for the asssessment of body composition: comparison with densitometry and anthropometry.
*European Journal of Clinical Nutrition* ; **43**: 779-791.

25. GEDDES LA AND BAKER LE.
1968
*Applied Biomedical Instrumentation 2nd Ed.*
New York : John Wiley and sons.

26. GIRANDOLA RN, WISWELL RA AND ROMERO G.
1977
Body composition changes resulting from fluid ingestion and dehydration.
*Res Q* ; **48(2)**: 299-303.

27. GOOVAERTS HG, DE VRIES FR, MEIJER JH, DE VRIES PMJM, DONKER AJM AND SCHNEIDER H.
1988
Microprocessor-based system for measurement of electrical impedances during haemodialysis and in postoperative care.
*Med Biol Eng Comput* ; **26**: 75-80.

28. GOU S, ROCHE AF, HOUTKOOPER L.
1989
Fat-free mass in children and young adults predicted from bioelectric impedance and anthropometric variables.
*Am J Clin Nutr* ; **50**: 435-443.

29. HAY IT.
1989
Age and admission weight as predictors of mortality in gastro-enteritis.
*S Afr Med J* ; **76**: 483-484.

30. HILL ID, MANN MD AND BOWIE MD.
1981
Hypernatraemic dehydration.
*S Afr Med J* ; **59**: 479-481.

31. HILL ID.
1981
*Hypernatraemic dehydration in children with diarrhoeal disease.*
University of Cape Town: MD Thesis

32. HILL ID.
1989
Oral rehydration therapy - South African Paediatric Association recommendations
*S Afr Med J* ; **76**: 461-462

33. HOFFER EC, MEADOR CK, SIMPSON DC.
1969
Correlation of whole-body impedance with total body water volume.
*J Appl Physiol* ; **27(4)**: 531-534.

34. HOFFER EC, MEADOR CK, SIMPSON DC.
1970
A relationship between whole body impedance and total body water volume.
*Ann NY Acc Sci* ; **197**: 452-461.

35. HOUSEHAM KC AND BOWIE MD.
1988
Epidemiological factors in acute infectious infantile diarrhoea in Cape Town.
*S Afr Med J* ; **73**: 346-349.

36. JENIN P, LENOIR J, ROULLET C, THOMASSET AL, DUCROT H.
1975
Determination of body fluid compartments by electrical impedance measurements.
*Aviat Spac Environ Med* ; **46**: 152-155

37. KATCHER AL, LEVITT M AND SWEET A.
1953
Alterations of fluid and electrolyte distribution and renal function in diarrhoea of infancy.
*J Clin Invest* ; **32**: 1013-1024.

38. KHALED AM, MCCUTCHEON MJ, REDDY S, PEARMAN PL, HUNTER GR AND WIENSIER RL.
1988
Electrical impedance in assessing human body composition: the BIA method.
*Am J Clin Nutr* ; **47**: 789-792.

39. KOOH SW AND METCOFF J.
1963
Physiologic considerations in fluid and electrolyte therapy with particular reference to diarrhoeal dehydration in children.
*J Paediatr* ; **62**: 107-131.

40. KUSHNER RF AND SCHOELLER DA.
1986
Estimation of total body water by bioelectrical impedance analysis.
*Am J Clin Nutr* ; **44**: 417-24.

41. LOGAN RW AND ARNEIL GC.
1984
Chapter 10 : Fluid, electrolytes and acid-base disturbances.
In : Forfar JO and Arneil GC eds. *Textbook of paediatrics 3rd Ed.*
Edinburgh : Churchill Livingston.

42. LOZANO A, ROSELL J AND PALLAS-ARENY R.
1990
Two-frequency impedance plethysmograph: real and imaginary parts.
*Med & Biol Eng & Comput* ; **28**: 38-42.

43. LUKASKI HC AND JOHNSON PE.
1985
A simple, inexpensive method of determining total body water using a tracer dose of $D_2O$ and infrared absorption of biological fluids.
*Am J Clin Nutr* ; **41**: 363-370.

44. LUKASKI HC, JOHNSON PE, BOLOCHUK WW AND LYKKEN GI.
1985
Assessment of fat-free mass using bioelectrical impedance measurements of the human body.
*AM J Clin Nutr* ; **41**: 810-817.

45. LUKASKI HC, BOLONCHUK WW, HALL CB AND SIDERS WA.
1986
Validation of tetrapolar bioelectrical impedance methods to asses human body composition.
*J Appl Physiol* ; **60(4)**: 1327-1332.

46. MCDOUGALL D AND SHIZGAL HM.
1986
Body composition measurements from whole body resistance and reactance.
*Surgical Forum* ; **36**: 42-44.

47. MACKENZIE A, BARNES G AND SHANN F.
1989
Clinical signs of dehydration in children.
*Lancet* ; **Sept 9**: 605-607.

48. MARTORELL R, HABICHT JP AND HAAS J.
1989
Predicting total body water from bioelectrical impedance in children.
*Ann Hum Biol* ; **16(2)**: 173-174.

49. MAYFIELD SR, UAUY R AND WAIDELICK D.
1991
Body composition of low-birth-weight infants determined by using bioelectrical resistance and reactance.
*Am J Cln Nutr* ; **54**: 296-303.

50. MEIJER JH, DE VRIES PMJM, GOOVAERTS HG, OE PL, DONKER AJM AND SCHNEIDER H.
1989
Measurement of transcellular fluid shift during haemodialysis: part 1 method. *Med & Biol Eng & Comput* ; **27**: 147-151.

51. MOLINA S, ARANGO T, PINEDA O AND SOLOMONS NW.
1987
Response of bioelectrical impedance analysis (BIA) indices to rehydration therapy in severe infantile diarrhoea.
*Am J Clin Nutr* ; **45**: 837 (abstract).

52. MORTIMER EA.
1987
Child health in the developing world.
In : Berhman RE and Vaughan VC eds. *Nelson Textbook of Paediatrics 13th Ed*

Philadelphia : WB Saunders.

53. NYBOER J.
1959
*Electrical Impedance Plethysmography.*
Springfield,Ill : Thomas.

54. NYBOER J.
1970
Electrorheometric properties of tissues and fluids.
*Ann NY Acc Sci* ; **170(2)**: 410-420.

55. PATTERSON R, RANGANATHAN C, ENGEL R AND BERKSETH R.
1988
Measurement of body fluid volume change using multisite impedance measurements. *Med & Biol Eng & Comput* ; **26**: 33-37.

56. PEARMAN P, HUNTER G, HENDRICKS C AND O'SULLIVAN P.
1989
Comparison of hydrostatic weighing and bioelectrical imedance measurements in determining body composition pre- and postdehydration.
*JOSPT* ; **May**: 451-455.

57. ROBSON A.
1989
The pathophysiology of the body fluids.
In : Berhman RE and Vaughan VC eds. *Nelson Textbook of Paediatrics 13th Ed.*
Philadelphia : WB Saunders.

58. SCHOELLER DA, VAN STATEN E, PETERSON DW, DIETZ W, JASPAN J AND KLEIN PD.
1980
Total body water measurement in humans with $^{18}O$ and $^{2}H$ labeled water.
*Am J Clin Nutr* ; **33**: 2686-2693.

59. SEGAL KR, GUTIN B, PRESTA E, WANG J AND VAN ITALLIE TB.
1985
Estimation of human body composition by electrical impedance methods: a comparative study.
*J Appl Physiol* ; **58(5)**: 1565-1571.

60. SEGAL KR, VAN LOAN M, FITZGERALD PI, HODGDON JA AND VAN ITALLIE TB.
1988
Lean body mass estimation by bioelectrical impedance analysis: a four-site crossvalidation.
*Am J Clin Nutr* ; **47**: 7-14.

61. SEGAL KR, BURASTERO S, CHUN A, CORONEL P, PIERSON RN AND WANG J.
1991
Estimation of extracellular and total body water by multiple-frequency bioelectrical impedance measurements.
*Am J Clin Nutr* ; **54**: 26-29.

62. SETTLE RG, FOSTER KR, EPSTEIN B AND MULLEN JL.
1980
Nutritional assessment: Whole body impedance and body fluid compartments.
*Nutrition and Cancer* ; **2** , 1:72-80.

63. SWANSON DK AND WEBSTER JG.
1982
Simple design of an impedance plethysmograph.
*Med & Biol Eng & Comput* ; **20**: 461-465.

64. TEDNER B.
1983
Equipment using an impedance technique for automatic recording of fluid-volume changes during haemodialysis.
*Med & Biol Eng & Comput* ; **21**: 285-290.

65. THOMASSET A.
1962
Bio-electrical properties of tissue impedance measurements.
*Lyon Med* ; **207**: 107-118.

66. TWYMAN DL AND LIEDTKE RJ.
1987
*Bioelectrical impedance analysis of body composition.*
RJL Systems technical manual.

67. YACH D, STREBEL PM AND JOUBERT G.
1985
The impact of diarrhoeal disease on childhood deaths in the RSA, 1968 - 1985.
*S Afr Med J* ; **76(4)**: 472-475.

68. ZHENG E, SHAO S AND WEBSTER JG.
1984
Impedance of skeletal muscle from 1 Hz to 1 MHz.
*IEEE Trans Biomed Eng* ; **31**: 477-481.

# APPENDIX A

## Determination of the volume of a conductor from its impedance

The resistance of an electrical conductor is dependent on its physical dimensions, its configuration and its resistivity. The resistance of a cylindrical electrical conductor of length (L) in centimeters, cross sectional area (A) in square centimeters and specific resistivity (rho) in ohm centimeters is given by the following formula:

$$R = \rho\frac{L}{A} \qquad \textbf{(A1)}$$

Since the product of length and area is volume (V) multiplyilng both numerator and denominator by length (L) gives:

$$R = \rho\frac{L^2}{V} \qquad \textbf{(A2)}$$

Rearranging equation A2 gives:

$$V = \rho\frac{L^2}{R} \qquad \textbf{(A3)}$$

For alternating currents impedance (Z) is used instead of resistance (R) and equation A3 can be written as:

$$V = \rho\frac{L^2}{Z} \qquad \textbf{(A4)}$$

Thus the volume of an electrical conductor can be calculated from the product of the specific resistivity of the conductor and its length squared divided by its impedance.

Density is equal to mass per unit volume. Hence mass can calculated using the following equation:

$$m = \sigma\rho\frac{L^2}{Z} \qquad \textbf{(A5)}$$

Where m = mass and $\sigma$ = density ( $\sigma$ is used here because $\rho$, the usual symbol for density, is also the symbol for resistivity ). The slope of a plot of mass on $L^2/Z$ is thus the product of density and resistivity.

## APPENDIX B

## Determination of the change in volume of a conductor from the change in its impedance

The change in volume of a conductor can be determined from the change in its impedance and this principle will be used to calculate percentage dehydration. If the length of a cylindrical conductor is constant and its volume increased by an increase in its cross sectional area then the change in its impedance (delta Z) is proportional to the change in volume (delta V):

$$\begin{aligned}\Delta V &= V_1 - V_2 \\ &= \rho\frac{L^2}{Z_1} - \rho\frac{L^2}{Z_2} \\ &= \rho L^2\left(\frac{Z_2 - Z_1}{Z_1 . Z_2}\right) \\ &= \rho L^2\left(\frac{\Delta Z}{Z_1 . Z_2}\right) \qquad \textbf{(B1)}\end{aligned}$$

## APPENDIX C

### Electrical model of the body

Biological tissue consists of numerous cells bonded together. The body fluids are distributed into intracellular (ICF) and extracellular compartments (ECF). These fluids have a high electrolyte content and are able to conduct electricity. The cell membranes contain a lipid bilayer which acts electrically as a dielectric and behaves in the same way as the dielectric of a capacitor does, it is able to block currents of low frequency and to allow only frequencies of high current to pass through the cell. Thus at low frequencies the current passes mostly through the ECF and at high frequencies the current passes through both fluid compartments. The electrical components of the body may be modelled thus:

The impedance of the ECF ($Z_e$) is :

$$Z_e = R_e$$

The impedance of the ICF ($Z_i$) is :

$$Z_i = R_i + X_c$$

$$= R_i + \frac{1}{j\omega c}$$

The total impedance is related to these by the following formula:

$$\frac{1}{Z} = \frac{1}{Z_e} + \frac{1}{Z_i}$$

Thus:

$$Z = \frac{Z_e \cdot Z_i}{Z_e + Z_i}$$

Therefore:

Multiplying both sides by the conjugate, the impedance of biological tissue can be expressed in complex number notation :

Multiplying both sides by the complex conjugate, the impedance of biological tissue can be expressed in complex number notation :

$$Z = \frac{R_i R_e - j\frac{R_e}{\omega C}}{R_i + R_e - j\frac{1}{\omega C}} \cdot \frac{(R_i + R_e) + j\frac{1}{\omega C}}{(R_i + R_e) + j\frac{1}{\omega C}}$$

$$= \frac{R_i R_e (R_i + R_e) + \frac{R_e}{(\omega C)^2}}{(R_i + R_e)^2 + \frac{1}{(\omega C)^2}} - j \cdot \frac{R_e^2}{\omega C (R_i + R_e)^2 + \frac{1}{\omega C}}$$

The resistive component of the impedance of biological tissue is thus given by the real part of the above equation :

$$R = \frac{R_i R_e (R_i + R_e) + \frac{R_e}{(\omega C)^2}}{(R_i + R_e)^2 + \frac{1}{(\omega C)^2}}$$

The reactive component of the impedance of biological tissue is thus given by the imaginary part of the above equation :

$$X = \frac{R_e^2}{\omega C (R_i + R_e)^2 + \frac{1}{\omega C}}$$

The magnitude of a complex number is the square root of the sum of the squares of the real and imaginary components. However for biological tissue the square of the real component is far greater than the square of the imaginary component. Reactance contributes negligibly to WBI which is why whole-body impedance and whole-body resistance differ by only 0.5% (Fuller). The WBI can thus be simplified by omitting the imaginary component and becomes :

$$WBI = \frac{R_i R_e (R_i + R_e) + \frac{R_e}{(\omega C)^2}}{(R_i + R_e)^2 + \frac{1}{(\omega C)^2}} \qquad \text{(C1)}$$

# Appendix D

## Tetrapolar Measurement of Whole-Body Impedance

The tetrapolar method of measurement of WBI is used to overcome the problem of skin impedance. Current flowing between two electrodes placed on the surface of the skin passes from one electrode through the impedance of the skin, through the impedance of the body fluids and then through the impedance if the skin again to the second electrode (see fig D.1).

Each of these impedances can be represented by the electrical model for biological tissue presented in appendix C. A circuit diagram of the impedance seen by two electrodes on the surface of the skin is given in figure D.2.

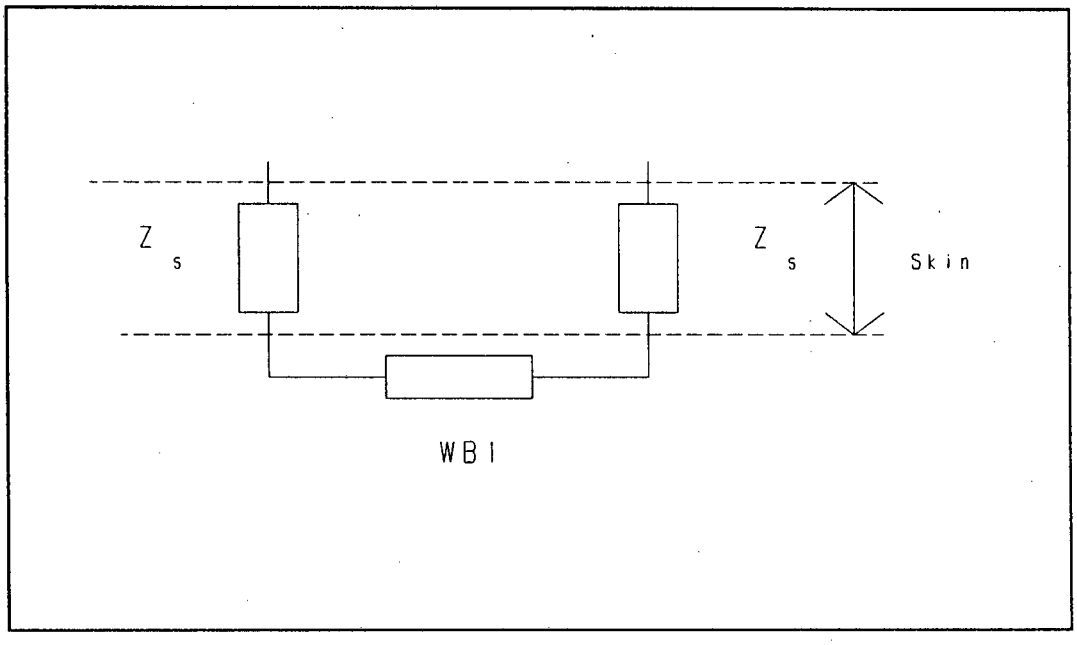


**FIGURE D.1 Impedance load of the constant current source**

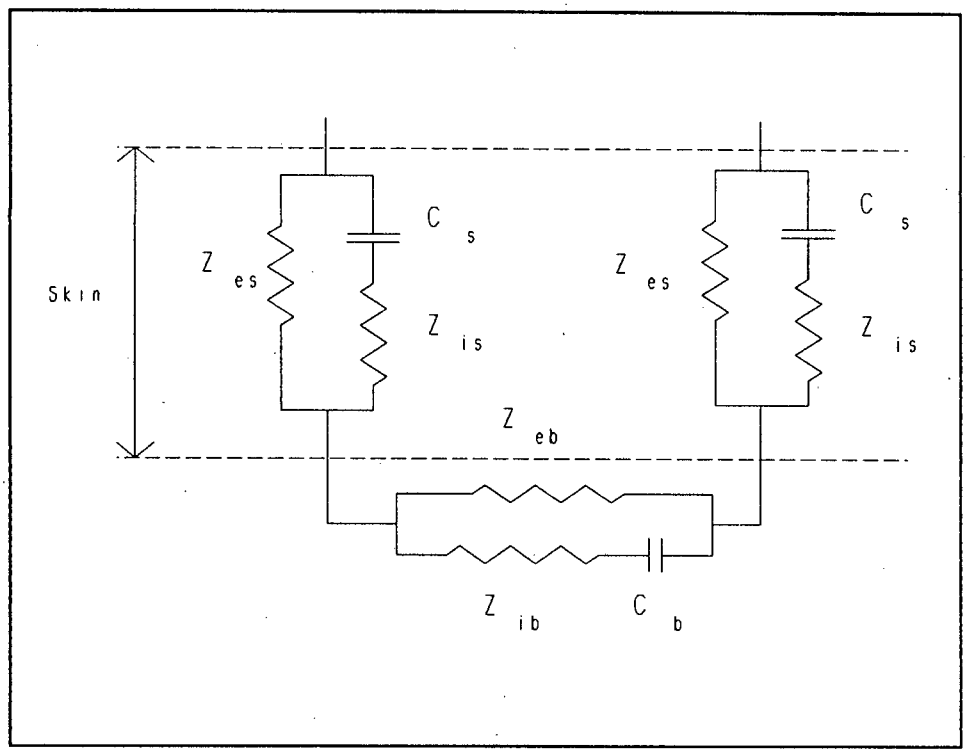


**FIGURE D.2 Elecrical model of the impedance load of the constant current source**

The tetrapolar method of measuring WBI involves passing an alternating current of constant peak amplitude through two electrodes placed on the surface of the skin. One electrode is placed on the hand and the other on the foot. A high impedance differential amplifier measures the voltage drop between these two points, using another pair of electrodes placed on the hand and foot proximal to the current injecting electrodes. The right side is used by convention. This circuit is shown in figure D.3.

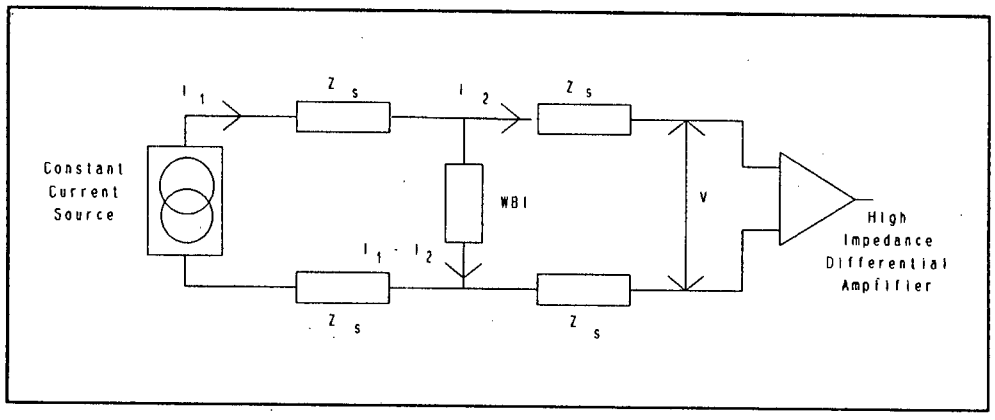


**FIGURE D.3 Circuit used to test the Variable Frequency WBI Analyzer**

The current flowing through the current injecting electrodes ($I_1$) is produced by the constant current generator and is set at a constant 300 µA RMS. The current flowing through the voltage sensing electrodes ($I_2$) flows through a high impedance differential amplifier and is only a few pA. The voltage measured is thus the sum of the voltage drop across the skin, the voltage drop across the body fluids and the voltage drop across the skin which is given as:

$$V = I_2 Z_s + (I_1 - I_2) WBI + I_2 Z_s$$

But:

$$I_2 \approx 0$$

Therefore:

$$V = I_1 \cdot WBI$$

Thus the skin impedance does not influence the measurement.
Rearranging in terms of WBI:

$$WBI = \frac{V}{I_1}$$

Which can be calculated if V is measured as $I_1$ is constant ( the output of a constant current source ).

## APPENDIX E

### Guidelines for the measurement of whole-body impedance in children

1. Insulating gloves must be worn so that the current does not travel through the body of the person holding the child which would result in a false reading.

2. Two pairs of electrodes are used. One pair is used on the right foot and the other on the right hand. Each pair consisting of a current electrode and a sensing electrode.

3. Right hand: the current electrode is placed just proximal to the second metacarpophalangeal joint and the sensing electrode is placed between the radial and ulnar styloid processes on the dorsal surface of the wrist. Care must be taken to ensure that sufficient electrode gel is used to make good contact.

4. Right foot: the current electrode is placed just proximal to the second metatarsophalangeal joint and the sensing electrode is placed between the lateral and medial malleoli on the dorsal surface of the ankle.

5. The child is placed on his/her back in the prone position.

6. The child's right arm and leg are held out to the side at 45 degrees.

7. The right arm and right leg must be held out to full length and the child must be motionless.

8. When holding the child care must be taken not to disturb the electrodes. The gloved hands holding the child should be distal to the current electrodes ie: holding the fingers and toes respectively.

# APPENDIX F

## Individual normal patients

| Number | Name | Sex | Impedance ( in Ω ) | Age ( in months) | Mass ( in kg ) | Height ( in cm ) |
|---|---|---|---|---|---|---|
| 1 | S.F.M. | M | 765 | 2.6 | 6.10 | 58.7 |
| 2 | S.M. | M | 725 | 1.1 | 5.38 | 56.9 |
| 3 | D.W. | M | 742 | 11.3 | 7.74 | 71.1 |
| 4 | S.G. | M | 590 | 22.6 | 14.50 | 87.6 |
| 5 | A.M. | M | 643 | 4.5 | 8.56 | 62.0 |
| 6 | V.N. | M | 575 | 6.5 | 10.40 | 69.1 |
| 7 | T.V. | M | 708 | 11.7 | 9.84 | 73.5 |
| 8 | M.M. | M | 798 | 5.3 | 7.96 | 62.0 |
| 9 | J.N. | M | 782 | 14.3 | 10.00 | 76.0 |
| 10 | E.L. | M | 813 | 11.4 | 9.64 | 74.0 |
| 11 | O.R. | M | 903 | 10.7 | 5.60 | 61.8 |
| 12 | B.M. | M | 856 | 7.8 | 8.62 | 78.0 |
| 13 | M.L. | M | 806 | 2.4 | 3.86 | 54.0 |
| 14 | M.B. | M | 753 | 7.1 | 7.22 | 65.7 |
| 15 | S.E. | M | 638 | 4.6 | 7.58 | 65.5 |
| 16 | F.M. | M | 650 | 1.7 | 5.80 | 58.3 |
| 17 | S.M. | M | 605 | 11.6 | 9.84 | 73.0 |
| 18 | A.T. | M | 788 | 6.1 | 8.40 | 66.7 |
| 19 | I.C. | M | 755 | 7.2 | 7.48 | 70.0 |
| 20 | R.J.N. | M | 706 | 5.5 | 6.82 | 64.3 |

| | | | | | | |
|---|---|---|---|---|---|---|
| 21 | R.D. | M | 750 | 17.3 | 10.00 | 85.0 |
| 22 | T.R. | M | 713 | 23.1 | 14.00 | 87.5 |
| 23 | M.G. | M | 729 | 16.1 | 9.50 | 75.5 |
| 24 | H.A. | F | 853 | 5.3 | 6.27 | 61.0 |
| 25 | C.W. | F | 723 | 6.6 | 6.46 | 64.5 |
| 26 | J.V. | F | 723 | 11.6 | 8.96 | 76.8 |
| 27 | N.P. | F | 675 | 7.8 | 9.73 | 71.2 |
| 28 | A.S. | F | 884 | 2.9 | 4.74 | 56.1 |
| 29 | N.N. | F | 648 | 2.8 | 5.24 | 59.0 |
| 30 | N.M. | F | 728 | 6.5 | 6.20 | 63.3 |
| 31 | N.S. | F | 893 | 7.7 | 7.68 | 67.0 |
| 32 | S.S. | F | 841 | 6.5 | 7.80 | 65.0 |
| 33 | N.G. | F | 710 | 1.8 | 4.90 | 58.0 |
| 34 | S.M. | F | 855 | 8.1 | 6.92 | 70.7 |
| 35 | N.B. | F | 722 | 7.1 | 7.20 | 64.5 |
| 36 | C.H. | F | 613 | 6.7 | 10.00 | 68.3 |
| 37 | G.S. | F | 758 | 6.8 | 7.22 | 64.6 |
| 38 | Z.H. | F | 783 | 5.9 | 6.30 | 64.0 |
| 39 | S.B. | F | 634 | 5.1 | 9.70 | 68.5 |
| 40 | F.N. | F | 860 | 12.7 | 11.50 | 87.0 |
| 41 | M.Q. | F | 793 | 17.4 | 10.50 | 80.5 |
| 42 | R.M | F | 824 | 21.1 | 12.00 | 87.5 |
| 43 | M.M | F | 768 | 14.1 | 10.50 | 78.0 |

# APPENDIX G
## Individual Dehydrated Patients

| Name | Age (months) | Height (cm) | Sex | Initial Mass (kg) | Final Mass (kg) | Percentage Dehydration | Initial WBI (Ω) | Final WBI (Ω) | Initial Sodium (mmol/L) | Initial Potassium (mmol/L) |
|---|---|---|---|---|---|---|---|---|---|---|
| OS | 9.1 | 72.0 | M | 7.08 | 7.86 | 9.9 | 1197 | 763 | 132 | 2.8 |
| ZB | 19.1 | 83.5 | M | 8.90 | 10.20 | 12.7 | 1207 | 784 | 129 | 1.8 |
| CT | 2.6 | 56.2 | F | 3.87 | 4.30 | 10.0 | 1273 | 807 | 132 | 2.5 |
| LB | 19.1 | 82.5 | M | 10.10 | 10.80 | 6.5 | 904 | 770 | 137 | 3.4 |
| NN | 2.2 | 49.9 | M | 2.68 | 3.20 | 16.3 | 1296 | 730 | 121 | 3.2 |
| SN | 2.9 | 59.5 | F | 4.15 | 4.72 | 12.1 | 953 | 595 | 130 | 1.6 |
| SS | 14.6 | 80.2 | F | 8.86 | 9.52 | 6.9 | 873 | 710 | 132 | 3.2 |
| SB | 9.4 | 70.1 | F | 7.52 | 8.02 | 6.2 | 874 | 720 | 136 | 2.9 |
| SK | 8.9 | 69.8 | M | 8.00 | 8.50 | 5.9 | 948 | 800 | 141 | 4.1 |
| ND | 3.1 | 59.5 | F | 5.46 | 5.85 | 6.7 | 847 | 638 | 138 | 3.8 |
| KN | 2.9 | 56.8 | F | 4.56 | 4.83 | 5.6 | 974 | 786 | 153 | 2.8 |
| PN | 18.5 | 74.1 | F | 6.50 | 7.26 | 10.5 | 1085 | 756 | 153 | 3.5 |
| PM | 11.1 | 73.3 | M | 8.44 | 8.82 | 4.3 | 1028 | 693 | 132 | 3 |
| CS | 4.9 | 54.5 | F | 3.64 | 3.88 | 6.2 | 1023 | 758 | 133 | 5.2 |
| KNT | 9.8 | 68.7 | F | 7.38 | 8.32 | 11.3 | 1099 | 653 | 128 | 2.2 |
| CJ | 6.4 | 65.3 | M | 5.46 | 6.20 | 11.9 | 890 | 680 | 142 | 3.5 |

# APPENDIX H

## Hardware - circuit diagram

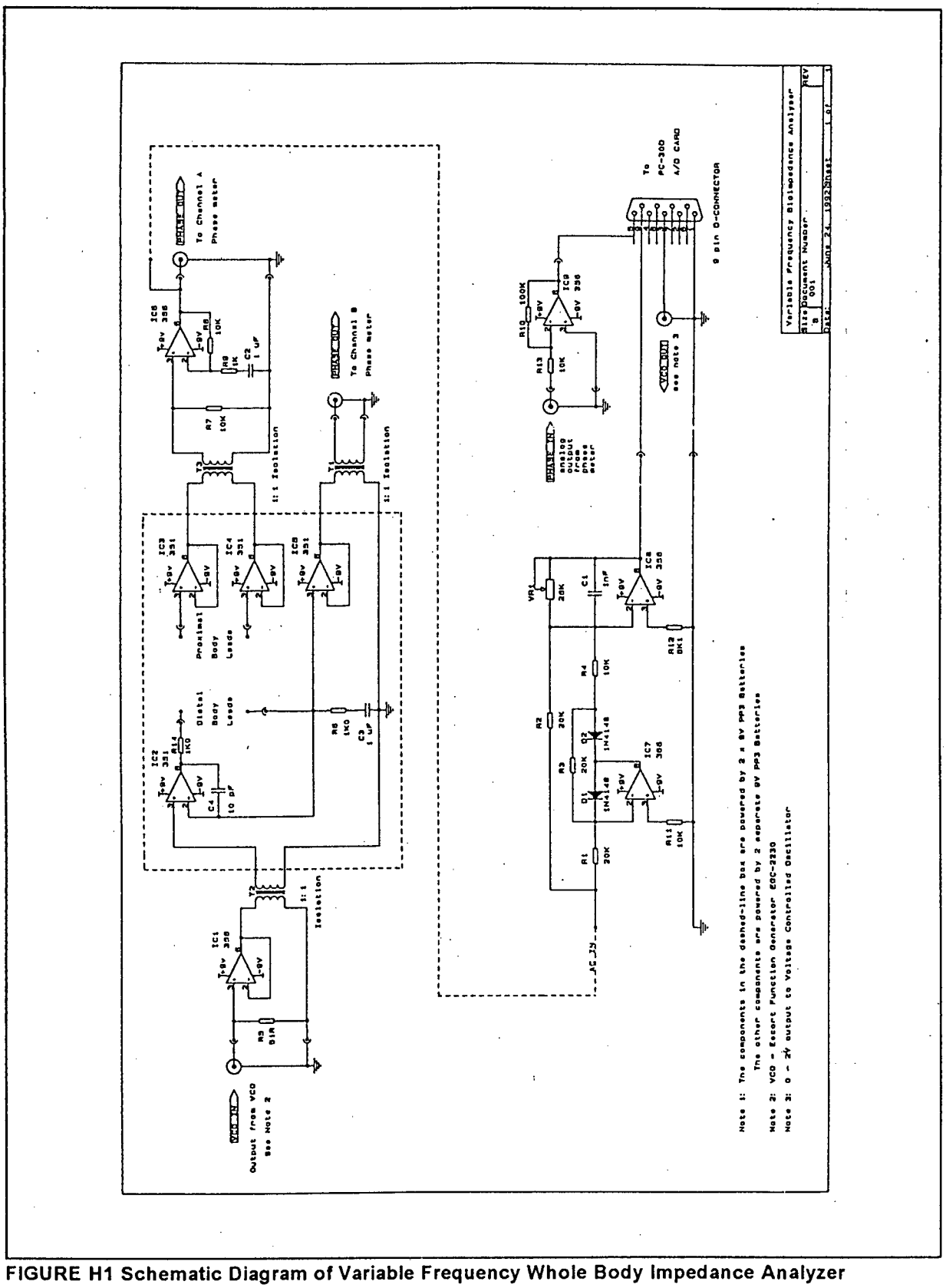


FIGURE H1 Schematic Diagram of Variable Frequency Whole Body Impedance Analyzer

# APPENDIX I

## System used for Testing of the Hardware

The hardware was tested using the circuit shown below. Two precision variable resistors were placed in series. These were 1433-T Decade Resistor boxes from General Radio USA. One was used to simulate the skin impedance and the other to simulate the WBI. The constant current source (red electrodes) was connected across both resistors as the constant current source must be able to supply a constant current through the skin impedance and the WBI. The high impedance differential amplifier was connected across one of the resistors. This resistor was used to simulate the WBI.

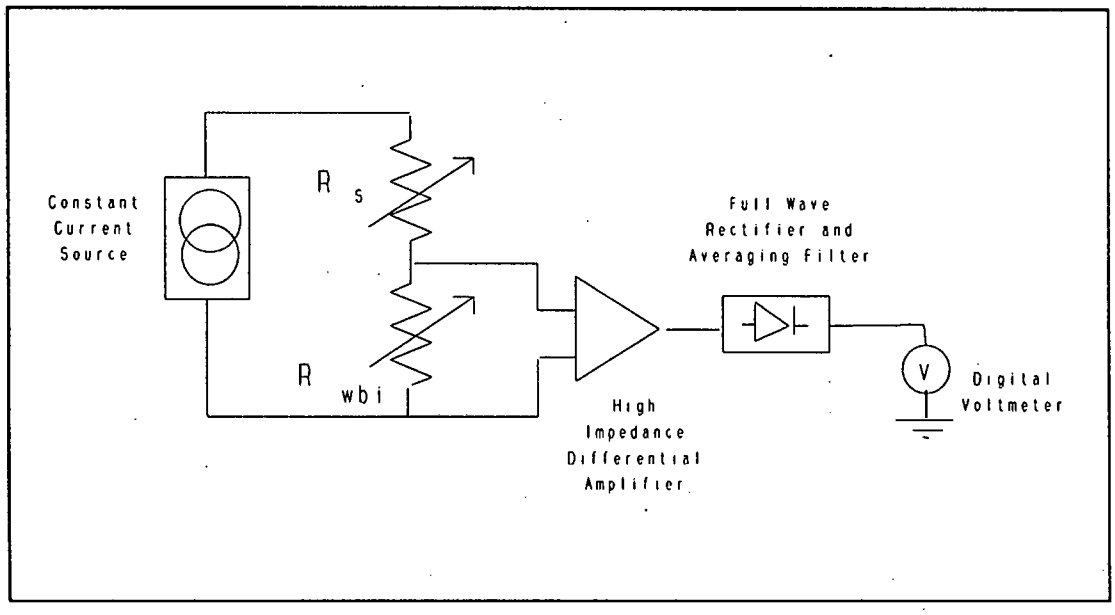


**FIGURE I.1 Circuit used to test the Variable Frequency WBI Analyzer**

Firstly the WBI resistor was set to 1 kΩ. The skin impedance resistor was then used to find the range over which the constant current source could operate with ≤ 1% error reading on the voltmeter. This determined the maximum skin impedance at which the constant current source could operate accurately. Secondly the skin impedance resistor was set to 1 kΩ and the WBI resistor was changed incremental from 200 Ω to 2000 Ω to determine the accuracy of the high impedance differential amplifier, full wave rectifier and averaging filter and the digital voltmeter.